

Powertrain optimization of a series hybrid race car

By

Albert Mathews

August 2009

Department of Mechanical Engineering

McGill University, Montreal, QC, Canada, H3A 2K6

A thesis submitted to

McGill University

In partial fulfillment of the requirements for the degree of

Master of Engineering

© Albert Mathews 2009

ABSTRACT

In recent years, we have witnessed the introduction of hybrid powertrains into the world of automobile racing. When compared to their conventional counter parts, hybrid powertrains demonstrate increased complexity with added degrees of freedom and technical barriers. For this reason, optimization of these systems becomes significantly more difficult requiring novel techniques.

This thesis documents the work performed to develop simulation techniques intended for the optimization of a series hybrid powertrain which was itself designed for an open wheeled, single seat race vehicle. The methodology employs computer simulation techniques such as driver-in-the-loop and forward facing powertrain models to optimize the vehicle powertrain for a specific set of known race conditions. Data obtained from an existing vehicle and its individual components, was used in the creation and validation of the models developed for this work.

The conclusions of the optimization process agree reasonably with the results from track testing of a subsequent vehicle equipped with a powertrain design based on the work performed. The simulation techniques employed here realized significant improvement in the vehicle performance and provided the ability to optimize the powertrain for any set of known race conditions.

RÉSUMÉ

Tout récemment, la motorisation hybride a fait son entrée dans le monde de la course automobile. Ce type de motorisation est beaucoup plus complexe à gérer et à optimiser qu'une motorisation conventionnelle à moteur thermique. Afin d'y parvenir, il est nécessaire d'utiliser de nouvelles techniques de pointe afin de réussir à obtenir d'excellents résultats malgré le grand nombre de variables et de restrictions inhérentes à la motorisation hybride.

Les travaux présentés dans ce document ont pour objectif le développement d'une méthodologie permettant d'optimiser la motorisation d'un véhicule de course existant. Le véhicule en question est de type Formule et comporte une motorisation hybride série. La méthodologie développée emploie des techniques de simulation informatique tel que "driver-in-the-loop" et "forward facing powertrain models". L'utilisation de ces techniques permet d'optimiser la motorisation complexe d'un véhicule de course hybride série pour des conditions de course connues. La création et la validation des modèles utilisés sont basées sur de l'information acquise lors de tests sur route d'un véhicule de course hybride série et lors de tests sur banc d'essai de composants individuels.

Les résultats obtenus via modélisation et simulation informatique concordent de façon adéquate avec les résultats obtenus sur piste lors d'essais fait avec une motorisation élaborée à partir de la méthodologie d'optimisation préalablement développée. Les techniques de simulation utilisées ont permis d'augmenter de façon significative les performances du véhicule de course utilisé. De plus, elles ont rendu possible l'optimisation des paramètres de motorisation hybride série pour des conditions de course connues.

ACKNOLEGDEMENTS

I would like to acknowledge Professor Peter Radziszewski and Professor Geza Joos for their valuable guidance throughout my research. Special thanks go to Benjamin Simard Lachance and Eugene Cojocar of the Exotypos team for their support with racing simulations as well as Jeff Turner, Joey Odman, Simon Ouellette, and all MHRT team members for their support and assistance. I would also like to express my appreciation for all McGill VERT Project Employees, McGill Machine Tool Laboratory and Mechanical Laboratory Technicians, and all MHRT team sponsors.

TABLE OF CONTENTS

ABSTRACT	iii
RÉSUMÉ	iv
ACKNOLEGDEMENTS	v
TABLE OF CONTENTS	vi
LIST OF FIGURES	viii
LIST OF TABLES	x
GLOSSARY	xi
1 Introduction	1
2 Literature Review	4
2.1 Vehicle Simulation.....	4
2.2 Driver-in-the-loop.....	5
2.3 Powertrains with CVTs	6
3 Defining Drive Train Performance	7
3.1 SAE Competitions	7
3.1.1 Formula Hybrid Competition	8
3.1.2 McGill University and the Formula Hybrid Competition.....	9
3.2 MHRT Vehicle	10
3.2.1 Drive Train Architecture	11
3.2.2 Chassis.....	12
3.2.3 Powertrain	12
3.2.4 Genset.....	13
3.2.5 Battery.....	14
3.3 Problem Statement	15
3.3.1 Review of Formula Hybrid Competition Results	15
3.3.2 Optimization Objectives.....	21
3.3.3 Aspects of Powertrain to be Considered	25
3.4 Chapter Conclusion.....	28
4 Methodology and Instrumentation.....	29
4.1 Methodology.....	29
4.1.1 Software Description.....	30
4.1.2 Software Operation	33
4.2 Instrumentation and Data Sets.....	36
4.2.1 Data Sets.....	37
4.3 Chapter Conclusion.....	42
5 Modeling and Validation of the MHRT Vehicle.....	43
5.1 Modeling of Vehicle System and Components in Simulink	44
5.1.1 Battery Model	46
5.1.2 Genset Model.....	49

5.1.3	Energy System Model Validation.....	57
5.1.4	Vehicle Load Model	59
5.1.5	Driver Model	74
5.1.6	Vehicle Model Validation	75
5.2	XMR Model.....	81
5.2.1	XMR Vehicle.....	81
5.2.2	XMR Track.....	83
5.3	Chapter Conclusion.....	84
6	Drive Train Optimization and Results	85
6.1	Genset Investigation.....	85
6.1.1	Outcome of MHRT Genset Improvement.....	87
6.2	Powertrain Investigation	88
6.2.1	XMR Trials.....	88
6.2.2	Simulink Output.....	91
6.2.3	Powertrain Investigation Conclusion.....	94
6.3	MHRT3 Results	96
6.3.1	MHRT3 Acceleration Performance	97
6.3.2	MHRT3 Lap Performance.....	99
6.4	Chapter Conclusion.....	102
7	Conclusion.....	103
8	Bibliography	106
	APPENDIX 1.....	111
	APPENDIX 2	112
	APPENDIX 3.....	113
	APPENDIX 4.....	114
	APPENDIX 5.....	116
	APPENDIX 6.....	120

LIST OF FIGURES

Figure 1: Block diagram of MHRT drive train architecture.....	11
Figure 2: 2008 FH endurance event voltage and current data.	20
Figure 3: Demonstration of the natural limiting effect of the powertrain.	24
Figure 4: Block diagram for the XMR simulator.	33
Figure 5: Block diagram of Simulink model.	34
Figure 6: Flow Chart illustrating indirect driver-in-the-loop simulation method.....	34
Figure 7: Model sub-system hierarchy.	45
Figure 8: System Model, level 1 in the hierarchy diagram.	45
Figure 9: Battery model validation against FH 2008 endurance event data.....	47
Figure 10: Block diagram of genset, level 2 in model hierarchy.....	49
Figure 11: Block Diagram of engine model: level 3 in model hierarchy.....	50
Figure 12: Genset fuel consumption relationship.	53
Figure 13: Sample plot for % error of genset current versus simulated engine RPM.	54
Figure 14: Governor model gain schedule.	54
Figure 15: Genset model validation against data set 3, battery is off.	55
Figure 16: Energy System Validation against 2008 FH endurance data.	57
Figure 17: Energy System validation charging close up.....	58
Figure 18: Energy System validation driving close up.	58
Figure 19: Vehicle load model block diagram: level 2 in model hierarchy.	60
Figure 20: Controller model efficiency map.	62
Figure 21: Map for rate of change of drive motor temperature.....	65
Figure 22: CVT3 Model, Motor RPM table.	67
Figure 23: CVT3 Model, DriveN pulley torque table.....	67
Figure 24: Shift Window Comparison of CVT1 and CVT4.	68
Figure 25: Vehicle drag, inertia, and traction limit model: level 3 in system model hierarchy. ...	69
Figure 26: MHRT2 Coast down data.	70
Figure 27: Formulation of vehicle drag relationship	71
Figure 28: MHRT3 Tire Longitudinal Force Data (48).....	73
Figure 29: Speed plot for complete model validation.	76

Figure 30: Drive motor RPM plot for complete model validation.	76
Figure 31: Drive motor current plot for complete model validation.	77
Figure 32: System voltage plot for complete model validation.	78
Figure 33: Battery current plot for complete model validation.	78
Figure 34: Genset current plot for complete model validation.	79
Figure 35: Average percent error of selected data channels for model validation.	80
Figure 36: XMR torque maps.	82
Figure 37: XMR model validation.	82
Figure 38: XMR track schematic.	83
Figure 39: Results for genset investigation.	86
Figure 40: Genset Thermal Testing Results.	88
Figure 41: XMR lap time results. See text for plot marker description.	89
Figure 42: Powertrain investigation motor temperature output.	91
Figure 43: Powertrain investigation SOC output.	92
Figure 44: Bar graph of motor temperatures from powertrain investigation.	93
Figure 45: Bar graph of final SOC values from powertrain investigation.	93
Figure 46: Acceleration results for the powertrain investigation.	94
Figure 47: Bar graph of decision matrix weighting schemes.	95
Figure 48: MHRT3 and model acceleration data.	98
Figure 49: Comparison of drag relationships for MHRT2 and MHRT3.	99
Figure 50: Motor temperature data and model validation for data set 4.	102
Figure 51: Chassis CAD views for MHRT3 (left) and MHRT2 (right).	111
Figure 52: Battery model relation for open circuit voltage to state of charge.	112
Figure 53: RPM per Volt relationships.	113
Figure 54: Torque versus current relationships.	113
Figure 55: Curve fits used to extrapolate CVT3 torque data.	115
Figure 56: Genset ratio optimization.	120

LIST OF TABLES

Table 1: LTC cell charge / discharge information (34).....	14
Table 2: Battery pack information for MHRT 1, 2 and 3.....	14
Table 3: 2007, 2008, and 2009 FH competition fuel allocations.....	17
Table 4: 2007 and 2008 FH acceleration event competition results.....	18
Table 5: 2007 and 2008 FH endurance event competition results.....	19
Table 6: CVT weights and springs used for the powertrain investigation.....	26
Table 7: Fixed ratios selected for the powertrain investigation.....	27
Table 8: Performance criteria for models.....	43
Table 9: Statistical analysis of battery model error.....	48
Table 10: Statistical analysis of genset model current error.....	56
Table 11: Statistical analysis of energy system model performance.....	59
Table 12: Configurations of CVT models.....	66
Table 13: Maximum Driving and Braking Forces.....	74
Table 14: Powertrain configuration identification table.....	89
Table 15: Fuel consumption data for the powertrain investigation.....	94
Table 16: Decision matrix for the powertrain investigation.....	96
Table 17: Vehicle speed statistics for different tracks.....	100
Table 18: Lap time statistics for data set 4.....	100
Table 19: Dynamometer data for CVT3.....	114

GLOSSARY

ABC – the coefficients for a curve fit vehicle drag model
AC – Alternating Current
ANSI – American National Standards Institute
AVL CRUISE – powertrain and vehicle dynamics simulation software
AVPRnet – Advanced Vehicle Powertrain Research Network, a Transport Canada initiative
AXE – product name for Alltrax Inc. electric motor controller
BEMF – Backwards Electromotive Force
BMS – Battery Management System
CAD – Computer Assisted Design
CSC – Clean Snowmobile Challenge
CVT – Continuously Variable Transmission
DC – Direct Current
DriveN – secondary/output pulley of the CVT
DriveR – primary/input pulley of the CVT
EX21 – product name for Robin Subaru engine
FH – Formula Hybrid
FSAE – Formula SAE
Genset – Direct current generator used for the series of MHRT vehicles
GPS – Global Positioning System
IEEE – Institute of Electrical and Electronics Engineers
LTC – Lithium Technology Corporation
M/G – Motor/Generator, the electric component of the generator
MATLAB – math computing software developed by The MathWorks
ME0709 – product name for Mars Electric permanent magnet motor/generator
MHRT – McGill Hybrid Racing Team
MRT – McGill Racing Team
PDF – Post Document Format
PI – Proportional Integral
PMG – Product name for Perm GmbH permanent magnet motor
PSAT – Powertrain Systems Analysis Toolkit
PWM – Pulse Width Modulation
rFactor – product name for Image Space Inc. racing simulator
rFactor Pro – product and company name for advanced racing powertrain simulation software
RPM – Revolutions per Minute
SAE – Society of Automotive Engineers
SOC – State Of Charge
VERT – Vehicle Engineering education Research and Technology transfer
XMR – X Motor Racing, racing simulator developed by Exotypos

1 Introduction

In recent years we have witnessed the introduction of hybrid powertrains into the world of automobile racing (1), (2), (3). When compared to their conventional counterparts, hybrid powertrains demonstrate increased complexity with added degrees of freedom and technical barriers (4), (5). The added degrees of freedom refer to the possibility of incorporating multiple energy flow pathways as a means to achieve some set of goals. Conventional powertrains on the other hand are typically restricted to unidirectional single pathway energy flows between the fuel tank and the wheels. For this reason, design based optimization of hybrid systems becomes significantly more difficult requiring novel techniques for optimization purposes (4), (5), (6).

During the past two decades there has been significant advancement in fields of vehicle dynamics simulation and powertrain simulation. In an effort to reduce cycle times, all large automotive companies have created in house simulations of virtually all aspects of the vehicle ranging from powertrain energy flows to vehicle crash worthiness. Powertrain simulation tools have become more popular due to the complexity of the ever greater numbers of hybrid powertrains reaching the market (7), (8). In the field of automobile racing, powertrain simulation has been adopted for both vehicle development and driver training purposes (9), (10). Race simulations which simulate vehicle dynamics in a three dimensional environment are typically used for driver training purposes but are now also being use for vehicle development (9). These simulations originated as entertainment media, but as the fidelity of the simulations increased, they became active development tools for race teams. They have become an important tool since they allow for investigations in absolutely non-varying environments which is not possible in the real world. Only in recent years has the ability to combine racing simulation with high fidelity powertrain simulations become a possibility. Known as “Driver-in-the-Loop” simulations, the goal is to simulate all physical properties necessary to create a virtual vehicle on a virtual track. Detailed tire-road interaction models taking into account heat, rain, wear, powertrain models incorporating clutch over heat and powertrain damage caused by accidents, aerodynamic changes caused by accidents, and other complex phenomena are now common. The fidelity of these simulations puts both the simulated vehicle and the driver as close to the real situation as possible allowing race teams to perform cost and time saving development not previously possible (9).

Broadly stated, the goal of the thesis is to perform a design based optimization for the McGill University hybrid race car using modern race vehicle and powertrain simulation techniques. The design based optimization approach is applied to the events of the 2009, Society of Automotive Engineers, Formula Hybrid (FH) competition¹.

The motivation for such an undertaking is drawn from the vehicle development cycles imposed on race vehicle design teams. These development cycles typically require teams to design, manufacture, and test their vehicle over the course of one year. Testing time is therefore extremely valuable and any preparation that can be done in advance is a competitive advantage. Specifically addressing the case of a student designed hybrid race car, simulation of the vehicle dynamics, powertrain performance, and their interactions can provide the team with knowledge and data which will help them maximize the effectiveness of their limited testing time. Taking a different look at the situation, if we compare a race vehicle with a conventional powertrain and one with a hybrid powertrain, the added degrees of freedom inherent with a hybrid powertrain significantly increase the design and optimization possibilities available (11). Therefore, if the physical vehicle cannot be on the test track for a sufficient amount of time to narrow down the available options to a small set with favorable performance under the given set of conditions, then vehicle simulation can provide the knowledge which will allow the designers to limit the availabilities to a reduced set for which there is sufficient testing time with the physical vehicle.

Therefore the objectives can be outlined as:

1. Identify areas of the drive train where significant improvements are possible.
2. Determine what actions should be taken in order to improve the performance of the MHRT vehicle for the FH dynamic events.
3. Predict the performance improvement of the system from a design based optimization.
4. Compare these predictions with measured performance of a second generation prototype.
5. Discuss any discrepancies between predictions and measurements.

Objectives one and two above form the subject of chapter 3. Chapter 4 then outlines the methodology developed to achieve the goal as well as the instrumentation employed in acquiring

¹ See (3) as well as sections 3.1.1 and 3.3.1 for details about the competition.

the necessary data. Chapter 5 presents all component and system models developed/modified and validated which are required to predict drive train improvements. Chapter 6 presents the investigations performed to produce the predictions as well as the final selections/suggestions which stem from these predictions. Included in chapter 6 are the comparisons of these predictions with data obtained from a subsequent prototype. Finally, a conclusion to the study with suggestions for improvement on the models and methodology is provided in chapter 7.

2 Literature Review

The literature review for this study covers three topics separately. Presented first is material covering the simulation of vehicles from both powertrain and vehicle dynamics perspectives, second are simulation studies involving driver-in-loop architecture; and third a brief review of material covering vehicle powertrains which include CVTs.

2.1 *Vehicle Simulation*

From a powertrain perspective, vehicle simulation is a relatively new tool which can be used to analyze and make predictions for parameters including powertrain efficiency, performance, emissions, and so on. Since becoming a valuable tool use for vehicle powertrain development, the primary use has been in the efficiency analysis and optimization of large and small road vehicles. Concerning hybrid powertrains, there is a wealth of information far beyond what is necessary for this literature review, therefore a few pertinent examples are reviewed; first a study which aims to predict the performance of a non-existing powertrain, second a study which analyzes an existing powertrain and explores possibilities for improvement, and third a study which compares the performance of different powertrains under identical conditions.

In (12), a detailed analysis of a diesel-hydraulic series hybrid is carried out with the goal of determining the impact of engine transients on round trip fuel consumption and emissions. The study employs engine-in-the-loop architecture to capture the real performance of the engine when submitted to the load requirement of the simulated hydraulic hybrid. Results demonstrate the value of powertrain simulation in producing large amounts of information at relatively low cost. The point is made clear that including real components in the simulation architecture (i.e. hardware-in-the-loop) is critical for certain studies. Finally, the main point made is that engine transients can have significant impact on the overall fuel economy and emission profile of large road vehicles. Importantly, these transient effects are not captured by quasi-static engine maps currently used for simulating engine parameters such as fuel consumption and emissions.

In (4), analysis is performed on the powertrain of an electric delivery vehicle. Strong and weak points are identified with subsequent investigations to evaluate the relative potential impact which various improvements could have on vehicle efficiency. The study concludes that a

properly sized traction motor offers the most economical improvement. This conclusion contradicted the preconception that an optimized regenerative braking strategy would offer the greatest improvement. This study is the type which is most in line with goals of this thesis investigation.

In (13), a study is performed to compare the trip efficiency of commuter buses using either a diesel engine or a fuel cell as the primary power source. Several scenarios are investigated to explore “the influence of key factors such as speed, acceleration, and road grade on fuel consumption for diesel and hydrogen fuel cell buses under real-world operating conditions.” The study concludes that a switch of primary fuel to hydrogen, obtained by means of steam reforming, may increase the fuel consumption and carbon-dioxide emissions while reducing other emissions profiles.

From a vehicle dynamics perspective, simulations are used for both road safety and race optimization investigations. For road safety, vehicle dynamics simulation are used for the development of control algorithms for air bags, control systems testing, driver training, stability analysis, active control development, etc. The studies typically employ high fidelity models for representing the vehicle inertia in three axes, suspension system, and road tire interactions. For racing, clearly high fidelity vehicle dynamics are required for investigation with both classical driver models and driver-in-the-loop architectures (14). In (15), a full vehicle dynamics model created using ADAMS Car is validated to determine the effectiveness with which race car simulations can be used for racing optimization. The study concludes that “the full vehicle ACAR model has potential as a valuable analysis tool for the FSAE racecar design process.”

In the thesis study presented here, a combination of the both modeling strategies used in (15) and (4) is proposed with the substitution of a driver-in-the-loop architecture for the model driver used in (15).

2.2 Driver-in-the-loop

The most popular application of driver-in-the-loop simulations is for entertainment purposes as racing video games. Besides entertainment, driver-in-the-loop simulations are used in academic and government sponsored studies, transportation industry, and automobile racing.

In academia, the most common use is for highway safety investigations. For investigations into the effects of alcohol consumption on driving ability, driver-in-the-loop is considered as a necessary tool (16), (17). In the field of vehicle control automation, such as vehicle stability control, speed control, and crash avoidance, etc; studies employing driver-in-the-loop simulation have shown to produce more realistic results compared to studies using simulations employing classic driver models (16), (17), (18). For example in (16), an Advanced Cruise Control system is developed with the control code validated using a multiple-driver-in-the-loop simulation platform. The authors explain how the use of a multiple-driver-in-the-loop platform provides the abilities to test the ACC code with realistic steering, throttle and brake inputs, and in addition to perform comparative studies of driver workload for various ACC models. A similar study is conducted in (19).

In automobile racing, both classic driver models and driver-in-the-loop simulations are used for vehicle development purposes. Simulations employing classic driver models are typically used to find theoretical performance maximums for a given configuration. Driver-in-the-loop simulations are most commonly used for driver training; however, they are preferred over classical driver models for determining optimal configuration for particular drivers or finding abilities of the vehicle that a non-adaptive driver model cannot (14). Leaders in the field of driver-in-the-loop simulation for racing applications include organizations such as AT&T Williams F1 (20) and rFactor Pro (9), due to the competitive nature of the industry, all technical information is proprietary and confidential.

2.3 Powertrains with CVTs

Powertrains incorporating CVTs as a means to couple the main power source(s) to the traction mechanism require different control strategies than powertrains incorporating classical sequential discrete transmissions. In (21), the effect of control structure on the performance of vehicles incorporating CVTs is investigated. The study explores different control options to convert driver throttle input into various vehicle commands such as engine throttle position and CVT shift ratio. The study suggests that although several solutions exist, none are perfect and require case specific refining dependent on the desired operation.

3 Defining Drive Train Performance

The performance of the MHRT vehicles did increase between 2007 and 2008. Accomplishing further improvement requires careful analysis of available data in order to determine the strengths and weaknesses. This chapter first presents a detailed description of the MHRT drive train followed by a review of past competition data which together provide the insight necessary to isolate the strengths and weaknesses. The chapter concludes by presenting the specific objectives of the powertrain optimization and the limitations imposed the optimization process.

3.1 SAE Competitions

The Society of Automotive Engineers (SAE) hosts a variety of university student oriented competitions. These competitions aim to provide practical experience in areas such as team work, project management, engineering design, manufacturing, etc. To achieve this, students from universities around the world form teams to design, manufacture and compete against each other with fully functional vehicles designed according to a set of rules provided by the SAE.

These SAE competitions are hosted annually around the world, all of which are based on one of five rule sets which are updated annually (22). The five rule sets are:

1. Aero Design
2. Clean Snowmobile Challenge (CSC)
3. Formula SAE Series
4. Baja SAE Series
5. Supermileage

In 2007 a new section of the Formula SAE Series specifically intended for vehicles equipped with hybrid drive trains was created. This new section makes use of much of the same rules as the parent Formula SAE Series but with drive train rules specific for hybrid technology. The two rules sets can be found on the respective competition websites as PDF documents (3), (22).

SAE student competitions are composed of both dynamic and static events. Static events require the teams to compose technical design reports and perform technical design and marketing presentations. Dynamic events differ widely depending on the nature of the competition and the

vehicle, for example the CSC will have emissions events, while the Formula SAE Series will have time trial events and the Baja SAE Series will have hill climb and rock crawl events.

3.1.1 Formula Hybrid Competition

The following description of the Formula Hybrid competition is available from the competition website (3):

“Formula Hybrid™ is a design and engineering challenge for undergraduate and graduate college and university students. They must design, build, and compete an open-wheel, single-seat, plug-in hybrid racecar. This car must conform to a formula which emphasizes drive train innovation and fuel efficiency in a high-performance application.”

“The competition is organized by Thayer School of Engineering at Dartmouth and carries the endorsement of the Society of Automotive Engineers, Inc. (SAE) and the Institute of Electrical and Electronics Engineers, Inc. (IEEE).”

Aside from the drive train, a major difference between the Formula SAE Series and the Formula Hybrid Competition is the allowance of teams to enter a vehicle in the Formula Hybrid Competition for multiple years. This is in contrast with the Formula Series which does not allow a vehicle to compete once a full year has passed since it was first entered in any of the Formula SAE Series competitions. This difference in the Formula Hybrid rules comes with restrictions; for example, older chassis must be modified to comply with all current Formula SAE Series safety regulations, while non-compliance with rules not related to safety is allowed. As such, Formula Hybrid teams may modify vehicles originally built for the Formula SAE Series, therefore allowing them to focus more time and resources on drive train design and innovation. The intention is to promote Formula Hybrid as a drive train design oriented competition.

The events at the Formula Hybrid Competition are:

- Static Events
 - Technical Design Presentation
 - Marketing Presentation
- Dynamic Events
 - Acceleration
 - Pure Electric Propulsion
 - Option of Hybrid or Electric Propulsion
 - Autocross
 - Endurance

Dynamic events are discussed in greater detail in following chapters. The static events are not part of the focus of this study.

3.1.2 McGill University and the Formula Hybrid Competition

For the inaugural year, 2007, and the following year, 2008, McGill University entered a modified vehicle originally entered in the Formula SAE Series event in Detroit, MI in 2005. This vehicle known as MRT7 was just one in a line of similar vehicles designed and manufactured by the McGill Racing Team (23).

The MRT7 was retrofitted with an electric drive train by students at McGill University in the academic year of 2005-2006 as part of an advanced vehicle research project known as the VERT (Vehicle Engineering education Research and Technology transfer) Project. Upon completion of the modified vehicle in the spring of 2006, McGill University was invited by the Thayer School of Engineering to demonstrate the vehicle at the New Hampshire Motor Speedway as part Thayer's initial push for the formulation of an SAE endorsed Formula Hybrid competition.

The following academic year (2006-2007) a formal rule set was produced for the inaugural Formula Hybrid competition in May 2007. A team of students at McGill University with the assistance of the VERT Project performed the necessary work to further modify the electric MRT7 to comply with the new rule set. The vehicle retained the electric powertrain and was fitted with a gasoline generator and appropriate battery pack for the competition. This original

design of a series gasoline electric hybrid was kept for the following year and remains as the hybrid platform for the McGill Hybrid Racing Team (24) for the 2009 Formula Hybrid Competition.

MHRT has performed well in the Formula Hybrid Competition placing first overall in both 2007 and 2008 (25), (26). Much of the success of the team is due to reliability of the drive train and on-board systems which allowed the team to be competitive in all dynamic events in both years. Although the team produced significant performance improvement between 2007 and 2008, it is believed that even further performance improvement is possible with the current platform. Herein lays the motivation for work documented in this thesis. From this point on, the McGill University Formula Hybrid entry vehicles will be described using the following names:

- 2007 entry – MHRT1
- 2008 entry – MHRT2
- 2009 entry – MHRT3

3.2 *MHRT Vehicle*

The McGill hybrid vehicle powertrain architecture is a gasoline-battery electric, series hybrid. The vehicle design employs a charge depleting strategy² for situations requiring extended operation. This design was chosen by the MHRT to reflect the requirements of the competition dynamic events. The electric powertrain and battery coupled together, act as a low-pass filter for the power requirement applied to the engine. This allows the engine to be operated at effectively constant power output. There are many citations in the literature regarding the benefits of such a setup when considering engine fuel efficiency and emissions (12). The series hybrid architecture is one of the more common architectures chosen by teams competing in the SAE Formula Hybrid Competition (27).

² A charge depleting strategy means that in addition to burning fuel to supply the vehicle with energy, the battery state of charge depletes over time thus adding supplemental energy.

3.2.1 Drive Train Architecture

Figure 1 shows a block diagram of the drive train³ architecture of all three MHRT vehicles built so far. The Genset block represents the gasoline engine and the electric motor/generator as one unit.

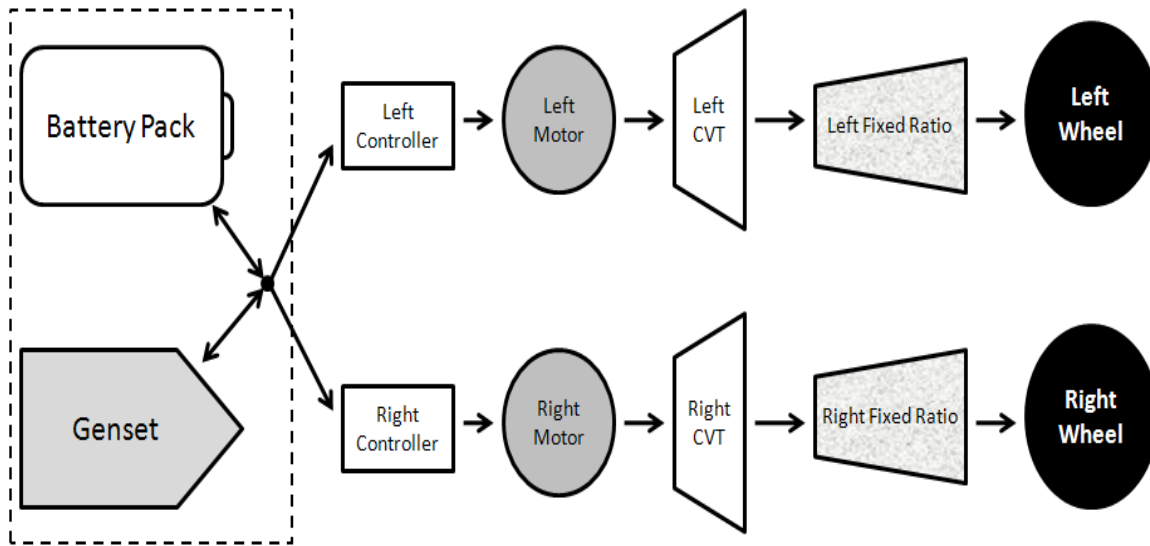


Figure 1: Block diagram of MHRT drive train architecture.

The components inside the dotted line together make up the energy supply system. The rest of the components are grouped together as the powertrain. The arrows in the block diagram illustrate the direction of energy flows. In regular operation, the genset acts as a continuous source of energy, the battery acts as a sink or a source of energy, while the powertrain⁴ acts only as a sink. Energy will flow from the battery to the genset (i.e. genset acting as energy sink) only to start the genset. The controllers do not have regenerative braking abilities hence energy will never flow from the controllers in the direction of the energy supply system. As the diagram shows, the hybrid architecture does not incorporate any power electronics governing the flow of energy between the battery and genset. Supervisory control systems monitor the interaction between the battery and genset as well as the condition of the battery; however, these systems

³ Drive train in this document refers to all component of a vehicle which forms the system that propels the vehicle.

⁴ Powertrain in this document refers to the set of components which propel the vehicle by converting energy from onboard storage. The battery and genset are not included in the powertrain.

have the restricted ability to turn off or turn on both the genset and the battery, they cannot otherwise control their actions. The interactions of this type of architecture are described in (28).

3.2.2 Chassis

As mentioned above, the chassis for both MHRT1 and MHRT2 was a modified chassis from the McGill Racing Team entered in the SAE Formula Series Detroit 2005 competition. The chassis is a steel space frame type with dual wishbone four-wheel independent suspension. Modifications to the chassis were restricted to the drive train compartment section of the frame, as well as the suspension setup.

The chassis for MHRT3 was custom built for the Formula Hybrid application by the MHRT. The MHRT3 chassis very closely resembles the chassis used for MHRT 1 & 2. CAD model views of the two chassis' are provided in appendix 1.

3.2.3 Powertrain

As shown in figure 1, all MHRT powertrains to date are composed of two independent systems each driving one of the rear wheels. Provided here is a point from description of the components of the powertrain:

- The motor controllers are Alltrax AXE 7234 direct current motor controllers. This controller is a phase width modulation type controller with an operational voltage range of 24 to 72 volts and a 30 second current rating of 340 amps (29).
- The drive motors are Perm Motor Company PMG 132 direct current motors. This motor is a permanent magnet pancake style motor rated at 72 volts with a 200 second current rating of 200 amps (30).
- The Continuously Variable Transmission (CVT) manufactured by CVTech is a rubber V-belt and pulley type CVT modified to be permanently engaged. The CVT DriveR (primary) pulley is a Powerbloc 50 with interchangeable weights and spring and the DriveN (secondary) pulley is a LP3 with interchangeable spring (31).
- Fixed Ratio is ANSI 40 roller chain and sprockets with a step down ratio between 3:1 and 5:1.

3.2.4 Genset

The Genset for all MHRT vehicles is composed of a single cylinder 4 stroke gasoline engine coupled with a permanent magnet direct current (DC) motor/generator (M/G). As described in (28), the genset supplies current to a DC bus common to the battery and the powertrain.

The genset in both MHRT1 and MHRT2 used a Robin Subaru EX21 (32) engine directly coupled to a Perm PMG 132 DC motor. This system was capable of outputting between 50 and 60 amps to a DC bus between 50 and 80 volts with a typical power output of between 3500 and 4500 Watts. Although this system was light, compact, and powerful enough for the job, it was plagued with temperature issues. The Perm PMG 132 was not designed to be operated when coupled to an external heat source such as an engine and therefore had the tendency to fail if operated for periods of time greater than 10 minutes.

The genset in MHRT3 uses the same engine but coupled via a chain drive to a Mars Electric ME0709 permanent magnet motor (33). This configuration does not suffer from the temperature issues due to the robust construction of the ME0709 and the excess heat dissipated by the chain drive as compared to the direct shaft coupling. The performance of this setup is comparable to that of the previous setup with added weight due to the greater weight of the ME0709 compared to the PMG 132.

In all configurations the engine throttle is controlled by a manufacturer installed mechanical governor. The governor is used to limit the engine speed such that the genset output voltage does not exceed the maximum voltage of the DC bus. This maximum voltage is determined by the battery, the battery management system, and other electrical components powered off the bus.

3.2.5 Battery

The battery packs for the MHRT vehicles are all composed of high power lithium-ion cells from Lithium Technology Corporation (34). These cells have a maximum voltage of 4.2V, minimum voltage of 3.0V, nominal voltage of 3.6V, and a capacity of 45 Ah at a C/5 discharge rate.

The charge/discharge ratings for the cells are provided in table 1:

Table 1: LTC cell charge / discharge information (34).

	Continuous	Peak
Discharge Current	270 A	500 A for 30 sec
Charge Current	90 A	270 A for 15 sec

The battery pack for MHRT1 contained 20 cells in series making a 72 volt nominal pack while the pack used for both MHRT2 and MHRT 3 contained 18 cells in series making a 65 volt nominal pack. The details of the different packs are listed in table 2.

Table 2: Battery pack information for MHRT 1, 2 and 3.

	MHRT1 2007	MHRT2 2008	MHRT3 2009	
Number of Cells	20	18	18	
Max Pack Voltage	84	75.6	75.6	V
Nominal Voltage	72	64.8	64.8	V
Min Pack Voltage	60	54	54	V
Pack Capacity	45	45	45	Ah
Pack Energy	3240	2916	2916	Wh

The condition/health of the battery pack for all MHRT vehicles is monitored by an I+ME Actia (35) battery management system (BMS) supplied by Lithium Technology Corporation. This system monitors cell voltages, pack current, and temperature in several key locations; it uses this information to determine the immediate health of the battery pack and whether it is safe for operation under the current conditions. The BMS controls a high voltage, high power relay which it uses to isolate the pack from all electrical circuits as it deems necessary.

3.3 Problem Statement

Recalling the objectives set to achieve the goal:

1. Identify areas of the drive train where significant improvements are possible.
2. Determine what actions should be taken in order to improve the performance of the MHRT vehicle for the FH dynamic events.
3. Predict the performance improvement of the system from a design based optimization.
4. Compare these predictions with measured performance of a second generation prototype.
5. Discuss any discrepancies between predictions and measurements.

Investigating different drive train architectures or the affects of substituting alternative components is not considered in this study. The goal is to improve the performance of the exiting architecture with the current selection of components. The architecture and component selection are considered as fixed for this study.

To clearly identify what areas are most in need of improvement it is necessary to review the performance of both MHRT1 and MHRT2 such that we have a clear picture of what were the strengths and weaknesses of each. Competition results as recorded by the Formula Hybrid track crew are available for both vehicles (25), (26). Data from the onboard data acquisition system of MHRT2 is only available for the endurance event of 2008, and even then it has its limitations⁵. As a result of this, comparisons here will be for most part based on competition results.

3.3.1 Review of Formula Hybrid Competition Results

The results from the FH competitions are available for 2007, 2008, and 2009. Although the results of the 2009 competition are presented, none of the data obtained from the 2009 competition or MHRT3 is used in the formulation of the specific objectives for the study or the models developed to accomplish the main goal. The 2009 data is presented along with the 2007 and 2008 data for reference purposes only.⁶

⁵ See section 4.2.1, paragraph “Data Set 1”

⁶ MHRT3 performed poorly in the 2009 FH competition due to mechanical issues not related to the work done for this thesis.

3.3.1.1 Formula Hybrid Fuel Allocation

Fuel allocation for both 2007 and 2008 were identical. The rules committee estimated an allocation amount based on fuel consumption of a Formula SAE Series vehicle performing the events of the Formula Hybrid competition, the committee then reduced the amount by 15% (36). The committee settled on an allocation of 4.712 liters; however, for each team, a volume of fuel equal in energy content to the storage capacity of their onboard accumulators is subtracted from the total allotment. The storage capacity of the accumulators and equivalent volume of fuel are calculated using data compiled by the Formula Hybrid committee.

For the 2007 and 2008 competitions, these fuel allocations along with a fully charged battery pack constitute the total amount of energy available to the team for the entire Formula Hybrid competition. McGill University completed all possible runs for all events for both 2007 and 2008 with approximately one liter of fuel remaining upon completion. Furthermore, noting the calculations for minimum required fuel economy, one would not expect that the fuel allocation would be a very restrictive design constraint for FH teams.

Table 3: 2007, 2008, and 2009 FH competition fuel allocations.

	2007	2008	2009	
Fuel Allocation	4.712	4.712	3.765	L
Cell Capacity	129.6	129.6	129.6	Wh
Equivalent Volume of Fuel per Cell	0.0536	0.0536	0.0536	L/unit
Number of cells	20	18	18	unit
Volume of Fuel Deducted	1.07	0.97	0.97	L
Fuel Received	3.64	3.75	2.8	L
Distances Required with Fuel Allocation ⁷	-	-	-	-
Acceleration ⁸	0.45	0.45	0	km
Autocross ⁹	2.8	2.8	0	km
Endurance	22	22	22	km
Total	25.25	25.25	22	km
Minimum Fuel Economy	18.66	18.66	17.11	L/100km
Alt. Units	12.6	12.6	13.75	MPG
Absolute Minimum Fuel Economy ¹⁰	20.0	20.0	17.11	L/100km
Alt. Units	11.76	11.76	13.75	MPG

3.3.1.2 Acceleration Event

As mentioned in section 1.1.1, this event has two categories, all-electric and uncontrolled, the latter meaning that the team has the choice to run in either all-electric, hybrid mode, or all-ICE. Table 4 summarizes the results from the 2007, 2008, and 2009 competitions. Conveniently, the acceleration event was conducted as a shortest time over a straight flat 75 meter course for all competition years.

Unfortunately, not all acceleration runs were recorded during the 2007 competition; however, there is still sufficient data on which we can draw some conclusions. The first point to note is that MHRT2 performed very poorly in the first electric run, this was due to a faulty throttle signal which was promptly remedied for the remainder of the 2008 FH Competition.

⁷ In 2009, fuel allocation were given for the endurance event only, the fuel used for the acceleration and autocross events was not monitored by the competition officials.

⁸ Acceleration event distance is estimated base on 75m length of acceleration course multiplied by the 6 runs allowed for each team.

⁹ Autocross event distance is estimated based on an average course length of 0.7 km multiplied by the 4 runs allowed for each team.

¹⁰ This measure of fuel economy is calculated for the case where a team would perform the minimum amount of distance for each event for which fuel is monitored (i.e. only perform one acceleration run of each type and one autocross run).

Table 4: 2007 and 2008 FH acceleration event competition results.

	2007	2008	2009	
Run #	Electric	Electric	Electric	
1	7.246	11.319	7.375	sec
2	n/r	6.736	9.001	sec
3	n/r	6.210	n/r	sec
4	n/r	n/r	n/r	sec
	Open	Open	Open	
1	7.366	6.777	7.999	sec
2	n/r	6.200	n/r	sec
3	n/r	6.134	n/r	sec
4	n/r	n/r	n/r	sec
	n/r = no record			

Comparing the results from the two categories, we see that neither MHRT1 nor MHRT2 performed significantly better in either category. This fact is due to the ability of the battery to maintain voltage while supplying the high current necessary for an acceleration run. For the 2008 event, the strategy adopted by the team was to alternate between categories while gradually increasing the motor current limit setting of the motor controllers. It is for this reason that we see similar improvement patterns between the two categories. One important fact, which we will see in greater detail in the chapters covering improvement in powertrain performance, is that the improvements observed in the 2008 are small compared to the increases in current limit that the team was imposing. Information about the current limit settings was not recorded; however, the team recalls the settings were increased from about 30% (approximately 110 amps) controller capacity to 70% (approximately 200 amps). For the case of MHRT2, it can be demonstrated that the improvements are only obtained for low vehicle speeds since another factor also governing motor current becomes dominant. The two limitations on motor current will from now on be referred to as the imposed limit, that which is imposed by the controller setting, and the natural limit. These limitations are discussed in detail in section 3.3.2.1.

MHRT2 did perform better in the acceleration event than did MHRT1, since the drive train configurations were virtually identical, the improvement is most likely due to an increased imposed motor current limit.

3.3.1.3 Autocross Event

The only data available for autocross events are the competition lap time results and unfortunately, the course for this event was very different in 2008 compared to 2007. Therefore it is impossible to draw any conclusions from a comparison of the competition autocross event results.

3.3.1.4 Endurance Event

The endurance event was conducted in a very similar manner for all competition years; therefore like the acceleration event, comparison of the competition results can provide some insight into vehicle performance.

The endurance event consists of a 22 kilometer course to be completed in less than 60 minutes total time (26). Each team must have two drivers, each completing 11 kilometers with a maximum time for driver change of 30 minutes. Driver change time is not included in the 60 minutes total time. Charging at stand still during driver change is permitted. Provided in table 5 are the competition results:

Table 5: 2007 and 2008 FH endurance event competition results.

	2007	2008	2009	
Distance	22	22	22	km
Number of Laps	32	40	24	
Lap Distance	0.69	0.55	0.92	km
Time Driver 1	0:27:26	0:16:42	0:28:10	hour:min:sec
Ave. Speed Driver 1	24.1	39.5	23.4	km/h
Time Driver 2	0:27:11	0:17:00	0:25:11	hour:min:sec
Ave. Speed Driver 2	24.3	38.8	26.2	km/h
Penalties	0:00:02	0:00:04	0:00:18	hour:min:sec
Total Time	0:54:39	0:33:45	0:53:39	hour:min:sec
Combined Ave. Speed	24.2	39.2	24.8	km/h

The results clearly show an improvement between 2007 and 2008. This improvement is due to the greater experience with vehicle and therefore greater confidence possessed by the team in 2008. In 2007 the team did not know how much energy per unit of distance the vehicle would

consume on average, and therefore operated the vehicle conservatively to maximize the chances of completing the event. In 2008, the team had invested significantly more time in track testing prior to the competition and therefore had greater experience and knowledge of the vehicle capabilities. This allowed the team to operate the vehicle much more aggressively in 2008. This is a clear case showing how important testing time is to the performance of the team at the competition; a lack of testing time reduces the ability of the team to make proper decisions which lead to a competitive advantage.

Figure 2 shows plots for system voltage and load current as recorded onboard MHRT2 during the 2008 endurance event. A brief description below explains the important features of the plots.

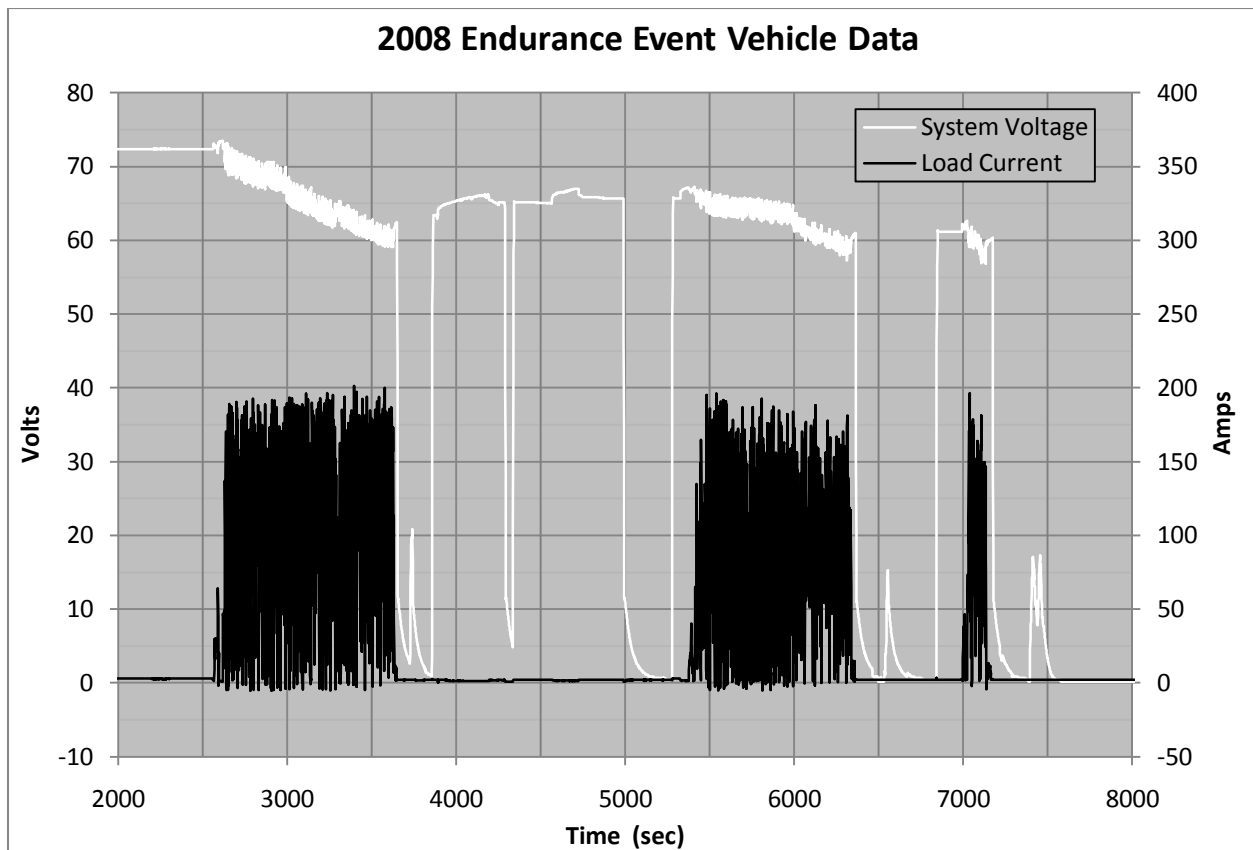


Figure 2: 2008 FH endurance event voltage and current data.

The system voltage refers to the voltage measured at the DC bus of the vehicle while the load current refers to the total current flowing from the bus into the motors controllers (i.e. the product of the system voltage and load current is the electrical power used to propel the vehicle including powertrain losses). Driver A begins just after 2500 seconds and ends near 3600.

B originally begins near 5400 seconds and is pulled of the course 2 laps early by competition officials at 6400 seconds. Driver B returns to the track between 7000 and 7200 seconds to complete the remaining 2 laps. During the break between drivers A and B, we see an approximately 500 second long charge beginning at 3900 seconds and another shorter charge at 4600 seconds lasting approximately 150 seconds, these will be known as charge 1 and charge 2 respectively. Another feature to note is at 3000 seconds and 6000 seconds we see a rapid drop in voltage in conjunction with an increase in the magnitude of the slope; this occurs because at these points the genset was manually shut off by the driver to avoid a possible over heat of the genset. At the end near 7200 seconds the loaded battery pack is at approximately 57 volts while at the beginning it was at approximately 70 volts, these correspond to roughly 90% and 15% state of charge (SOC).

Further on we will see how simulation of the genset and battery together forced to produce the load current can provide significant insight into the area of large potential improvement for the genset.

3.3.2 Optimization Objectives

From the review of the competition data from 2007 and 2008, we can now identify the strengths and weaknesses of the MHRT vehicles. From these we extract the aspects of the drive train on which to focus the effort.

The vehicle strengths are:

- Reliability: the 2007 and 2008 MHRT vehicles completed all required events in a competitive manner.
- Energy efficiency: the 2007 and 2008 MHRT vehicles completed all the required events with excess fuel remaining.

The vehicle weaknesses are:

- The natural tendency for the powertrain to limit the drive motor current and hence power output as the vehicle accelerates to higher speeds as noted in section 2.2.1.2.
- The limited amount of energy supplied by the genset during the endurance event due to over temperature issues.

3.3.2.1 Powertrain Investigation Objectives

The natural tendency for the powertrain to limit its own power output is a perfect case for investigation via modeling and simulation. Not only can the simulations themselves provide valuable insight into the dynamics of the system, but the process of creating the models gives the modeler an in depth understanding of the system components. This understanding assists greatly in understanding the system dynamics. For this reason, the first weakness listed above will be the primary focus of the modeling and simulation investigation of this study. Presented below is a brief description of the operational principle of CVTs and a definition of the guiding theory behind the powertrain improvement strategy.

3.3.2.1.1 Operation Principle of CVTs

A CVT operated by continuously varying the ratio between the input and the output so as to produce the desired torque and speed transfer ratios. The CVT used for the MHRT is a self governing V-Belt and pulley type CVT. The sheaves of each pulley on the CVT can slide along their respective rotating axes which changes the diameter at which the belt rides on each pulley. Typically, each pulley has one fixed sheave and one movable sheave. By changing the diameter of each pulley relative to the other, the transfer ratio is changed. Since the belt cannot change in circumference, one pulley must reduce its diameter as the other increases.

The self governing function of this type of CVT is accomplished using springs, helical interfaces, and centrifugal weights; each produces a force which acts axially on the movable sheaves. Generally, the centrifugal weights produce speed sensitivity while the helical interface produces torque sensitivity. The springs are used as added tuning elements. By changing the mass of the weights, the spring rates, the helical angle, the operation of the CVT can be tuned to achieve various transfer ratio control requirements. In this study, the mass of the weights and the spring rate in the primary pulley are the subjects of interest.

3.3.2.1.2 Definition of Guiding Theory

As noted in section 3.3.1.2, the power limitation of the powertrain exists in two forms, an imposed limit and a natural limit. The imposed limit comes from manually setting the current limit in the motor controllers. The natural limit is a manifestation of the interaction between the components of the powertrain. In effect, the configurations of the CVT and fixed ratio govern the speed relationship between the vehicle rear wheels and the drive motors; for a given wheel speed, two different CVT configurations will most probably not lead to the same motor speed. What is important is that from equations 3 and 4 in section 5.1.2.2, we see that the motor speed is directly related to the backwards electromotive force (BEMF) produced by the permanent magnet motors. If we consider the voltage supplied by the battery to be constant, then the motor equations also show that as the BEMF increases, the amount of current which the constant voltage can push through the motor armature is reduced. This limitation of armature current as the motor speed increases is the natural limiting effect of the powertrain. In reality, this effect is magnified since the battery voltage decreases as the discharge current increases; this is shown by equations 1 and 2 in section 5.1.1. The natural limiting effect is demonstrated using recorded data in figure 3. The two sets of plots shown in figure 3 represent the motor current and vehicle speed for the same powertrain performing two separate acceleration runs. Each run is performed with the identical configuration except for different imposed current limits; 110 and 200 amps. As the data shows, the imposed limit is the dominant factor but only up to a certain speed, after which, the natural limit becomes the dominant factor. The imposed limit is the dominant factor at low vehicle speeds because the BEMF of the motors is small enough such that the battery is capable of pushing current up to and beyond the imposed limit. As the vehicle and motors accelerate, the natural limiting effect of the BEMF takes over. Therefore, to achieve the objective of mitigating the natural limit of the powertrain, we will need to lower the speed of the motors relative to the speed of the vehicle. Fortunately, the CVT is the ideal device to regulate the operating speed of prime movers relative to load speed. In section 5.2.1, figure 36 shows model output for maximum torque for two powertrains with different CVTs, this demonstrates how we can change the power availability simply by changing the CVT configuration. It is also important to note that simply lowering the speed arbitrarily may have negative affects with respect to both power output and reliability of the system. Careful attention to all details simultaneously, is therefore necessary for this investigation.

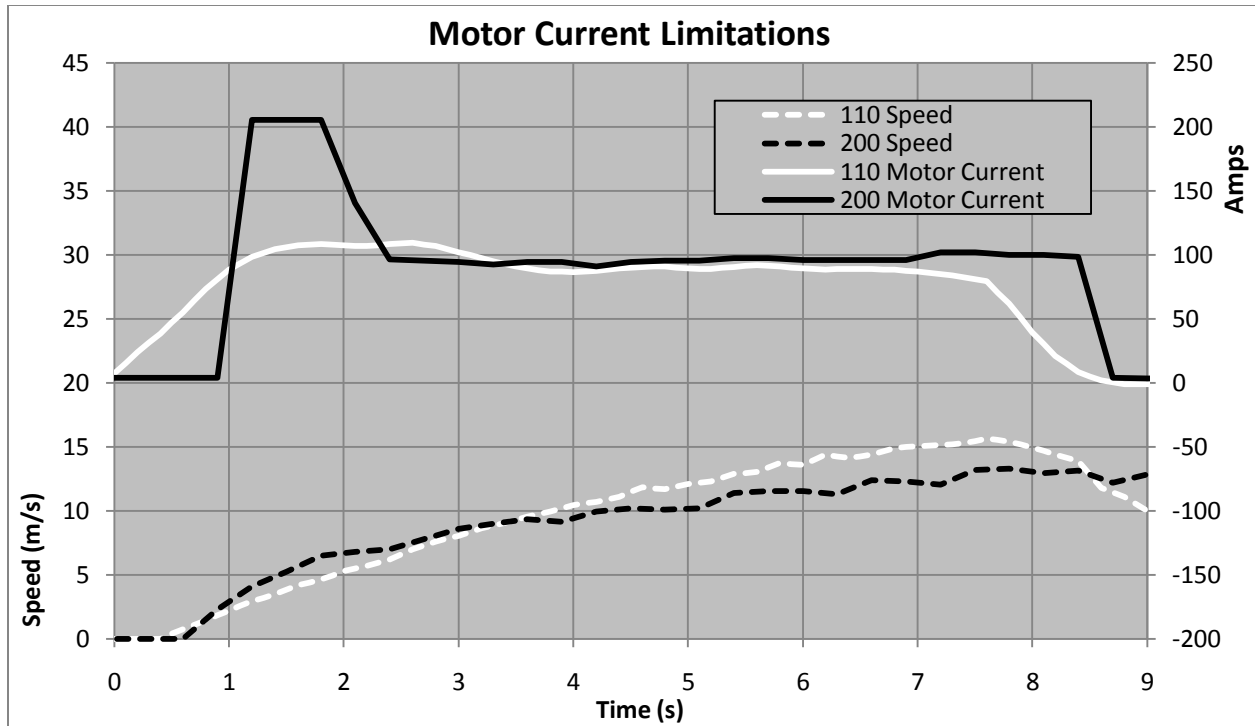


Figure 3: Demonstration of the natural limiting effect of the powertrain.

3.3.2.2 Genset Investigation Objectives

Using models to predict failures and failure modes of complex components is a difficult task requiring significant confidence in the predictive ability of the models. As we will see later on, developing parameterized thermal models for electric motors is quite difficult. Although an attempt is made, and some conclusions drawn, the confidence in the model is not sufficient to employ modeling and simulation as the sole strategy to mitigate the thermal issues with the genset. For this reason, the second weakness listed above will be investigated using the simulation capabilities developed here; however, the simulations will not be used to mitigate the thermal issues themselves, but rather to determine how to allocate resources dedicated for genset improvement. To do this, we will investigate how other possible modifications influencing the energy supplied by the genset compare to the potential increase in energy that can be achieved by a total mitigation of the thermal issues. These results can help place priority on which modifications to focus on in order to maximize the energy supplied by the genset.

The following sections describe what options are available with respect to the powertrain and genset which can be explored in order to achieve the goal.

3.3.3 Aspects of Powertrain to be Considered

Here we identify all the components of the drive train which are to be considered as modifiable to accomplish the specific objectives as described above. Note, as mentioned previously, alternatives to the components which are currently used for the drive train are not considered. The components which are considered to be modifiable for the powertrain and genset investigations are listed and explained in the sections 3.3.3.1 and 3.3.3.2 respectively. Some components will be considered as non-modifiable for certain reasons; these components will remain non-modifiable for both investigations. The components which are considered non-modifiable are:

- Battery Pack: the battery pack specifications of 65 V nominal and 45 Ah are constant.
- Controllers: the current limit setting on the motor controller is fixed at 200 amps. Since the car has two drive motors and controllers, this equates to a maximum load current of 400 amps. This limit reflects the current carrying capacity of the high power conductors used for all MHRT vehicles.
- Perm PMG drive motors: the drive motors are non-modifiable by design.
- The CVT DriveN (secondary) Pulley: the DriveN pulley is considered as non-modifiable for this investigation. It is possible to modify the torque response characteristics of the CVT by changing the spring in the secondary pulley; however, this option was not considered and the DriveN pulley was left in its stock configuration.
- Half Shafts: the shafts connecting the wheels to the output of the fixed ratio are non-modifiable since this component is constrained by the physical design of the vehicle.
- The wheels and tires: the wheels and tires are considered non-modifiable for this investigation as a requirement of the MHRT.

3.3.3.1 Powertrain Investigation

The components considered as modifiable for the powertrain investigation are:

- The CVT DriveR (primary) Pulley: the DriveR pulley has two modifiable parameters: the mass of the centrifugal weights, and the compression characteristics of the spring.
- The Fixed Ratio: the fixed ratio is modifiable.

For each of the components considered to be modifiable, there are a limited number of parameters which can be varied as well as a limit on the extent to which these parameters can be varied. These limits are discussed here.

The DriveR pulley is directly driven by the drive motor. This pulley has two modifiable parameters which both influence the operational characteristics of the CVT. The DriveR pulley uses a set of centrifugal weights and a spring which interact with each other to govern the relationship between the DriveR pulley rotational velocity and the CVT ratio. The SAE publication (37) provides an in depth explanation of the dynamics of CVTs and how the weights and spring influence the CVT operation. The spring and weights can be interchanged with other springs and weights of different functional value supplied by the CVT manufacturer. Table 6 contains the chosen set from the available options:

Table 6: CVT weights and springs used for the powertrain investigation.

Weights		Springs	
275	g	12.2	N/mm
400	g	18.1	N/mm

The original configuration of MHRT2 used 275 gram weights and an 18.1 N/mm spring. To decrease the speed of the motor it is necessary to either increase the mass of the weights, decrease the stiffness of the spring, or both. For this reason, only heavier weights and softer springs than those used for MHRT2 were chosen. As described in section 5.1.4.3, the chosen weights and springs can be mixed and matched to form four CVT configurations.

The fixed ratio is a roller chain reduction. The practical limits imposed on the variation of the ratio are due to the size constraints of the large and small sprockets. The smallest sprocket available which suits the application is twelve teeth while the largest sprocket which can fit inside the available space is sixty teeth. The fixed ratio used on both the MHRT1 and MHRT2 was a 3.75 reduction with twelve and forty-five tooth sprockets.

The sprockets and ratios chosen for this study are provided in table 7:

Table 7: Fixed ratios selected for the powertrain investigation.

Ratio	Small Sprocket	Large Sprocket
5	12	60
4.62	13	60
4.29	14	60
3.75	12	45
3.46	13	45
3.21	14	45

Between the four possible CVT configurations, and the six ratios chosen for the investigation, a total of twenty-four possibilities exist. All twenty-four will be included in the powertrain investigation.

3.3.3.2 Genset Investigation

The components considered as modifiable for the genset investigation are:

1. Engine throttle governing mechanism
2. Transmission ratio between the engine and generator

The engine throttle has in the past been governed by the manufacturer mechanical governor which directly governs the throttle based on engine speed. Alternatives to this mechanism will be introduced and investigated to gauge their ability to increase the energy supplied by the genset. The effect of these alternatives will be compared to the effect of mitigating the thermal issues. The limits imposed are those of practicality (i.e. systems that are impossible to make or relatively high in complexity are not considered).

In the past the transmission ratio has been a 1:1 ratio using a direct shaft to shaft coupler. Here, the variation of this ratio is investigated and the effects compared to that of total mitigation of the thermal issues. The limit set on variation of this ratio is a practical one similar to that set on the fixed ratio for the powertrain investigation.

3.4 Chapter Conclusion

Sections 3.3.2.1 and 3.3.2.2 together provide detailed descriptions of the areas of the drive train where significant improvement is possible. We can elaborate on objectives 1 and 2 by defining specific objectives as follows:

1. Mitigate the natural power limitation of the powertrain without compromising the vehicle reliability during an FH endurance event.
2. Determine how best to allocate resources devoted to genset improvement.

Clearly defined specific objectives provide the necessary information required to develop an appropriate methodology to achieve the goal.

4 Methodology and Instrumentation

Chapter 4 describes methodology developed to achieve the objectives. Included in this chapter is a detailed description of the data sets used in the creation and validation of the vehicle and component models. Tools and instrumentation used to gather data are documented as well.

4.1 Methodology

Modeling and simulation of complex systems and their interacting components implies the use of computer software due to the vast amount of computations required. The selection of the software used for any modeling and simulation endeavor requires detailed description of the problem in order to ensure that the software possesses all the capabilities necessary to solve the problem. The specific problem stated above is one of powertrain optimization for a race vehicle. There are many commercially available software packages which are capable of performing high fidelity powertrain simulations for optimization purposes (38); however, upon closer inspection, these software packages do not exactly fit the criteria derived from the problem statement. Extensive research has shown that all currently available powertrain simulation software packages perform powertrain simulations based on a fixed drive cycle input¹¹. This means that if the model has shown to have sufficient power available to match the speeds and accelerations of a given fixed drive cycle, any modifications made to the model which would in theory increase the vehicle's ability to accelerate, and/or reach higher top speeds, will not produce different results. The results will be identical since the model will follow the fixed drive cycle in both cases, before and after modifications. Therefore, since the goal of this work is to optimize the performance of a race car, the model must be capable of capturing the effect of increased power availability on the lap time of the vehicle for a given race track. This means that rather than simulating a vehicle and powertrain which are required to follow a fixed drive cycle, the vehicle and race track must be simulated in order to determine whether an increase in power is actually beneficial with regards to lap time. For the specific case of the McGill hybrid vehicle, there are many factors which must be monitored, and the results of these compiled to determine whether

¹¹ A fixed drive cycle as defined here is at minimum a vehicle velocity schedule, or worded differently, a speed requirement over time. Many standardized drive cycles exist today for the purpose of comparing production vehicles.

overall improvement has been achieved. These factors include, but are not limited to, lap time, state of charge of the battery, acceleration performance, drivability, thermal effects of various components, and efficiencies at the system and sub-system levels. This concept of comparing the benefits of improved lap times versus the possible negative effects on the components of the vehicle is the primary objective of the software, model, and simulations. The remainder of this section is devoted to exploring the options available for performing such simulations and describing the final selection.

4.1.1 Software Description

In the world of powertrain simulation software, there are two dominant architectures: forward facing models and backward facing models. A detailed description and comparison of these is provided in the report “AVPRnet Simulation Infrastructure” produced for the Transportation Development Center of Transport Canada by McGill University (38). Most relevant to this study, the report identifies the ability of forward facing models to capture the real world limitations of the components of a powertrain. Forward facing models accomplish this by having information flowing in two directions, from the driver through the drive train to the road, back from the road to the driver. This in turn produces one or more feedback loops which mimic the natural feedback loop interactions of real systems (39). For this study, this ability is an absolute necessity since the objective of the powertrain investigation is to mitigate the natural tendency of the powertrain to limit the power output of the motors. For this reason, forward facing architecture is a requirement imposed at all levels of system modeling.

Forward facing simulations made to simulate a vehicle on a track are typically known as driver-in-the-loop since a human is put in control of the vehicle inputs (i.e. steering, throttle, and brakes). Using a graphical display showing the simulation output, the driver is able to control the vehicle as it progresses around the track. Clearly there are two flows of information occurring in such a system, one from the driver to the model, and one from the model back to the driver.

Fortunately, due to a large worldwide community of virtual automobile racing, software which is capable of simulating a vehicle and track in a forward facing manner exists in abundance. Currently available automobile racing simulators developed by both private groups and open-source communities have received equal if not greater resources devoted to simulation fidelity

compared to commercially available powertrain simulation software. However, the powertrain architectures of these racing simulators are virtually all limited to conventional powertrains¹². To date, only one software package, rFactor Pro (9), claims to have the ability to perform driver-in-the-loop simulations for any powertrain architecture desired. This ability is achieved through the coupling of the well known racing simulator rFactor (40), with the widely used graphical coding simulation software, MATLAB Simulink (41). This coupling allows the user to replace the conventional powertrain model of rFactor, with any powertrain which can be modeled in Simulink (9). Unfortunately, neither private nor academic licenses for rFactor Pro are available which means that in order to develop driver-in-the-loop simulation capabilities for the MHRT, the next logical option is to investigate the possibility of combining the capabilities of a racing simulator, with those of a powertrain simulator. There are two methods to accomplish this with of two software packages, directly or indirectly.

1. Directly implies coupling via communication patch develop specifically for the purpose which allows the two software to communicate in real time.
2. Indirectly implies operating the two software packages in a step by step fashion using the saved output of one, as the input to the other.

Direct coupling is effectively what rFactor Pro does with rFactor and Simulink; a real time communication link is setup between the two software packages and multi-channel data flows seamlessly, from one to the other, and back again.

Due to the amount of in depth knowledge of racing simulators required to accomplish either method, the cooperation of an existing racing simulator development group was sought. The team from Exotypos, the developers of X Motor Racing (XMR) (42), showed the greatest amount of enthusiasm for the project, and since the XMR simulator physics are highly user configurable, XMR is the logical choice. The Exotypos team agreed that in exchange for the right to include the MHRT vehicle in the official version of XMR, they would provide, within available resources, the technical assistance to modify the XMR simulator for the needs of this study.

¹² Conventional powertrains are those employing an internal combustion engine coupled with mechanical clutches and transmissions.

The following modifications to the official release of XMR were performed:

1. A physical model of MHRT2 was created. This included the creation of the suspension and chassis geometry. In addition, a three-dimensional visual representation of MHRT2 was created. The parameters affecting the performance of the vehicle, such as mass, peak power, tire grip, etc., are input by the user with the assistance of the XMR Vehicle Physics software provided with the simulator software.
2. A physical model of the 2008 Formula Hybrid Competition endurance event race track was created. This model was created to the specification of the MHRT. The model included cones placed to identify the course of the 2008 event, and a start/new lap line for data acquisition within the racing simulator.
3. A data output feature capable of saving all desired data to external files was created. The format of the data was defined by the MHRT.

The option of creating a direct patch between XMR and other software was investigated but later dropped due to the limited resources and time available. Therefore, using the modified version of XMR, the indirect approach was taken.

The software chosen to simulate the powertrain is MATLAB Simulink. Simulink forms the backbone of several commercially available powertrain simulation software packages (43), and as mentioned above, Simulink is used effectively with rFactor Pro for a similar application as intended here. The versatility provided by Simulink makes it a popular choice in the field of powertrain simulation.

4.1.2 Software Operation

Figure 4 is a block diagram representing functionality of the XMR simulator, note the forward facing architecture.

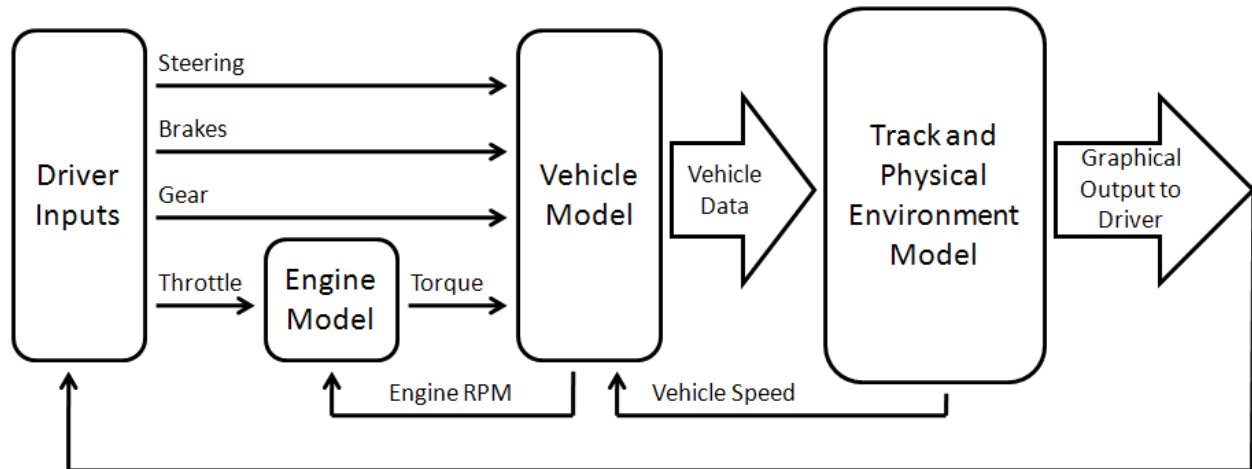


Figure 4: Block diagram for the XMR simulator.

The driver inputs consist of a steering wheel and pedal set which together form the user interface for a personal computer. The vehicle, engine, and physical environment models represent the XMR software. The vehicle and engine models are almost completely user configurable using the Vehicle Physics software supplied with the XMR software. Here, the engine model has been shown separately from the vehicle model since this is the main focus of this study. For the purpose of this study, all vehicle parameters excluding the engine model torque curve were tuned to acceptable values, and then held constant for conduct of each trail set. The two sets of trails performed with XMR are outlined in detail the section 6.2.1. The model parameters, and track definition details are discussed in section 5.2.

Figure 5 is a block diagram of the Simulink model developed for the study; again note the forward facing architecture.

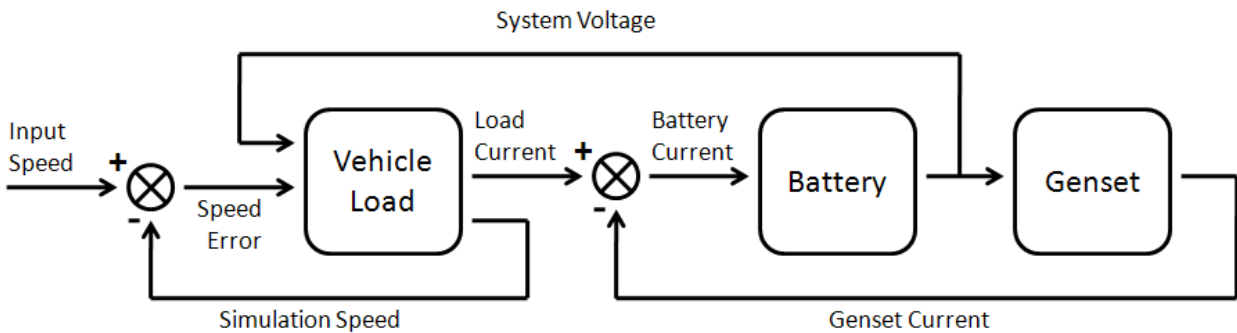


Figure 5: Block diagram of Simulink model.

This model is setup to accept a fixed drive cycle as its input. Using this input, the driver model controls the vehicle model such that it follows the drive cycle as closely as the model restrictions will allow.

The indirect methodology proposed for the XMR and Simulink models described above is illustrated in figure 6:

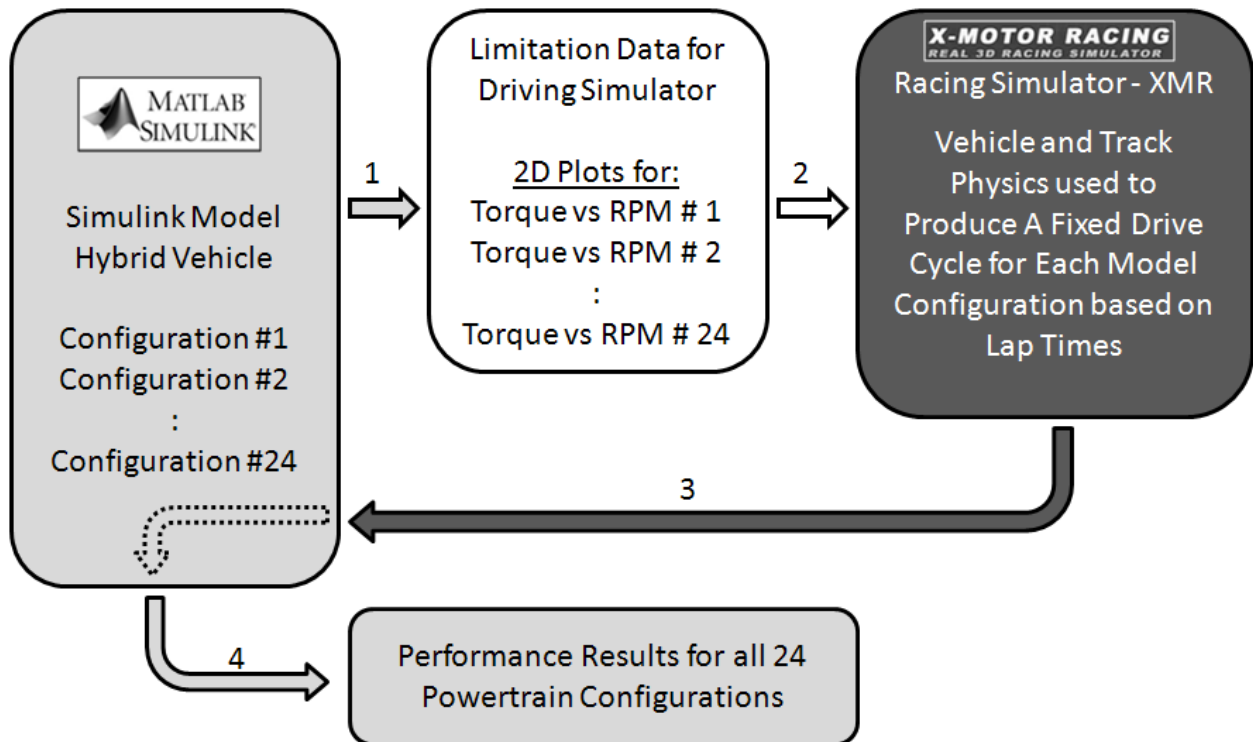


Figure 6: Flow Chart illustrating indirect driver-in-the-loop simulation method.

The methodology illustrated by the flow chart is described in detail here:

- Step 1. The Simulink model is used to produce maximum torque curves for each powertrain configuration which can be input into the racing simulator. These curves must have the format typical of maximum torque curves for an engine since this is information used by the XMR simulator for its engine model. With reference to figure 1, the curves are produced for the output of the CVT (DriveN pulley); this method effectively packages the battery, controller, motor, and CVT as one unit providing a single curve relating the maximum torque available at the CVT output to the RPM (revolutions per minute) at the CVT output. As such, one can see how packaging these components all into one unit creates a simplified “engine model” capable of recreating the imposed and natural limits of the given powertrain configuration. These curves are produced by bypassing the driver block in the Simulink model, and directly feeding in a full throttle signal to the vehicle model. Allowing the model to accelerate from zero velocity to its maximum velocity while recording the torque produced at the CVT output and the RPM of the CVT output, provides the necessary information to formulate the torque-RPM curves required for the XMR model.
- Step 2. The torque-RPM curves are input into the XMR model one at a time. For each torque curve (or powertrain configuration), the vehicle is driven around the defined track for a sufficient number of laps until the driver feels that he/she cannot make better average lap times. As described in section 6.2.1, the order in which the configurations are driven is not held constant to reduce the influence of driver improvement on the lap times. The results of these trails can be used to compare the different configurations based on lap time.
- Step 3. The lap times, and the instantaneous vehicle forward velocity sampled at 10 Hz, are recorded for each configuration and used to create fixed drive cycles representing a full SAE Formula Hybrid endurance event. A drive cycle (or velocity schedule) is created by repeating the fastest three laps until the vehicle has covered approximately 11 km, then 20 minutes of dead time representing driver change time is inserted for charging purposes, and following the driver change the 11 km section

is repeated. Note that this cycle reflects the data recorded for the 2008 endurance event shown in figure 2.

- Step 4. The Simulink model is run for each fixed drive cycle created. This produces the simulation prediction for how the given powertrain configuration performs during an endurance event. These results can be compared to see how the different configurations performed with respect to important factors such as SOC depletion, drive motor temperature, etc.

To compile the information provided by the XMR and Simulink simulations, a weighted decision matrix is used to rank the powertrain configurations against a set of selected criteria. These criteria are: acceleration time, lap time, final SOC value, and the average motor temperature as seen during sustained driving. The weights assigned to the criteria are effectively a judgment decision made by the designer(s) of the MHRT vehicles. The individual assignment of weights to the criteria determines the importance that the designer feels the criteria has on the success of the vehicle in the FH dynamic events. Since assigning the weightings is based on judgment, 4 top members of the MHRT including the author each provide a weighting scheme. The decision matrix will be evaluated for each scheme to see how sensitive the outcome is to different weighting schemes. The decision matrix, also known as a Pugh's Matrix, is a typical mechanical engineering design process. The decision matrix process is documented in (44), (45) (46).

4.2 Instrumentation and Data Sets

Data on which all the work here is based was acquired from MHRT2, MHRT3, and their individual components. Data from MHRT3 is used only of comparison of the model predictions and is not used for development of the models themselves. This section describes the data sets, and if possible, the equipment used in gathering the data. The following list briefly describes the data acquisition equipment:

- Equip. A. Isaac Data Acquisition System – The V7 Pro from Isaac Instruments is a general purpose reconfigurable data acquisition system. The system consists of a central recorder with interchangeable peripheral sensors (47).
- Equip. B. VERT Project Dynamometer – The dynamometer is equipped with an AC induction motor and a two-way power flow drive/regenerative unit which is

connected to grid power. The dynamometer table is reconfigurable and capable of accommodating the PMG motor and CVT. Torque and RPM data are provided by a non-contact type sensor from S. Himmelstein & Co.

Equip. C. Multi-meters and current clamps.

Equip. D. Scale – A&D GF-3000 Precision Balance. The scale range is between 3100g and 0.5 g with a repeatability of 0.01g.

Equip. E. Custom Data acquisition system developed by MHRT for the 2009 competition.

The equipment listed here may be referred to using the abbreviated list index, for example the Isaac system may be referred to as Equip. A.

4.2.1 Data Sets

Below is the list of data sets used for this study; these data sets will be referred to using their respective index:

Data Set 1. Formula Hybrid 2008 Endurance Event Data

Data Set 2. VERT Project Summer 2007 Data

Data Set 3. May 12th, 2008 Test Day Data – MHRT2

Data Set 4. June 13th, 2009 Validation Data – MHRT3

Data Set 5. CVT Dynamometer Data

Data Set 6. PMG Dynamometer Data

Data Set 7. Genset Fuel Consumption Data

Data Set 8. Electric Snowmobile Data

Data Set 9. Manufacturer Data

Data Set 10. Formula SAE Tire Testing Consortium Data

Data Set 11. Formula Hybrid 2009 Endurance Event Data

Data Set 12. Genset Thermal Testing Data

All component models were created and validated using data from at least one of these sets. It will be clearly stated which set was employed for each task in the sections describing the individual models. Provided here is a description of each set and their limitations. Due to the unfortunate poor operating condition of MHRT3 during the 2009 FH competition, the majority of the data recorded cannot be used productively for this study.

Data Set 1

Data for the 2008 Formula Hybrid competition endurance event was recorded using Equip. A. Figure 2 is a sample of this data.

The limitations of this data are:

- The GPS speed data is not sufficiently accurate to formulate an endurance event drive cycle.
- The wheel RPM sensor was improperly configured such that no data for wheel RPM was recorded.
- Controller throttle position was not recorded; therefore this data cannot be used as an input for a full vehicle model.
- No fuel flow data.

Data Set 2

Over the course of the summer of 2007, the VERT Project conducted many experiments with components of MHRT1 in an effort to develop computer models for these components. Experiments were conducted to explore the operation of the motor controllers, the motors, the genset, and the batteries. Equip. A, Equip. B, and Equip. C, were used to gather this data. The limitations of this data are:

- The batteries modeled by the VERT Project were not the lithium-ion batteries used for the MHRT vehicles.
- The genset data did not include fuel flow data.
- The motor data did not include thermal data.

Data Set 3

Following the 2008 FH competition, MHRT2 was taken to an open parking lot for testing. Included in these tests were several coast downs from top speed and two tests where the vehicle was operated under genset power only. Equip. A was used to gather the data. The limitations of this data are:

- No left wheel RPM sensor.
- CVT configuration was not changed.

Data Set 4

Following the 2009 FH competition, MHRT3 was taken to an open parking lot for a series tests. These tests were aimed at gathering information on vehicle performance for different CVT configurations. A 75 m acceleration course and an auto cross course were setup to gather data from the vehicle while operating under similar conditions as would be expected during an FH competition. CVT setups 1, 2, and 4 were all tested with a fixed ratio of 3.75. This data was recorded using Equip. E. The limitations of this data are:

- Several times the vehicle's main DC bus lost power causing the data for that session to be lost. Unfortunately, time did allow for all lost data to be recreated. Autocross type data for CVT setups 1 and 4 is limited compared to CVT2.
- No fuel flow data.

Data Set 5

Data required to formulate data tables for CVT models was gathered using Equip. B and Equip. C. This data was obtained by using a PMG and an AXE controller to drive the CVT as they do in the vehicle. Battery power was provided by the MHRT pack. The output of the CVT, the DriveN pulley, was connected to the dynamometer. Tabulated data for motor voltage and CVT output torque was taken by: 1) fixing the output speed of the CVT using the dynamometer and 2) fixing the motor current using the controller throttle. The equations used to model the motor, equations 1 and 2, were used to transform the recorded motor voltage and current into CVT input speed and torque. Limitations to this data are:

- For CVT DriveN speed between 600 and 1000 RPM, high torque transfer tended to cause large fluctuations in the CVT ratio which in turn, caused large scatter in output data. No usable data could be gathered for high output torque in this speed range.
- The precision of Equip. C for these tests was insufficient. Motor voltage requires 3 or 4 very reliable significant digits, Equip. C provided 2.

- Motor current is difficult to keep fixed due to the dynamic interaction of the battery and load.
- Maximum torque and power transfer capabilities of the CVT could not be attained for speeds above approximately 1000 RPM due to limited power available from the electric drive train.

Data Set 6

The PMG 132 was connected directly to the dynamometer and tested in both generating and motoring regimes. Data intended for the functional model as well as the thermal model was gathered using Equip. B, Equip. C, and Equip. E. The main limitation of this data is the fidelity of the thermal model. Limited resources and time did not allow for sufficient tests to be performed.

Data Set 7

Data for the fuel consumption of the genset was gathered using Equip. C and Equip. D. The test was performed by having the genset charge the battery at constant current for different values of current and voltage. The full voltage range was covered by beginning the test with a completely empty battery and conducting test until the BMS would no longer allow charging. Tests were performed for a set amount of time and the total mass of fuel removed from the tank was recorded using Equip. D. During these tests the voltage and current output from the genset was recorded using Equip. C. This data is limited with respect to the variation of the engine throttle; only one test was performed at approximately 75% throttle while all other tests the throttle was close to 100%.

Data Set 8

Data taken from testing of an electric snowmobile prototype using the same cells as the MHRT vehicles was used in the development of the battery model. This data was recorded using Equip.

A. The limitations of this data are:

- The data does not extend into areas of low SOC.
- Discharge current remains below 150 A.
- Charge current remains below 20 A.

Data Set 9

Manufacturer data is available for most of the components used for the MHRT powertrain. Data such as engine torque curves, PMG armature parameters, and battery cell parameters have proven to be very useful in the development of the models. Clearly this data is limited by that which is supplied by the manufacturer, not all manufacturers provide the data required.

Data Set 10

The Formula SAE (FSAE) Tire Testing Consortium produces tire performance data for FSAE style tires. The data provides correlations between longitudinal/lateral forces exerted by the tire for a set of varying tire parameters such as slip angle, slip ratio, camber, and ventricle load. This data is limited to small ranges and/or few data points for some parameters (48).

Data Set 11

During the majority of the 2009 FH competition, MHRT3 suffered from numerous technical difficulties. Due to these difficulties, the available data cannot be used productively for the majority this study. However, unlike the 2008 endurance event data, the RPM sensors on the wheels were operational and for a few laps out of 24, MHRT3 managed to produce competitive lap times. This data is useful for a statistical comparison of vehicle velocity with that of other data and simulations.

Data Set 12

Following the implementation of the decisions made by the MHRT regarding the genset, thermal testing was conducted to validate that the solution was in fact reliable. This data includes temperature channels for three points on the genset and one for ambient temperature.

4.3 Chapter Conclusion

The methodology described above determines the work involved to accomplish the objectives of this study. First, data to develop and validate both the XMR and Simulink models must be acquired. Second, models must then be developed and validated. Validation of the models requires that a minimum of one cycle of the method must be completed for the powertrain configuration for which the largest amount of field data exists. As we will see, the configuration for which there is the most data is the configuration used for the 2008 Formula Hybrid competition.

For the powertrain investigation, cycles of the method illustrated in figure 6 must be conducted for each powertrain configuration as outlined in section 3.3.3.1. Once completed, the data acquired must be analyzed and a suggestion made regarding the configurations with the greatest potential.

For the genset investigation, the genset model can either be used alone, or with the rest of the vehicle to investigate the gains of various possible improvements. A discussion of these results and suggestions made for the 2009 MHRT design together complete this investigation.

All data used for development and validation of models as well as subsequent comparison of model prediction is presented and described in section 4.2.

A discussion of the outcome of each investigation and comparisons of the predictions with data acquired from a subsequent prototype form the conclusion of the main objectives. Finally, suggestions for future work and areas of improvement conclude the study as a whole. The following chapters present in detail the work outlined here.

5 Modeling and Validation of the MHRT Vehicle

This chapter describes in detail the development and validation of all models created for this study. In (49), the following definition of model validation is provided:

“To produce credible simulation results the simulated environment must be realistic and validated using accepted practices. Model validation should be performed at the lowest level that can be supported by test data in addition to the vehicle level to build confidence that the models can be used for vehicles other than the specific one(s) used for validation.

Confidence in a model should be based on the accuracy of the model relative to test data, and the repeatability of the test data should be considered as well. For example, if a model yields results with 3% error versus test data, then conclusions from simulations can only be made when differences are greater than 3%. However, if system response data exhibits a repeatability of only 5%, then the validation error is at least 5%.”

The concept and process of validation as described in the quote above is maintained throughout this study. Statistical analyses of the validations are provided to give insight into the model performances; however, as noted by (49), due the unavailability of test data this is not always possible.

There are no concrete criteria applied to the performance of the models since it may prove to be beyond the scope of this study to create all system and component models which attain some predefined level of accuracy. The criteria are applied suggestively in order to avoid the situation where time and resources devoted to a given model impede the completion of the study within the required timeframe. Applying the criteria in a suggestive manner means that if a model satisfies the criteria it is considered sufficient for the needs of the study; however, if an initial attempt at a model does not satisfy the criteria, additional resources are devoted to improve the model performance. The criteria applied to the models are provided in table 8:

Table 8: Performance criteria for models.

Model Level	Average Value of the Percent Error
System Model Signals	10%
Component Model Signals	5%

System level validation criteria in the literature are typically in the range of 5% average error (39), (50). These criteria however are only applied to final values of energy consumption trackers (i.e. integrated signals such as SOC, Overall Fuel Economy, etc.); these signals do not demonstrate high frequency fluctuations during vehicle operation when compared to signals such as electrical currents and mechanical torques. The criteria provided in table 8 reflect the fact that in this study the criteria will be applied to model signals which typically demonstrate greater average error than integrated signals. As we will see, the error demonstrated by the energy tracking signals in this study satisfies the commonly applied 5% criteria.

There are two system models, the Simulink full system model and the XMR model. Component models will only be referred to in the Simulink model since the ability to test components of the XMR model is not available. Component models refer to the battery model, the CVT model, the motor model, energy system model, genset model, etc.

5.1 Modeling of Vehicle System and Components in Simulink

The diagram in figure 7 shows the hierarchy of the model and sub-systems. This structure is categorized into 4 levels: level 1 is the System Model; level 2 models are the driver, vehicle load, battery, and genset; level 3 models are those contained within the level 2 models; and level 4 model are those contained within level 3 model (i.e. the drag load model is level 4).

Figure 8 depicts a block diagram of level 1, note the forward facing architecture. Since the throttle signal can never be larger than unity, a constant input speed which is larger than the maximum capabilities of the simulation leads to a constant speed error equal to the difference between the capabilities of the simulation and the input speed. This is one example of how forward facing models capture the natural limits of systems and their individual components.

This structure of a vehicle system model is typical of currently available advanced vehicle simulation software such as PSAT, and AVL CRUISE (38). There is no output shown for the structure since the output depends on which aspects of the vehicle are under investigation. For example, if the battery SOC is the parameter of interest, then an output would be indicated at the battery block.

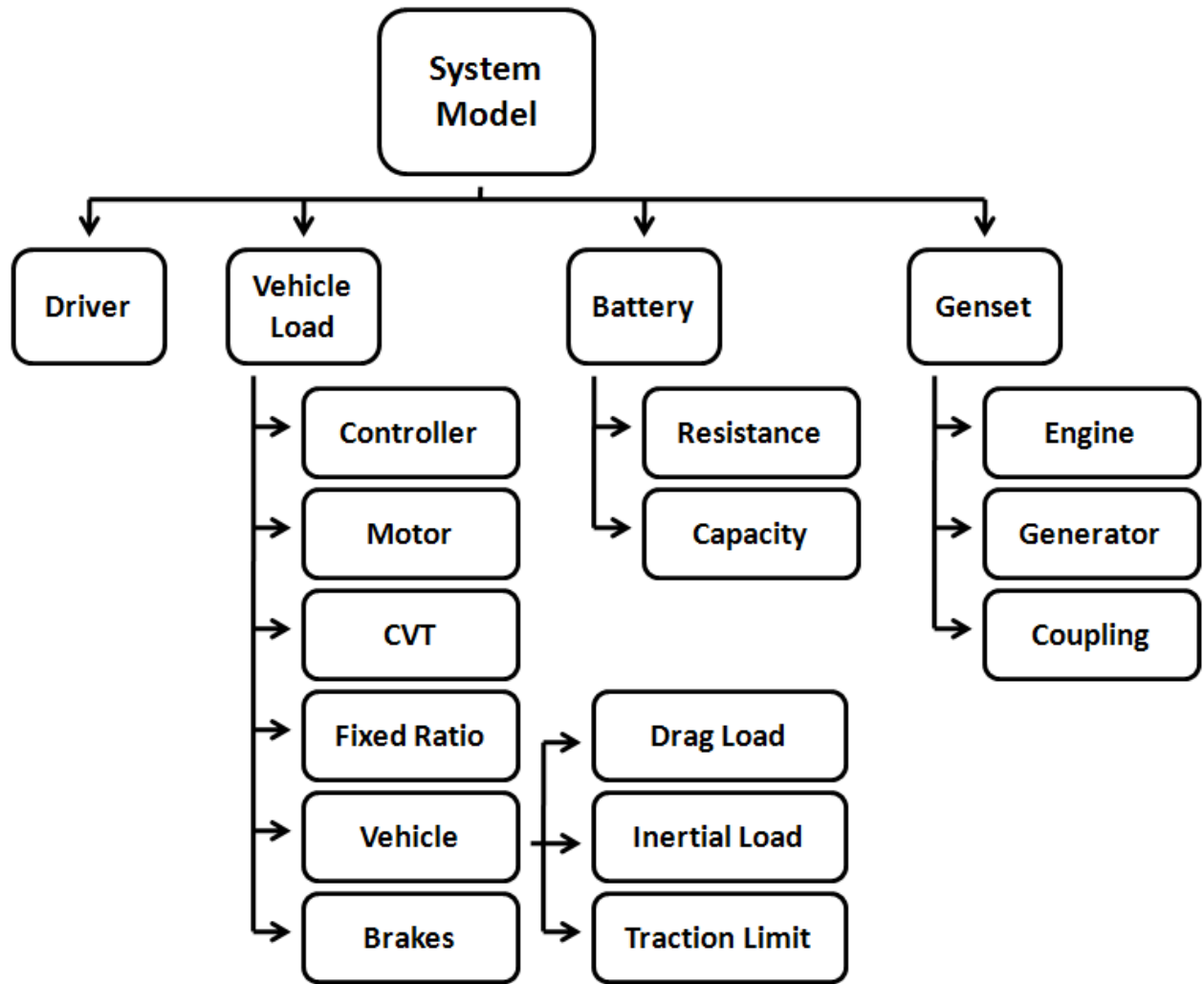


Figure 7: Model sub-system hierarchy.

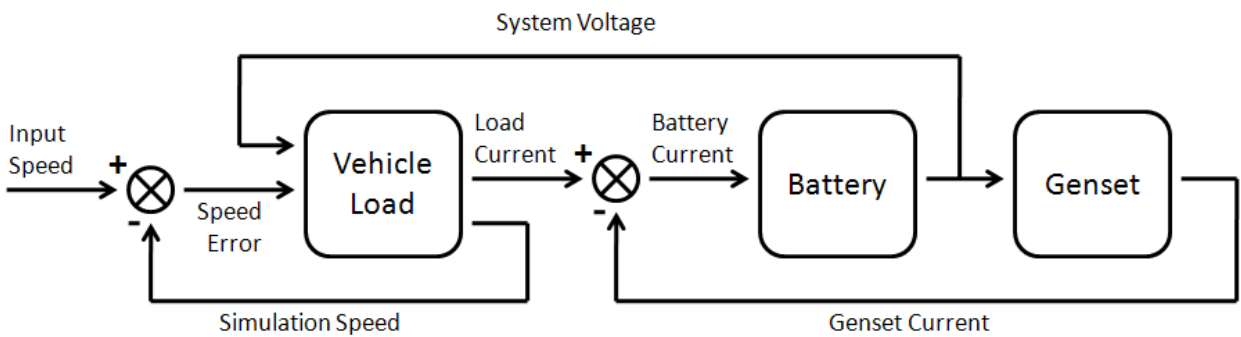


Figure 8: System Model, level 1 in the hierarchy diagram.

All Simulink simulations are run with fixed time step of 0.01 seconds using the “ode3 (Bogacki-Shamane)” solver. Data recorded from the models is sampled at 10 Hertz.

5.1.1 Battery Model

In the field of battery modeling there exist many different basic theories on which to base a battery model (51). These theories vary from simple and basic in nature to complex. The simpler models are typically based on data tables created using experimental data while some more complex models are based on the fundamental chemistry of the cells. Each has its advantages and disadvantages in terms of model fidelity and effort of creation. Some examples from (51) are:

- Resistive
- Series Resistive Capacitive
- Parallel Resistive Capacitive

The resistive type is chosen for the initial attempt. The resistive model functions by using the current demand over time to: 1) keep track of the energy removed or added to the battery over time, and 2) to estimate the instantaneous voltage drop at the battery terminals produced by the current demand. In doing so, the model is able to estimate the instantaneous terminal voltage of the battery for any given current input. This type of battery model is outlined in detail in both (28) and (51). The model can be represented by equations 1 and 2.

$$V_{TERM} = V_{OC} - I_{BATT} \times R_{INT} \quad Eqtn. 1$$

- V_{TERM} is the voltage as measured at the terminals of the battery.
- V_{OC} is the open circuit voltage measured at the terminals of the unloaded battery.
- I_{BATT} is the current flowing through the battery. This current is positive for discharging and negative for charging.
- R_{INT} is the parameter used to relate the change in terminal voltage due to the current flowing through the battery. The parameter is known as the internal resistance.

$$V_{OC} = V_{OC}(SOC) \times \left(SOC_{INIT} - C_{CAP} \times \int_0^t I_{BATT} dt \right) \quad Eqtn. 2$$

- $V_{OC}(SOC)$ is a function or table relating the open circuit voltage to the state of charge (SOC) of the battery. The table used for this study is provided in appendix 2.
- SOC_{INIT} is the initial SOC of the battery.
- C_{CAP} is the constant defining the capacity of the battery. The value used here is 45 Ah (34).

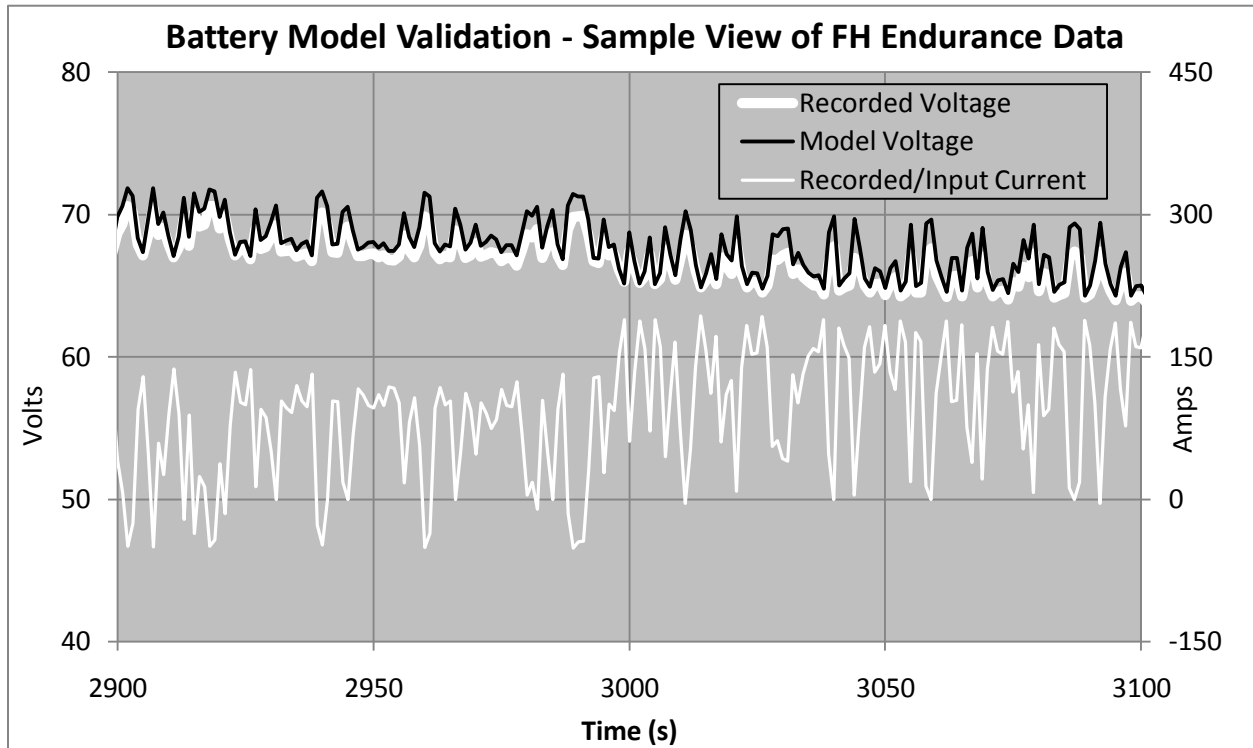


Figure 9: Battery model validation against FH 2008 endurance event data.

Figure 9 depicts a graph of the battery model voltage output super-imposed on the voltage data from the 2008 FH endurance event. The recorded voltage and current in figure 9 are the same as shown in figure 2; however, the view in figure 9 shows only a sample so that we can see clearly how the model follows the recorded voltage. The sample view shows a 200 second window approximately centered at the point when Driver A turns the genset off; this allows us to see how the real battery and battery model each respond to the two characteristically different current demands. Before the genset is turned off, the current demand switches sign regularly. A statistical analysis of the error between the model voltage and recorded voltage shows that the resistance type model developed here is adequate for the needs of the investigation. Table 9

provides the statistical analysis of the percent error of the battery model for the first segment, driver A, of the 2008 endurance event.

Table 9: Statistical analysis of battery model error

Average Value of % Error	Standard Deviation
1.269	1.016

Note that the average error is within the 5% average error criteria applied to component models. A positive error here indicates that the model generally overestimates the voltage. This makes sense because a resistive type model, unlike a real battery, instantly regains voltage once the load is removed or reduced. Due to the time constants involved with chemical mixing and other physical properties, a real battery will demonstrate a lag when regaining voltage as load is removed or reduced. For this reason, a resistance type model properly tracking SOC will continuously overestimate voltage for current inputs with large fluctuations in magnitude. Closer inspection of the graph reveals that when the load is rapidly removed, the model regains voltage faster than the real battery.

The battery model was created using data sets 1, 2, 3, and 8, and as shown in figure 9, it was validated as a component model against data set 1. Using the same data set in both the creation and validation of a model is not common practice and should be avoided; however, since the goal for battery model is simply to respond as closely to the real battery as possible, all options were pursued to refine the accuracy of the battery model. No attempt was made in this study to model the battery temperature, as we will see in section 6.3.2; battery temperature does become important with more powerful powertrain configurations and should be considered in future work.

5.1.2 Genset Model

The genset model consists of five main components:

- Engine Model
- Motor/Generator (M/G) Model
- Engine-Motor Coupling Model
- Genset Fuel Consumption Model
- Engine Throttle Controller Model

In order to be accommodated into the system model, the genset model must be created to accept system (battery) voltage as an input, and output the current which it is capable of producing. Independent of the presence of a load, the battery and genset form a self-balancing system. As explained in (28), the engine does not possess sufficient power compared to the battery to govern the system voltage; this fact is demonstrated by the voltage plot in figure 2 which remains virtually unaffected by the disappearance of the current supplied by the genset. Therefore, as the battery voltage fluctuates, the genset naturally adjust its operating point such that it always remains within its limits.

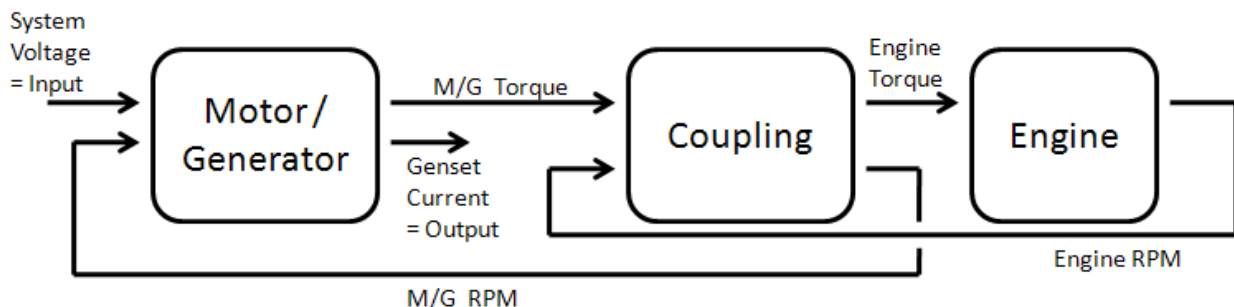


Figure 10: Block diagram of genset, level 2 in model hierarchy.

Figure 10 shows a block diagram of the genset model. Note again the forward facing architecture which does not force the simulation outside the capabilities of the physical components being modeled.

5.1.2.1 Engine Model

The engine model is typical of the low fidelity models common to racing simulators. This type was initially chosen because it can be easily created from manufacturer data. The model consists of three elements:

- Data table with the maximum torque as a function of the rotational speed.
- Inertia of the rotating mass.
- Throttle control.

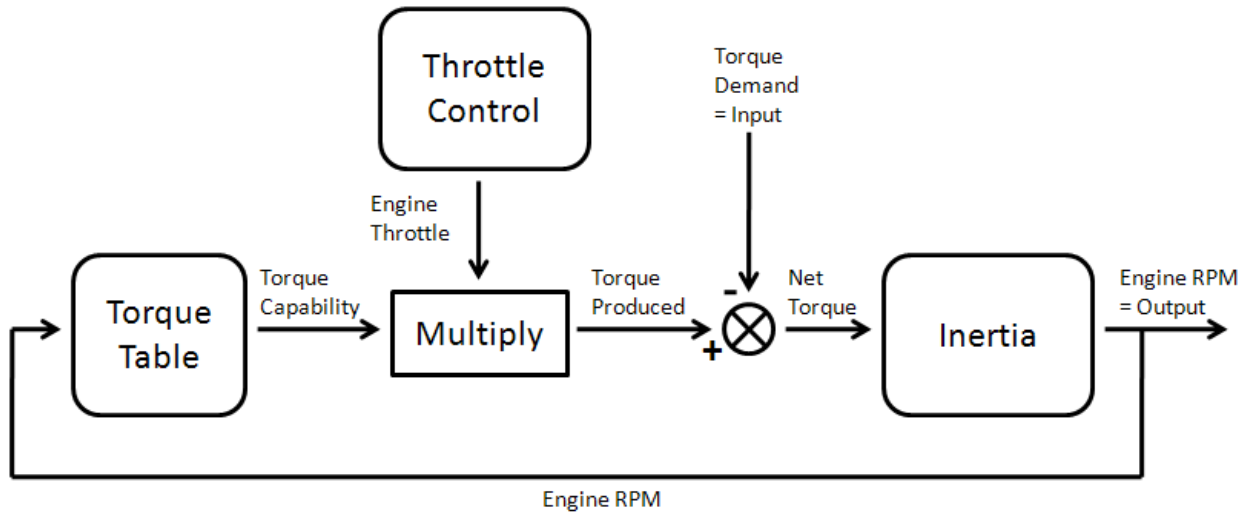


Figure 11: Block Diagram of engine model: level 3 in model hierarchy.

As can be seen from the genset validation graph in figure 15 and statistical analysis in table 10, this type model has sufficient fidelity for the needs of both investigations.

The engine model was created using data set 4 and manufacturer data for the torque-RPM relation. The value used for the rotational inertia is 60 RPM/N-m (30).

5.1.2.2 Motor Generator Models

The PMG 132 and ME0709 permanent magnet motors can be modeled using the set of equations shown here:

$$I_{MOTOR} \times R_{COIL} = V_{APPLIED} - [C_{SPEED} \times \omega] \quad Eqtn. 3$$

$$T_{MOTOR} = C_{TORQUE} \times I_{MOTOR} \quad Eqtn. 4$$

- $V_{APPLIED}$ is the voltage as measured at the terminals of the motor.
- C_{SPEED} is constant relating the rotational velocity of the motor to the backwards electromotive force produced by the motor. The constant value is 54 RPM per Volt (30), and appendix 3.
- ω is the rotational velocity of the motor in RPM.
- I_{MOTOR} is the current flowing through the armature of the motor.
- R_{COIL} is the real part of the complex impedance of the armature. The resistance value is 0.016 Ohms (30).
- T_{MOTOR} is the torque produced by the motor.
- C_{TORQUE} is a constant relating the current flowing through the armature to the torque produced. The constant value is 0.1933 N-m per Amp (30), and appendix 3.

Using these two equations and the inputs as shown in figure 10 we can calculate the outputs required by the genset model. This simplification does neglect certain features such as inductance and friction; however, as can be seen from the genset validation graph in figure 15 and statistical analysis in table 10, this type of model has sufficient fidelity for the needs of both investigations.

Graphs showing the relations used to evaluate the constants for both motors are available in appendix 3. The data sets used to formulate these relations are:

- PMG: Data set 6 and manufacturer data.
- ME 0709: Manufacturer data.

The model of the PMG is used for both the genset and the drive motors. The drive motor model has the added capability to estimate the motor temperature from the current, this aspect of the

drive motor model will be described in detail in section 5.1.4.2. The temperature estimation feature used for the drive motor model is not employed for the investigation of genset thermal issues due to a lack of failure criteria for the PMG when operated in the genset configuration. Perm provides temperature failure criteria for the PMG when operated as a drive motor where the only source of heat is that generated by the current flowing through the armature. The failure criteria provided does not hold for the genset configuration due to the added heat flux from engine through the shaft coupling to the PMG. Tests have shown that the provided failure criteria cannot be used to prevent failure in the PMG when used as a generator for the genset.

5.1.2.3 Genset Coupling Model

The coupling model for the genset allows for ratio and efficiency parameters to be adjusted according to the coupling being simulated. The efficiency factor models the torque loss of the coupling mechanism. Since the torque signal in the genset model flows in the opposite direction of the power flow, the efficiency factor must then be greater than or equal to unity representing an equal or greater torque experienced by the engine compared to M/G. The high efficiencies of the direct shaft-to-shaft couplers and chain drives used for all MHRT genset configurations have negligible losses (52), for this reason the efficiency factor is disregarded for all investigations.

5.1.2.4 Genset Fuel Consumption Model

This part of the genset model tracks the cumulative volume of fuel consumed by the engine using the genset electrical power output. Figure 12 shows the relationship between the volumetric fuel consumption rate and the genset electrical power output formulated from data set 7. The curve fit also depicted in figure 12 is represented by equation 5:

$$y = -0.00000015x^2 + 0.0012x - 0.23, \quad R^2 = 0.986 \quad \text{Eqtn. 5}$$

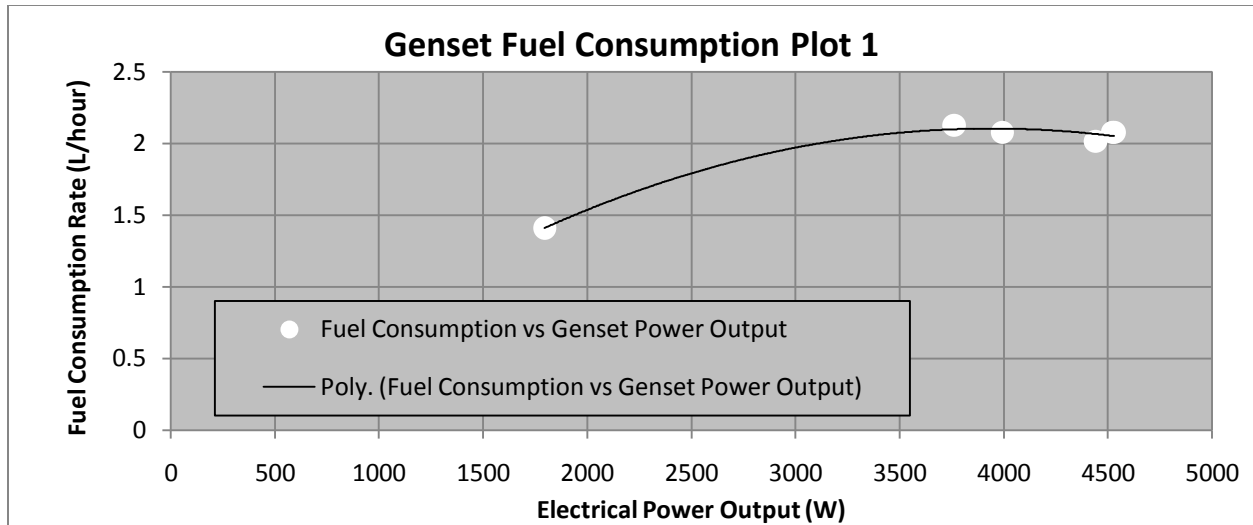


Figure 12: Genset fuel consumption relationship.

Equation 5 is used in the model to calculate the fuel consumed for each time step of a simulation. These calculations are integrated over time to calculate the total volume of fuel consumed by the genset for a given simulation.

5.1.2.5 Engine Throttle Controller Model

The engine throttle is controlled by the manufacturer installed mechanical governor. The governor has a classical design using springs and centrifugal weights which interact to keep the engine speed below a preset RPM value. The relatively complex configurations of the springs and weights, and the continuously changing geometry of the lever arms relative to the springs, together make it very difficult to formulate an analytical model. As such, rather than modeling the governor system as it exists, an attempt is made to model the governor using classic proportional, derivative, and integral control elements to see if sufficient fidelity can be achieved by these means. The controller is designed to act on the error between the simulated engine RPM and a preset desired RPM value. Several attempts were made using simple proportional, proportional-integral, and proportional-integral-derivative controllers; however none of these provided sufficient accuracy in reproducing the effect of the governor on the genset output. Finally, using a series of trials with a range of gain values for a proportional controller; a group of plots was created showing the error between the simulated genset current over the RPM range in which genset operated. Figure 13 is an example of one such plot.

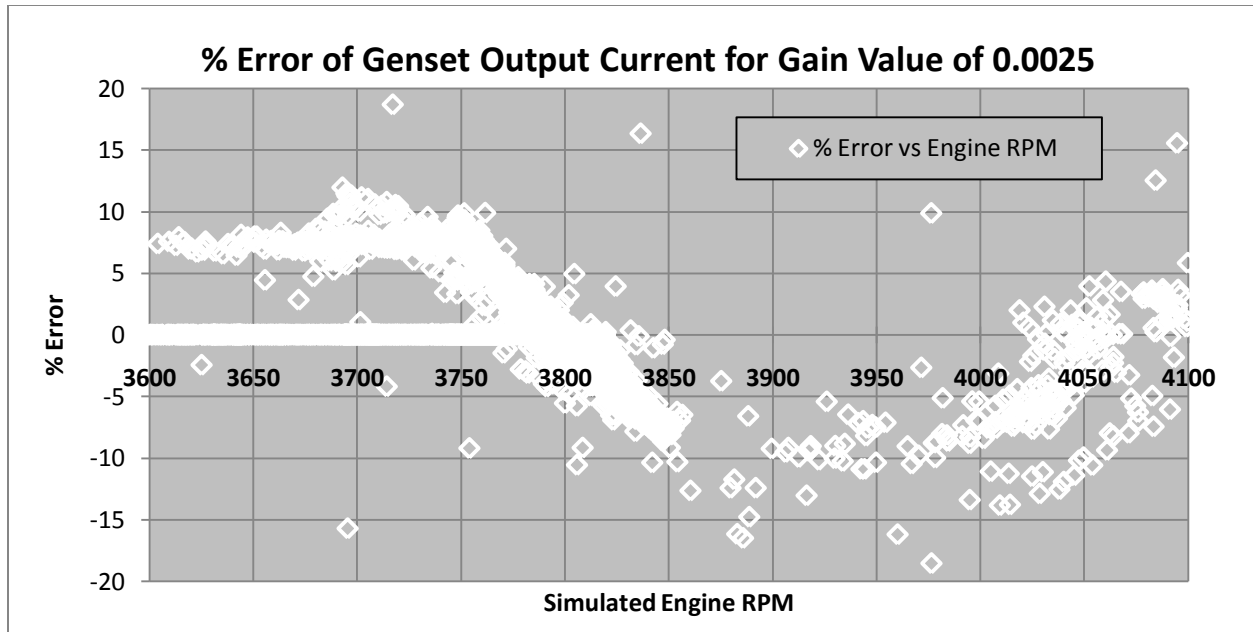


Figure 13: Sample plot for % error of genset current versus simulated engine RPM.

Each plot in the series has a similar trend in that the data crosses the zero percent error line at an easily identifiable location, for the gain value 0.0025 shown in figure 13; the data crosses the zero error line at approximately 3800 RPM. Using similar results from the entire series of plots; a gain schedule for the governor model can be created. The final gain schedule chosen for the governor model is plotted in figure 14.

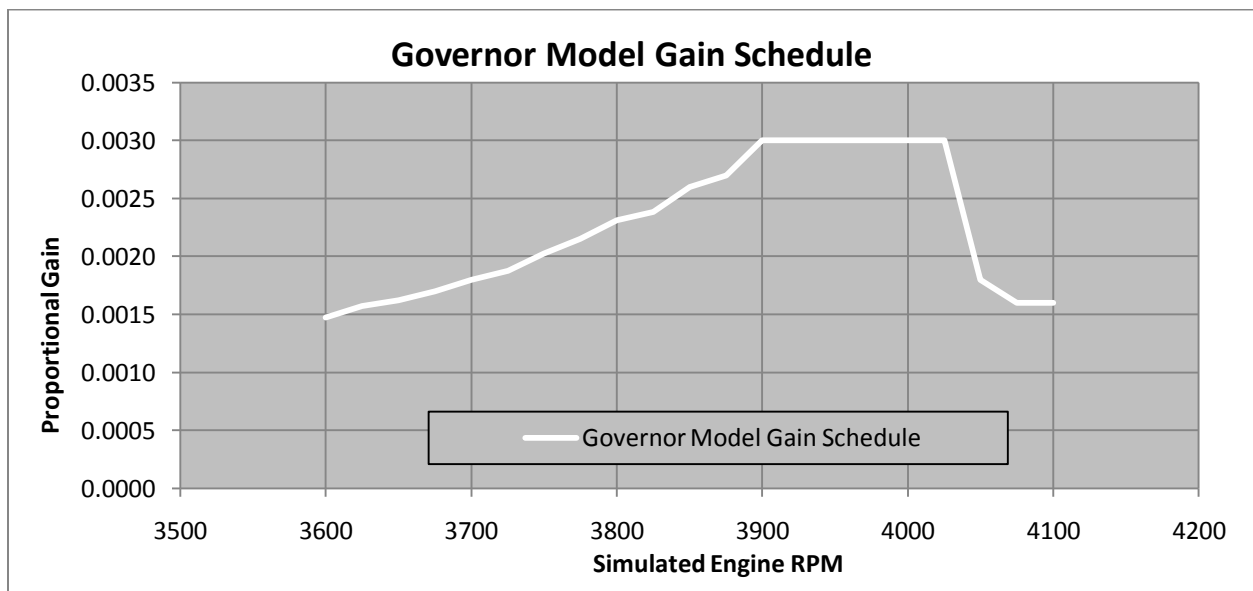


Figure 14: Governor model gain schedule.

The throttle signal produced by the governor model is derived from the product of the gain value with the RPM error between the simulation and the reference value.

5.1.2.6 Genset Model Validation

Here the genset model is validated against a section of data set 3 in which the vehicle was operating under genset power only. Operating the vehicle under genset power only allows the system voltage to fluctuate beyond the range expected when genset is operated with battery. This validation shows how the genset model responds when asked to provide large currents beyond its capabilities. The results are shown in figure 15. A validation where the model is operated under typical conditions with the battery is provided in section 5.1.3. There, the genset model and battery model together, are validated against the 2008 FH endurance event data. For the validation in section 5.1.3, the genset and battery model are setup as shown in figure 8 forming the energy system model, and the input is the recorded load current from the 2008 FH endurance event. This energy system model validation provides a statistical analysis of the genset model operating under typical conditions, a summary is provided in table 10. Data points for which the vehicle is off and non-operational are excluded from the analysis.

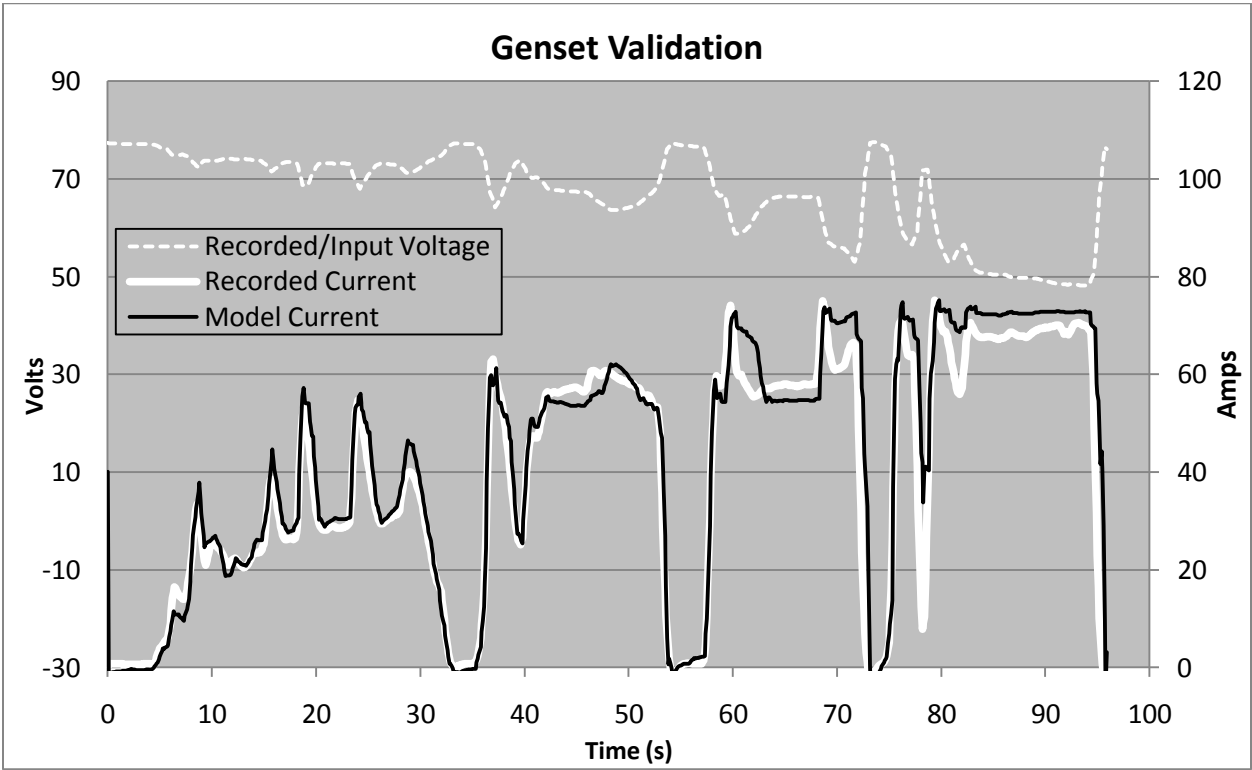


Figure 15: Genset model validation against data set 3, battery is off.

As we can see in figure 15 the genset model reproduces the response of the real genset adequately. After approximately 60 seconds when the loads approach the maximum capabilities of the engine, the model accuracy decreases. Most important is the constant error between approximately 85 and 95 seconds. This indicates that the model may be over estimating the capabilities of the genset. From the statistical analysis of the validation against FH data in table 10, we see that in fact the opposite appears to be the case. A negative value for average percent error indicates that the model is underestimating the current produced by the genset over the course of the endurance event.

Table 10: Statistical analysis of genset model current error

Average Value of % Error	Standard Deviation
-2.614	13.37

Note that the average error is within the 5% average error criteria applied to component models. There are two sources causing the genset model to underestimate current:

1. The battery model: as we can see from figure 15, the genset produces less current when the input voltage is relatively high. Recalling that the battery model regains voltage faster than the real battery under conditions of decreasing load, we would expect that the modeled genset would then see on average a higher voltage than did the real genset thus lowering the current output of the model relative to the recorded data.
2. The engine model throttle control: The mechanical governor installed on the engine is not a simple proportional or proportional-integral controller. The device includes many different interacting lever arms and springs which produce a relatively complex control signal. The model developed for this device performs sufficiently well as long as its reaction does not affect the input into the genset model; such as in figure 15. However, when the effects of the governor model are allowed to affect the input signal to the genset model, as with the endurance event validation where the battery voltage (also the genset input) changes as the genset current fluctuates, a greater amount of noise is apparent in the current output from the genset model.

5.1.3 Energy System Model Validation

The energy system model consists of the battery model coupled with the genset model. This is the same validation data as used for the statistical analysis of the genset model performance. Here, the energy system model is required to produce the current demand from the vehicle load during the 2008 FH endurance event as recorded onboard MHRT2. Figures 16, 17, and 18 show respectively, the complete validation, a close up of the first charging session, and a close up of the second driving session when driver B shuts off the generator.

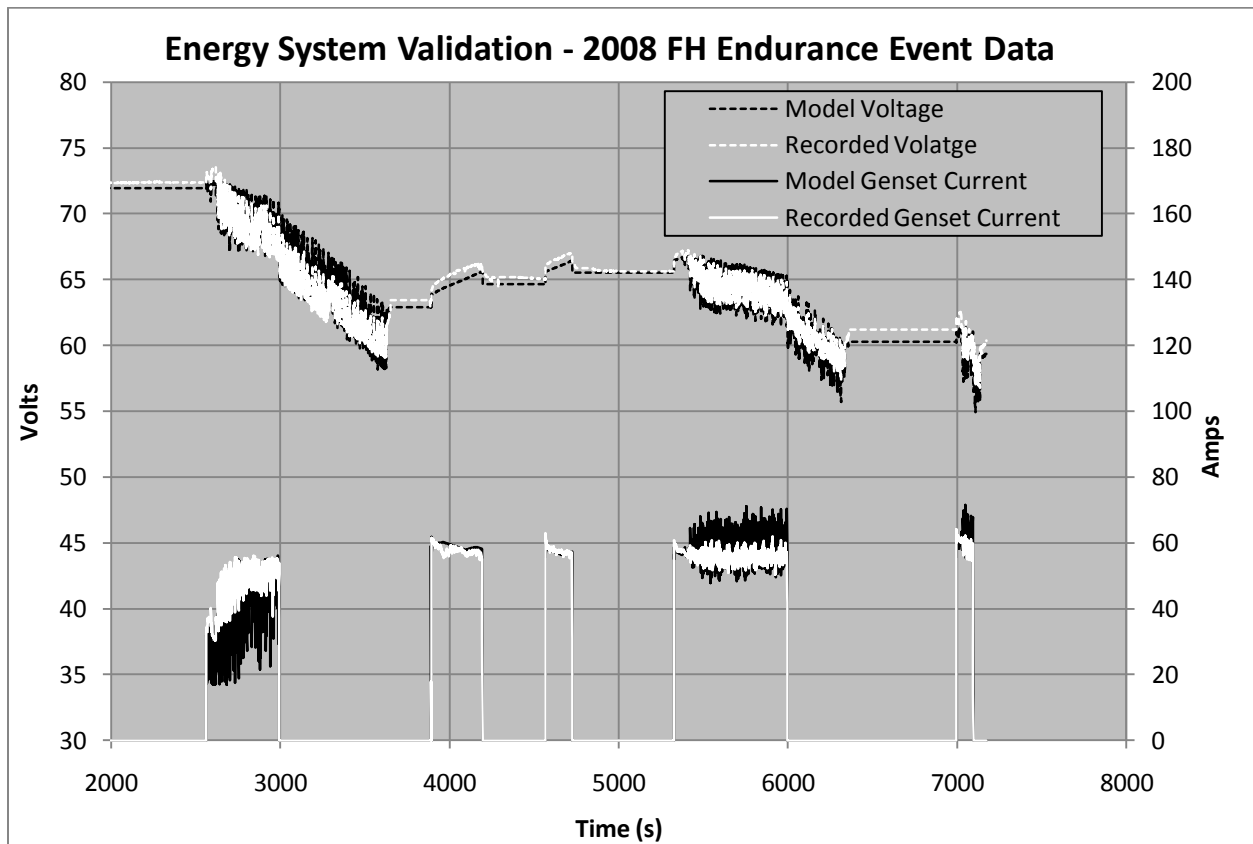


Figure 16: Energy System Validation against 2008 FH endurance data.

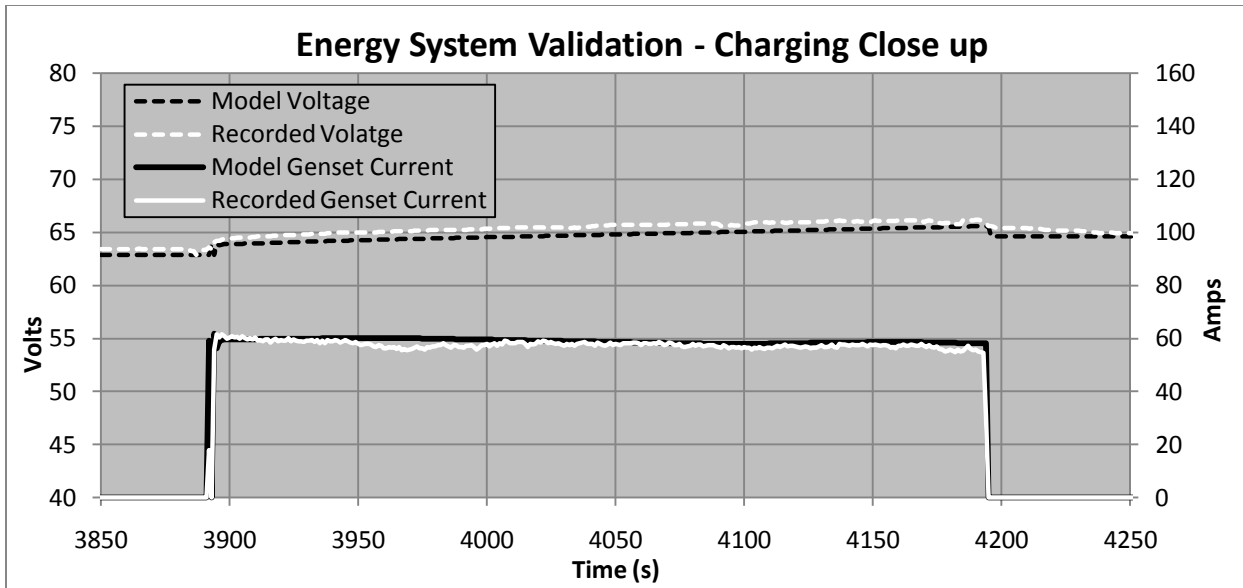


Figure 17: Energy System validation charging close up.

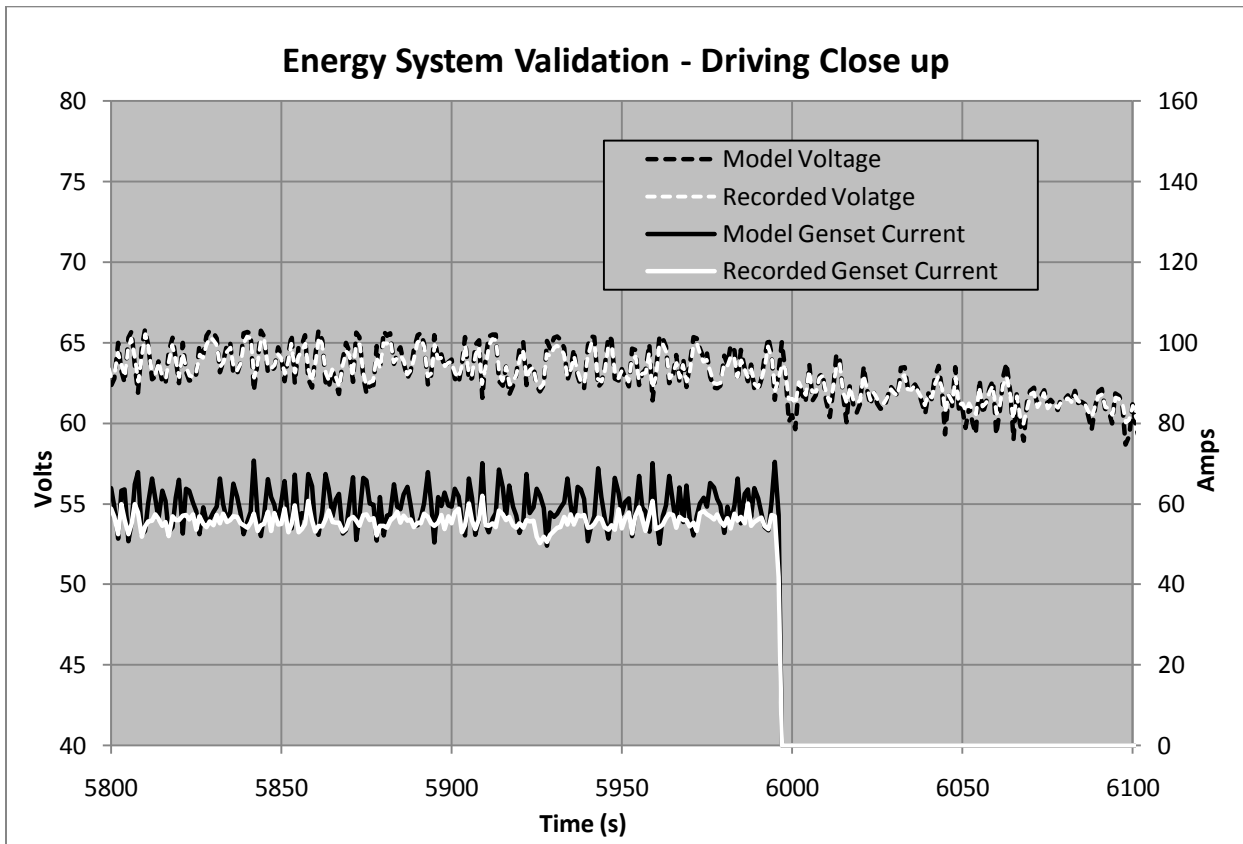


Figure 18: Energy System validation driving close up.

As we can see from figures 17 and 18 the model reproduces the system voltage very well both in charging and driving conditions. Figure 16 shows that the model signals tend to fluctuate more

than the real system which would indicate that the damping of the modeled system is lower than that of the real system. Recall from the genset section that as the number of feedback loops being simulated is increased, the relative magnitude of signal fluctuations becomes greater in the model compared to the real system. Specifically, the genset model was able to very closely reproduce the recorded current when its output did not affect the input voltage. However, when the battery model is introduced and the number of feedback loops is increased, the genset current output fluctuations increase relative to the recorded signal. A statistical analysis of the energy system model performance is provided in table 11. The genset current error during driver A is large and negative. This error is caused both by the relatively rapid recovery of the battery and error originating from the engine throttle control gain schedule.

Table 11: Statistical analysis of energy system model performance.

Data Section	Generator Current		System Voltage	
	Ave. % Error	Standard Deviation	Ave. % Error	Standard Deviation
Driver A	-18.52	14.47	0.20	0.94
Charge 1	2.46	1.92	-1.12	0.18
Charge 2	-0.78	5.77	-0.93	0.07
Driver B	4.89	24.39	-0.09	0.65
All	-2.61	13.37	-0.29	0.83

Although the energy system model error for this section of the data is beyond the criteria set for component models, we see that over the course of the endurance event, the genset current error is acceptable. Finally, the fact that the error for system voltage is small with respect to the 5% error criteria for component models indicates that the energy system model performs very well for tracking the SOC of the battery throughout an endurance event. This will be useful for the genset prioritization investigation since we measure genset improvement by monitoring the battery SOC over an endurance event and compare it to a baseline SOC trace.

5.1.4 Vehicle Load Model

As shown in figure 7, the vehicle load model contains the powertrain and vehicle resistance models. Here a brief description of the vehicle model and its representative block diagram are

given. Following this, each component model is explained in detail as with the energy system model. Individual validations are not provided for all components.

The block diagram for the vehicle load model is shown in figure 19, again note the forward facing architecture. In the vehicle model, only one group consisting of one controller, one motor, one CVT, and one fixed ratio is modeled. The outputs of this group are doubled before being passed on to the neighboring blocks in the system model. The signals which are doubled are the controller current and the wheel torque. This way the energy system is required to produce the current required for two identical powertrains (in the system model this is called the “load current”), and the vehicle experiences twice the amount of wheel torque produced by one powertrain.

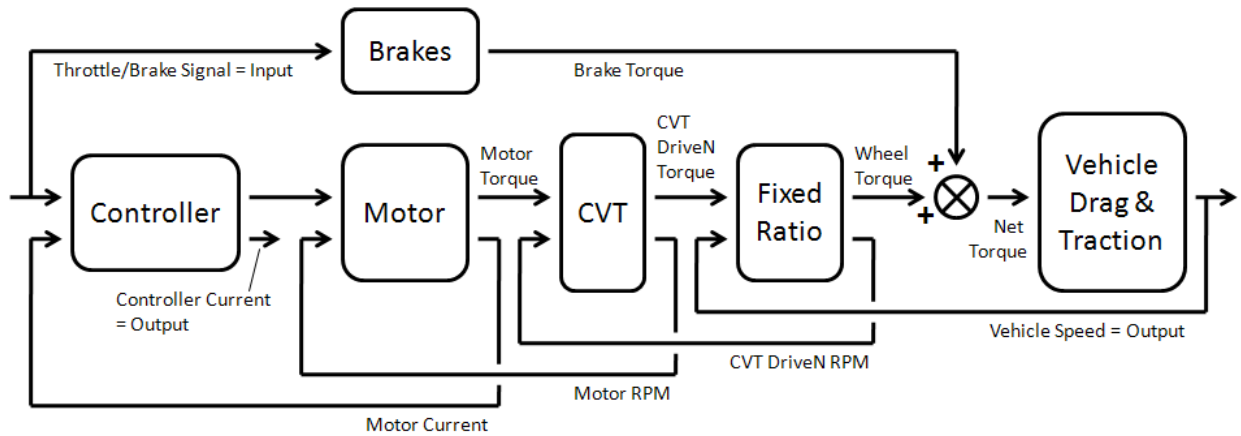


Figure 19: Vehicle load model block diagram: level 2 in model hierarchy.

5.1.4.1 Motor Controller Model

The motor controller used for all MHRT vehicles is a standard DC motor controller which uses pulse width modulation (PWM) to control the applied voltage at the motor terminals according to equation 6:

$$V_{APPLIED} = V_{TERM} \times Throttle\ Signal \quad Eqn.6$$

- $V_{APPLIED}$ is the voltage as measured at the terminals of the motor.
- V_{TERM} is the instantaneous voltage of the battery, as in equation 1.

- Throttle Signal is a value between 0 and 1 defined by the throttle input to the controller, a value of 1 is full or 100% throttle. This parameter is also known as the duty cycle of the controller.

The inductance of the motor acts as a low pass filter for the high frequency PWM signal such that the armature current remains a relatively smooth signal. Using the throttle input and other user specified parameters such as motor current limit, the controller modulates the applied voltage to produce the desired performance. For example, if the current limit is set at 100 amps and the motor speed and throttle signal are such that $V_{APPLIED}$ would produce a current larger than 100 amps, the controller current limit function steps in which adds another factor to equation 6 as follows:

$$V_{APPLIED} = V_{TERM} \times Throttle\ Signal \times Current\ Limit\ Factor \quad Eqn.7$$

Here the current limit factor is also a value between 0 and 1 which is determined by the PID current control circuit using the error between the measured armature current and the current limit value.

There are three features of the motor controller that must be modeled:

1. Modulation of $V_{APPLIED}$.
2. Control of armature current according to current limit.
3. Controller efficiency appearing as voltage drop across the controller.

The motor current limit as imposed by the controller is modeled by applying a maximum value to the current as calculated by the motor model. This will be presented in the drive motor model section.

The motor controller model is represented by equation 8:

$$V_{APPLIED} = V_{TERM} \times Throttle\ Signal \times Efficiency\ Factor \quad Eqn.8$$

The throttle signal comes from the driver block as shown in figure 8. The efficiency factor comes from a data table formulated from data set 2. The efficiency map has two inputs; throttle value and motor current. The surface representing the controller efficiency map is shown in figure 20.

The current which flows from the energy system to the controller, named “load current” in figure 8 is determined by the total current for both drive motors and the duty cycle of the controllers. As mentioned above, the controller current is doubled as it is passed on to the energy system model. As theory would suggest and experiments show, the motor current and controller current differ by a factor equal to the duty cycle. This occurs because at duty cycles lower than one, the controller main transistor set is non-conducting for a fraction of the time. During this time, armature current continues to flow through a bypass circuit designed into the controller to accommodate the armature inductance. This circuit is known as the Freewheel Diode. The load current, the current passed on to the energy system model, is governed by equation 9.

$$I_{LOAD} = I_{MOTOR} \times Throttle\ Signal \times 2 \quad Eqtn.9$$

- I_{MOTOR} is the motor current as in equations 3 and 4.

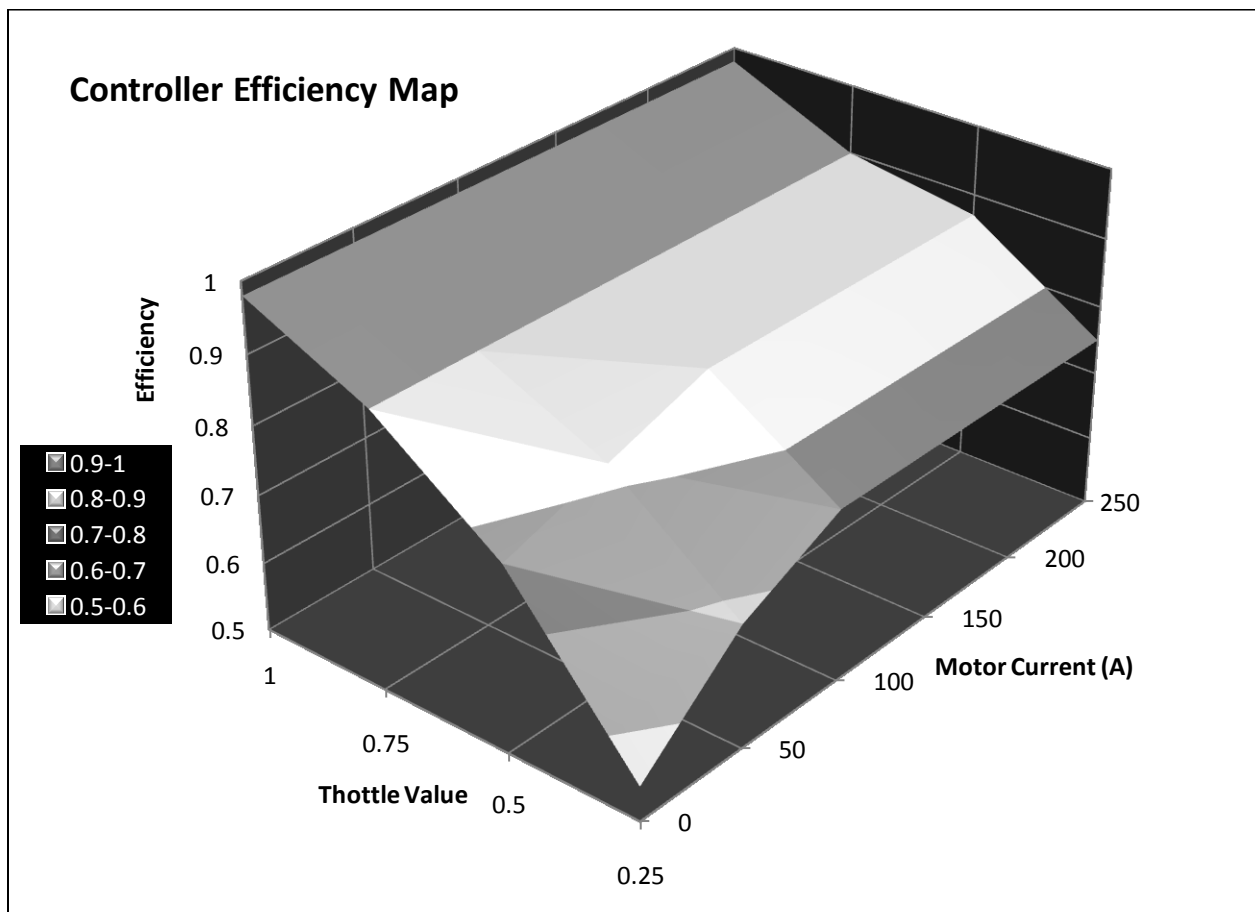


Figure 20: Controller model efficiency map.

5.1.4.2 Drive Motor Model

The drive motor model uses the same governing equations as those used for the M/G model but with added capability to estimate the motor temperature.

Other added features, such as inductance and rotational inertia were investigated for the motor model. These effects are modeled using equations 10 and 11 shown here:

$$I_{MOTOR} \times R_{COIL} = V_{APPLIED} - [C_{SPEED} \times \omega] - \left[C_{INDUCTANCE} \times \frac{dI_{MOTOR}}{dt} \right] \quad Eqtn. 10$$

- $C_{INDUCTANCE}$ is the inductance of the motor armature. The inductance value is 19 μ H.
- $\frac{dI_{MOTOR}}{dt}$ is the time derivative of the motor current.
- All other variables are the same as in equations 3 and 4.

The torque produced by the drive motor is calculated using equation 11:

$$T_{MOTOR} = [I_{MOTOR} \times C_{TORQUE}] - \left[C_{INERTIA} \times \frac{d\omega}{dt} \right] \quad Eqtn. 11$$

- T_{MOTOR} is the net torque produced.
- $C_{INERTIA}$ is the moment of inertia of the armature about its rotational axis. The constant value is 0.025 $\text{kg}\cdot\text{m}^2$ (30).
- $\frac{d\omega}{dt}$ is the angular acceleration of the armature.
- All other variables are the same as in equation 4.

The overall fidelity of the model did improve by adding the inductance and inertia features; however for some signals such as battery current and voltage, these features caused undesired fluctuations. The final model does not include the inductance and inertia features.

Equation 10 is where the controller current limit is applied in the model; a cap is placed on the value calculated for motor armature current. Since the result of equation 10 is used to calculate the torque produced by the motor as well as the current demand passed on to the controller, applying the cap on the result of equation 10 effectively reproduces the effect of the imposed controller current limit.

The motor temperature prediction feature of the motor model was developed to assist in the powertrain investigation. An estimation of motor temperature, and therefore a prediction of failure, is very helpful since the goal of the powertrain investigation is to increase the power output of the motor by increasing the current without affecting reliability. The failure criteria used for failure prediction is provided by Perm, the manufacturer of the PMG. The failure criterion is given as a temperature limit of 120° Celsius as measured by a thermocouple placed at a specific location on the PMG brush holder. In the model, the temperature is predicted by estimating the instantaneous rate of change of the temperature for the given operating conditions and integrating this signal over time. The parameters which define the operating condition are motor temperature, ambient temperature and motor current. Although the motor is designed to act as its own cooling fan, the motor speed was not found to have a significant impact on the rate of change of temperature. Due to limited resources, it was not possible to obtain data for ambient temperatures above the room temperature; therefore only one map was created for an ambient temperature of approximately 25° Celsius.

In the model, the rate of change of temperature is determined by two inputs: the motor temperature relative to ambient, and the motor armature current. The output is the rate of change of temperature in degrees Celsius per second. The surface representing the data obtained is shown in figure 21:

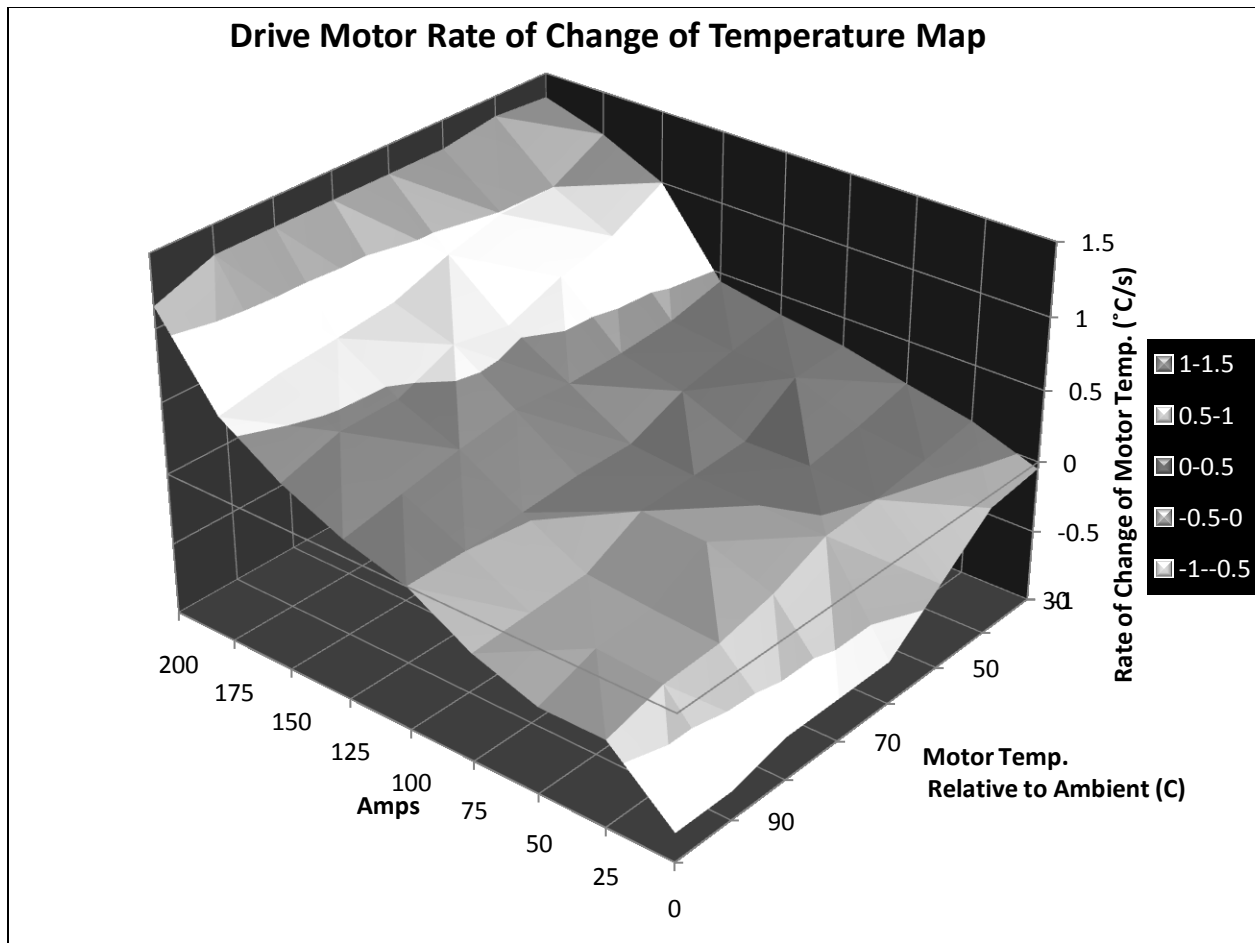


Figure 21: Map for rate of change of drive motor temperature.

Note that the data for the motor temperature map does not extend below 30 degrees above ambient. As the model cools down to below 30 degrees above ambient, Simulink must extrapolate this map in order to make the computation. By inspection we can see that for zero motor current, this map will show zero change in temperature over time for approximately 25 degrees above ambient. This causes the temperature prediction to reach an asymptote at approximately 50 degrees as the model cools down. This fact is not a major issue for this study since from an initial state of 25 degrees; the motor temperature rapidly climbs above 50 degrees for typical loading conditions. A validation of this map can only be provided using data from MHRT3 since no other vehicles were equipped with motor temperature sensors; this validation is provided in section 6.3.2.1.

5.1.4.3 CVT Model

The model developed for the CVT must have the specific structure as depicted in figure 19. The model must output the motor RPM and the DriveN pulley torque using the DriveN pulley RPM and the motor torque as inputs. Similar to the battery, the complexities of the CVT are such that a parameterized model is simpler to create compared to an analytical model. The CVT model must be capable to correctly predict the power transfer efficiency, and the ratio of torque loss to speed loss for all operating conditions. Creating an analytical model with these capabilities is beyond the scope of this investigation; therefore a parameter model was developed. The parameter model developed for this investigation captures these aspects of the CVT and reproduces them identically as measured during the dynamometer tests. The down side of the parameter model is that for different configurations of the CVT, all new data must be taken to create the data tables which make up the model.

The model consists of two data tables, one for each output parameter. Each data table uses both the DriveN pulley RPM and the motor torque as inputs to determine its output. These tables were created from Data Set 5. The details for each configuration model are provided in table 12. The discussion describing the logic behind these selections is provided in section 3.3.2.1.

Table 12: Configurations of CVT models.

	CVT1	CVT2	CVT3	CVT4
Spring (N/mm)	18.1	12.2	18.1	12.2
Weights (g)	275	275	400	400

Figures 22 and 23 respectively show the surfaces which represent the CVT3 data tables for the motor RPM and DriveN pulley torque. The data used to create the data tables for the CVT models had to be extrapolated since the acquired data was limited by the capabilities of the test equipment.

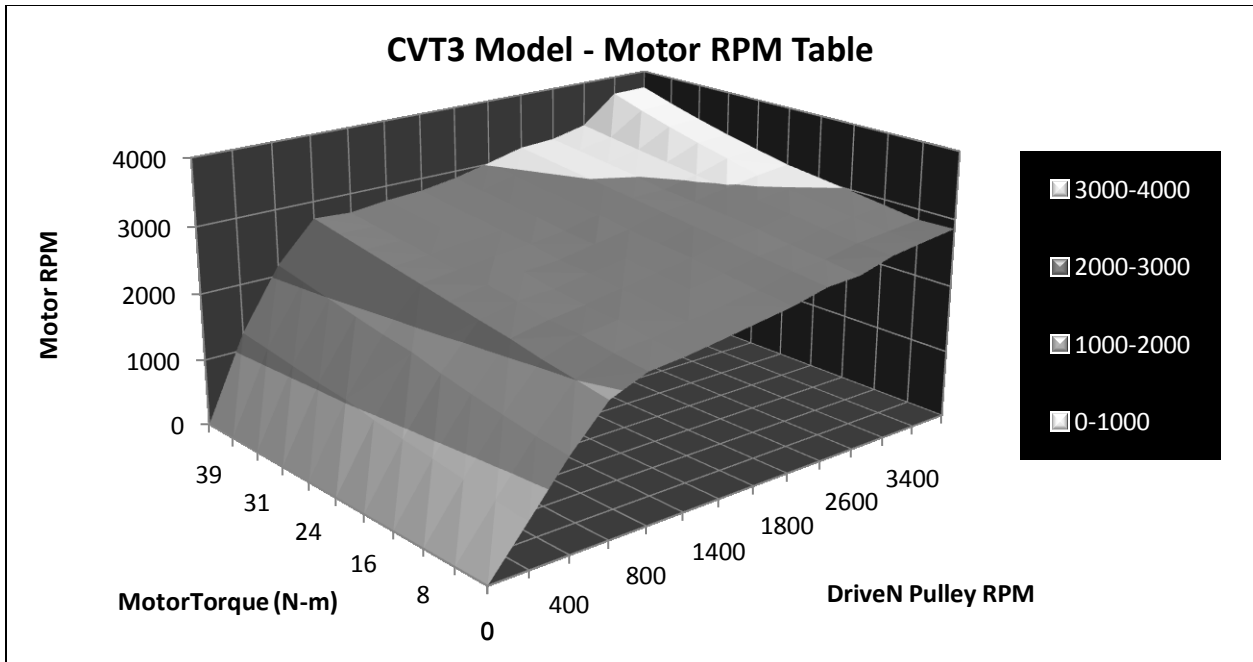


Figure 22: CVT3 Model, Motor RPM table.

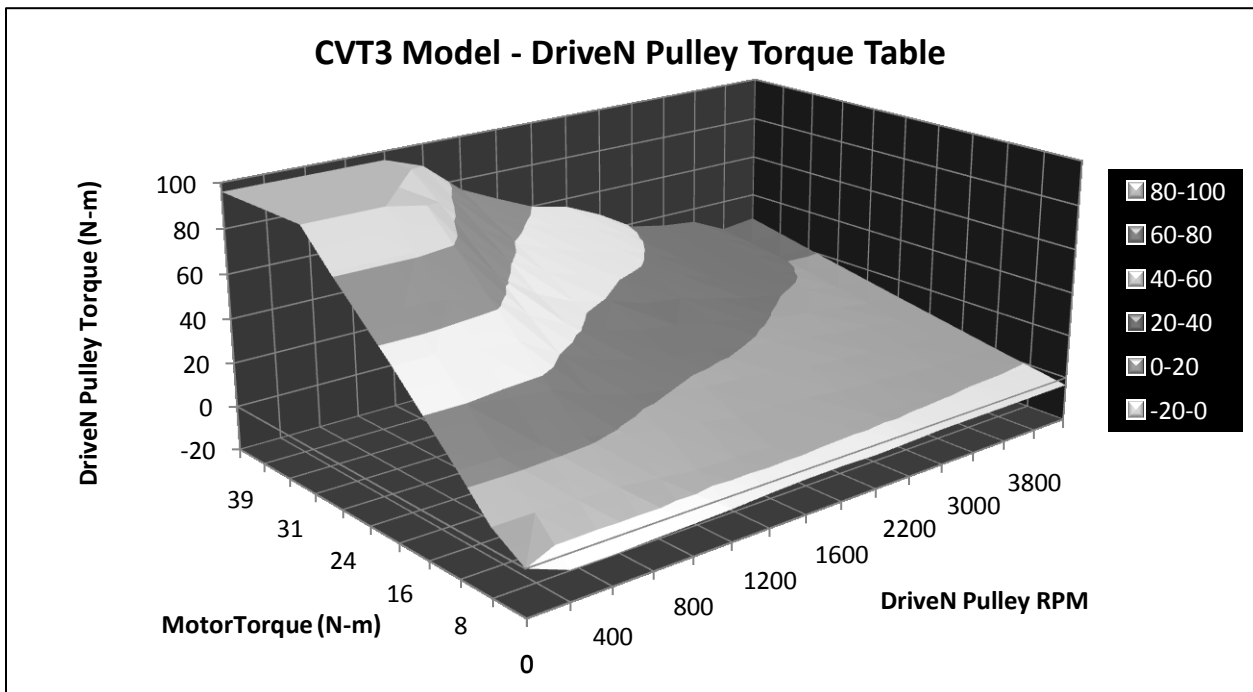


Figure 23: CVT3 Model, DriveN pulley torque table.

To ensure that torque transfer was not limited in the model due to a lack of data for high torque transfer, curve fits for the RPM and torque relations were used to extrapolate the output data in

order to form a non restrictive model. In an effort to avoid having the model transfer impossibly high torque values, all torque output for a given model was capped using the torque transfer value recorded when the CVT was noticeably slipping at lower speeds. The data shows clearly that once slippage occurs, transferring more torque was not possible. An example of this extrapolation procedure is provided in appendix 4.

All CVTs demonstrate the same basic shape for the surfaces which related the inputs to the outputs, as well as the surfaces which represent their efficiencies. The main noticeable difference between the four CVT models is seen in the maximum torque output at high speeds. Increasing the mass of the weights or decreasing the stiffness of the spring tends to increase the output torque for these higher speeds. This occurs because making these modifications to the CVT DriveR pulley configuration causes the CVT shift window to exist at lower motor speed. This in turn keeps the motor at a lower speed relative the DriveN pulley and as we can see from equation 9, for all other variables held constant, a lower motor speed produces a greater motor current and hence greater motor torque output. Figure 24 shows the placement difference of the CVT shift window between CVT1 and CVT4.

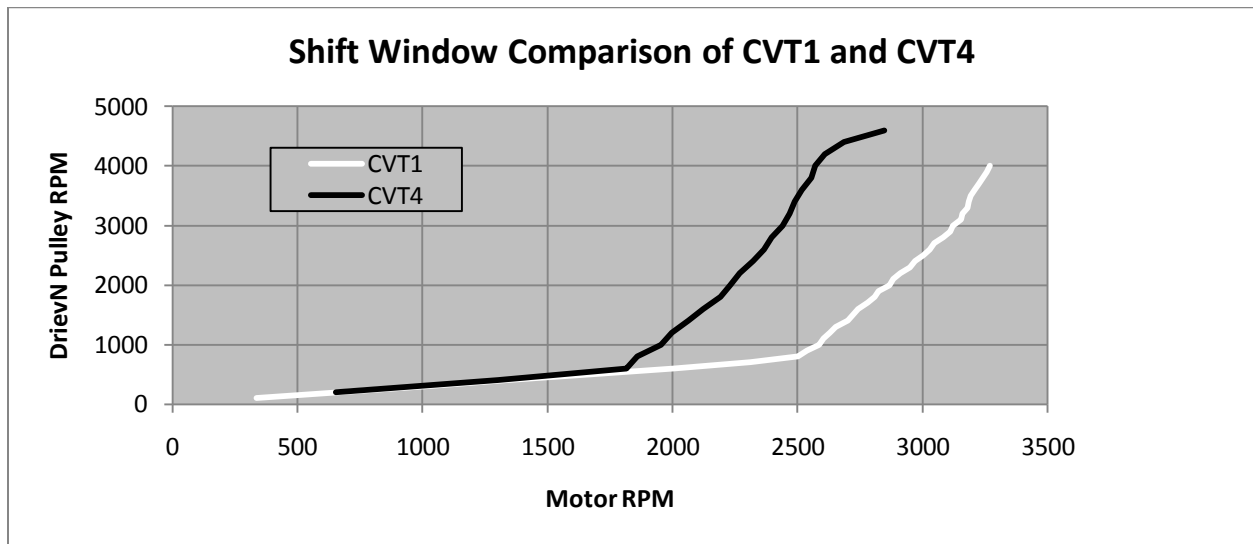


Figure 24: Shift Window Comparison of CVT1 and CVT4.

Note how the change in slope for CVT4 occurs at lower motor RPM, approximately 1800 RPM for CVT4 and 2500 RPM for CVT1. Also note how the slope of the CVT4 plot decreases at 2600 Motor RPM, this indicates that the shift window for CVT4 lies between 1800 and 2600 Motor RPM. In section 5.2.1, figure 36 shows model output for maximum torque for two powertrains

with different CVTs, this demonstrates the difference in power availability from different CVT configurations.

Finally, note that in figure 23, we see that for values of motor torque approaching zero, the output torque of the model is negative. This occurs because the input torque is not sufficient to overcome the friction associated with the CVT's V-belt and pulley design. This means that in reality this negative torque is experienced by the vehicle as a drag load if insufficient throttle is applied. We will come back to this in the vehicle model drag section.

5.1.4.4 Fixed Ratio Model

The fixed ratio model for the vehicle load block is identical to the genset coupling model with one difference. For the genset coupling model the torque data flows in the opposite direction of the power flow through the coupling. The opposite case is true for the fixed ratio model, the torque data flows in the same direction as the power flow. The efficiency factor is again disregarded for all investigations.

5.1.4.5 Vehicle Drag and Traction Model

This level 3 block of the system model shown in figure 25 includes models for the vehicle rolling and aerodynamic friction, the vehicle linear inertia, and the vehicle traction limit.

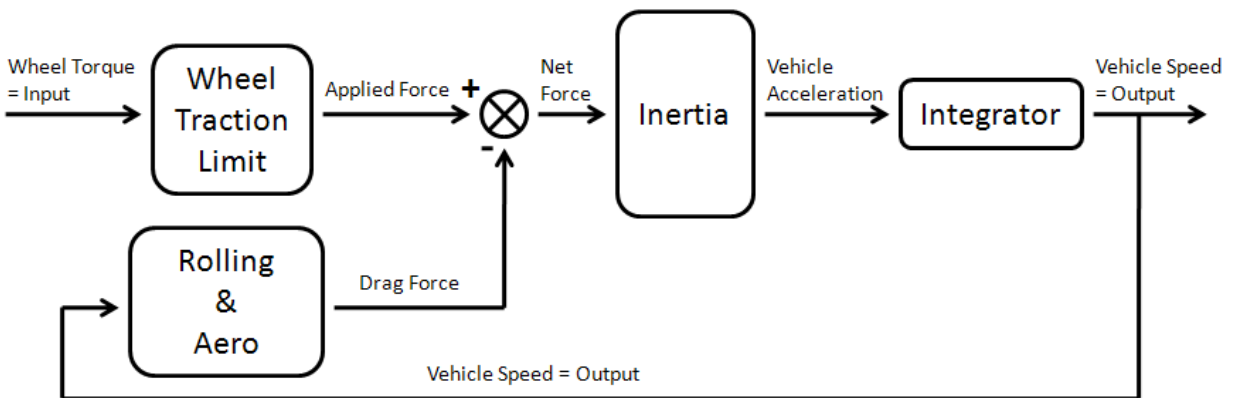


Figure 25: Vehicle drag, inertia, and traction limit model: level 3 in system model hierarchy.

5.1.4.5.1 Vehicle Inertia

The vehicle inertia is an application of Newton's Second Law:

$$a_{VEHICLE} = \frac{F_{NET}}{m_{VEHICLE}} \quad Eqtn. 12$$

- $a_{VEHICLE}$ is the acceleration of the vehicle.
- F_{NET} is the net force on the vehicle.
- $m_{VEHICLE}$ is the mass of the vehicle. The mass of MHRT2 including a 64 kg driver is 390 kg. MHRT3 with the same drive is 409 kg.

5.1.4.5.2 Rolling and Aerodynamic Drag

In the literature and commercially available software, rolling resistance and aerodynamic drag models can exist in two different forms, ABC curve fit models and physics based models (53). ABC curve fit models use information extracted from a vehicle coast-down test to formulate a relationship between the vehicle speed and the drag force acting on the vehicle. The “ABC” comes from the typical quadratic shape of these relationships where A, B and C are the coefficients of the quadratic equation. Physics based models rely on analytical relationships between vehicle speed and aerodynamic drag using drag coefficients and cross sectional area. Here we use coast-down tests performed with MHRT2 to formulate an empirical ABC relationship between the vehicle speed and the drag force. Data set 3 contains three coast-down tests; these are shown in figure 26.

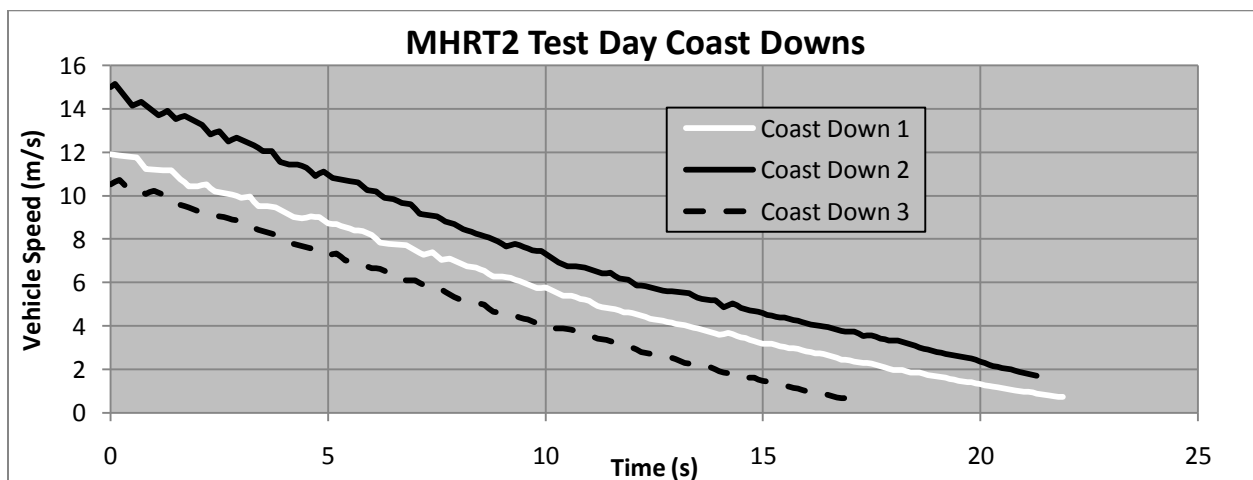


Figure 26: MHRT2 Coast down data.

To formulate an ABC model for a typical vehicle using the data in figure 26, the time derivative is taken to find the acceleration and then Newton’s Second Law is applied to find the resulting drag force with respect to vehicle speed. The result of these calculations performed for the plot “Coast Down 3” is shown in figure 27 as “Drag Calculated from Coast Down”. This plot is then extrapolated to higher speeds using a curve fit. Note that here the curve fit is a cubic function; this is due to the greater effect of the non-linear CVT drag at lower speeds compared to aerodynamic and rolling resistance effects.

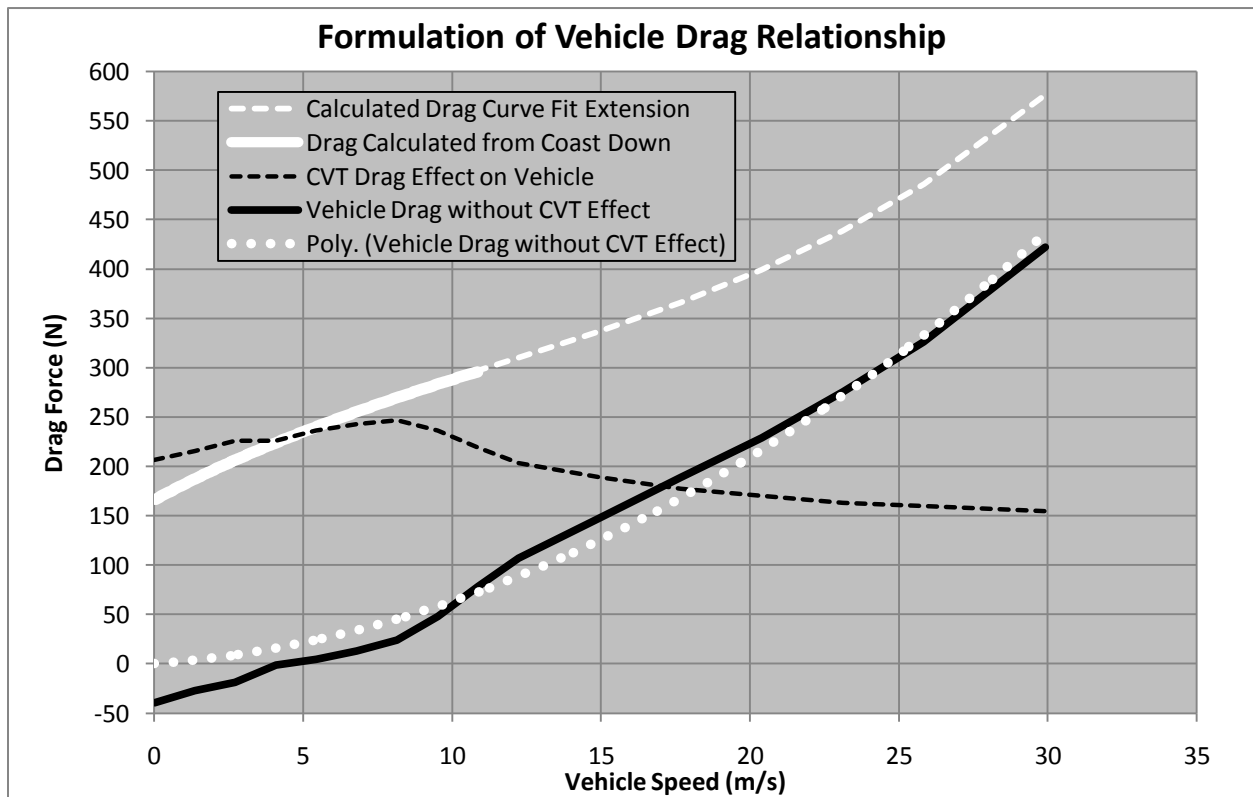


Figure 27: Formulation of vehicle drag relationship

The drag relationship represented by the curve fit also includes the drag force imposed on the vehicle due to the permanently engaged CVTs. Since the CVT models output negative torque for zero input torque, which then produces a drag effect in the vehicle model, it is necessary to subtract this portion of the drag from the total measured force from the coast down. The plot “CVT Drag Effect on Vehicle” in figure 27 shows the drag effect imposed on the vehicle by both CVTs. The plot “Vehicle Drag without CVT Effect” is the result of subtracting the CVT drag effect from the measured drag of the coast down. Noting that the plot “Vehicle Drag without CVT Effect” is negative for speeds below 5 m/s, it is necessary to use a curve fit with a forced

zero crossing to represent the vehicle drag in the model. The negative portion of the vehicle drag plot is caused by experimental error and data acquisition error. Forcing the vehicle drag to be zero at zero speed suggests that without the CVTs engaged the vehicle as has no rolling resistance. The rolling resistance contribution of the CVTs represented by the plot “CVT Drag Effect on Vehicle” therefore makes up the total rolling resistance of the vehicle. Although this is physically impossible since the tires will have their own rolling resistance, modeling the vehicle drag in this way reflects the reality of the relative resistances of the CVTs and the tires. This is indeed confirmed in reality by manually pushing the vehicle with and without the CVTs engaged. The drag relationship shown in figure 27 and represented by equation 13 is used for the final model for all investigations.

$$Drag (N) = 0.233v^2 + 2.177v; R^2 = 0.9773 \quad Eqtn. 13$$

- v is the vehicle velocity in meters per second.

5.1.4.5.3 Wheel/Tire Traction Limit

The wheel model converts the applied wheel torque into force applied on the vehicle. This conversion must be applicable for both acceleration and braking torques. Since a tire in contact with a road surface has finite traction the wheel model must do more than simply multiply the applied torque by the effective tire radius. There are many different forms of traction models sited in the literature (54), (55), (10). These models can be theoretical models, empirical models or semi-empirical models (a combination of the two), in all cases empirical data is typically required to tune the model for the specific conditions desired. The main parameter in the majority of models is the slip ratio, the relative velocity between the tire and road surface. Computing slip ratio requires the combined rotational inertia of the tire and the mechanical componentry directly attached to it (56). A simpler approach employed by the PSAT software does not require calculation of the slip ratio which eliminates the necessary feedback loop (57). The approach applies a maximum value to the acceleration and braking traction forces which can be applied to the vehicle using the maximum coefficient of friction between the tire and the road as well as the vertical load supported by the tires applying the torque.

Figure 28 shows the relationship between slip ratio and longitudinal force (acceleration/deceleration) for the racing tires used for MHRT3¹³ in several different situations, the data is from data set 10. In the plot the vertical load and tire camber are varied as well as slip ratio. The maximum vertical load applied provides the greatest longitudinal force at approximately 0.1 slip ratio. The slip ratio in this plot has been normalized by the vehicle speed.

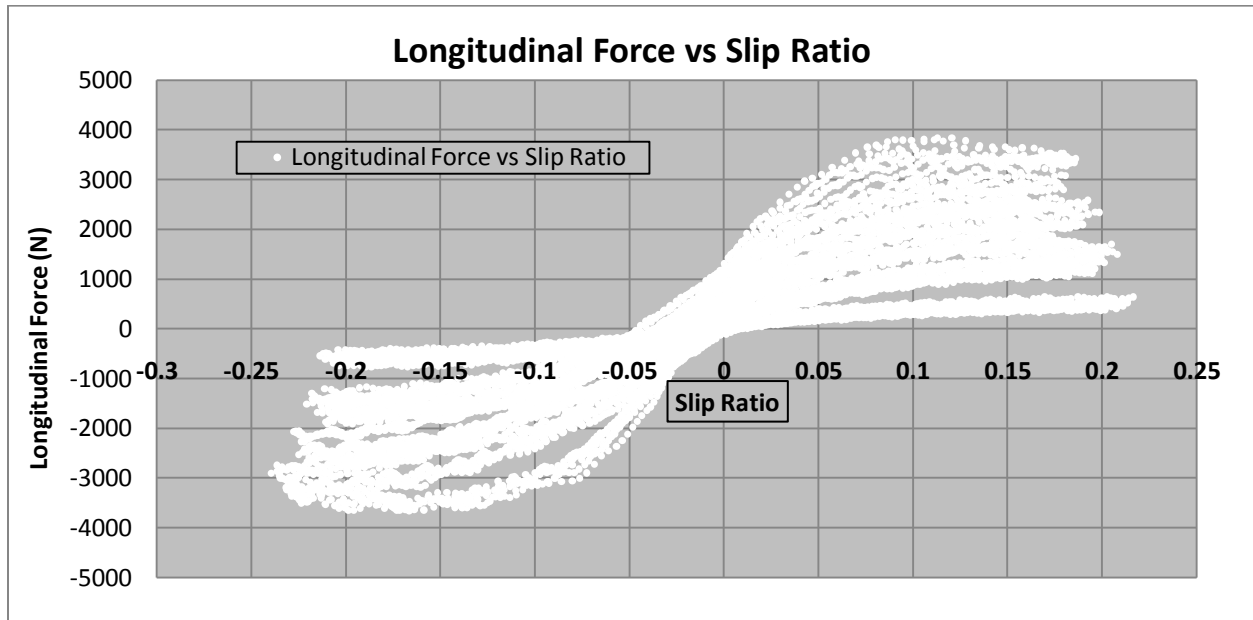


Figure 28: MHRT3 Tire Longitudinal Force Data (48).

Knowing that the maximum applied load for the data is approximately 1550 N, and that the maximum longitudinal force as taken from the plot is approximately 3800 N, we can estimate the maximum longitudinal coefficient of friction for the MHRT3 tires to be approximately 2.45. This is the value used for the maximum coefficient of friction for the tire model.

Finally, the wheel circumference and radius are held constant at 1.53 meters and 0.244 meter respectively. Maximum applicable forces are summarized in table 13.

5.1.4.5.4 Brakes

The brake model applies to all four wheels of the vehicle model. Braking torque is output when the throttle signal input is smaller than zero. The brake model consists of a maximum braking

¹³ Tire data for the MHRT2 tires is not available.

torque which is multiplied by the throttle signal to output fractional values of this maximum. The maximum torque is equal to the sum of the total braking torque necessary to lock all four wheels.

To accommodate the fact that there are four braking tires and only two driving tires, the traction model uses the maximum coefficient of friction multiplied by the vertical load on the tires doing the work which in turn imposes a maximum longitudinal force. Therefore, the maximum forward longitudinal force is the maximum coefficient of friction multiplied by the vertical load over the rear wheels, while the maximum reverse longitudinal force uses the vertical load over all four tires. Table 13 provides the numerical values for these forces.

Table 13: Maximum Driving and Braking Forces

Vehicle Mass with Driver	390	kg
Vertical Load on All Tires	3826	N
Max. Braking Force	9373	N
Vertical Load on Rear Tires	2104	N
Max. Driving Force	5155	N

5.1.5 Driver Model

A driver model is effectively a closed loop controller acting on the speed error of the simulation relative to the drive cycle speed. A driver model may take the form of proportional, proportional integral, proportional integral derivative, fuzzy logic, and other common types of closed loop controllers. Driver models which were explored for this study include:

- Proportional
- Proportional, Integral
- Proportional, Integral with non-saturating and resetting Integrator
- Proportional, Integral, Derivative

All driver models have advantages and disadvantages. Here the advantage is experienced as a smaller speed error while the disadvantages were experienced as large fluctuations in some system signals. Generally, the closer the simulation was made to follow the drive cycle speed, the greater the fluctuations in some system signals, primarily the drive motor current. This is caused by the reaction rate of the controller, as the reaction rate is increased; the sensitivity of the

system also increases causing fluctuations in certain signals to be relatively large in magnitude. Listed here are some examples of the control system tuning techniques explored¹⁴:

- Zeigler and Nichols Open Loop Tuning
- Ziegler and Nichols Closed Loop Tuning
- Trial and Error

Recalling from the methodology section that the drive cycles for the Simulink model are produced using a racing simulator with a track design that may or may not reflect the design of the future FH endurance track; it is safe to assume that even if the Simulink model does not follow the drive cycle perfectly, that useful results can still be obtained. The important concept is to compare the various powertrain configurations in a controlled manner. Therefore the final decision is to use a driver model which sacrifices some accuracy in following the drive cycle while providing better confidence in quality of the results with respect to important system signals such as motor current.

The driver model is a proportional controller with unity gain acting on the speed error in meters per second.

5.1.6 Vehicle Model Validation

Data Set 3 is chosen for the complete model validation since it provides the greatest amount of data channels from which comparisons between the recorded data and the model output can be made. The section of Data Set 3 chosen is 350 seconds in duration performed entirely with the genset operating as well as the battery. The motor controller current limit was set at approximately 110 Amps. Data from the 2008 FH endurance event would be ideal; however, recalling from section 4.2.1 that a drive cycle could not be formulated from this data, it is clear that the endurance event data cannot be used for the complete model validation. The following series of figures shows plots of comparisons between the model output and the recorded data for selected data channels. Here, the complete model is setup as depicted in figure 8.

¹⁴ Note that since the Simulink model cannot be represented in the frequency domain by a classical s-function, we are limited to empirical controller tuning methods.

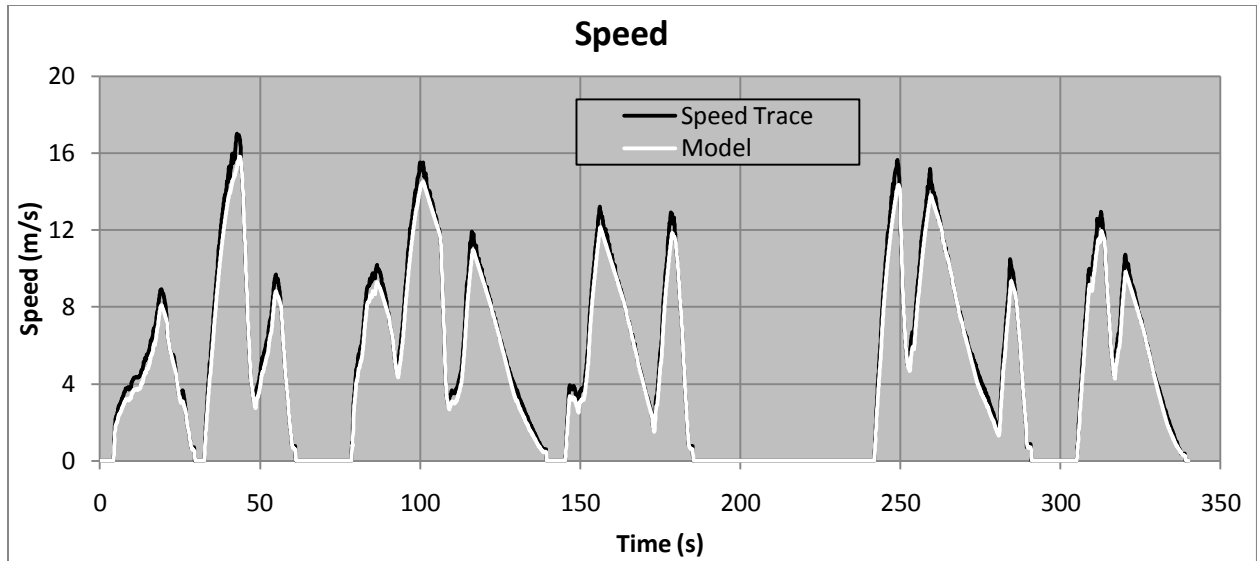


Figure 29: Speed plot for complete model validation.

Figure 29 is a good illustration of the consequences of using a proportional controller for a driver model on the input tracking ability of the model.

An important feature to note in figure 30 is the gap present as the motor RPM is decreasing. The gap indicates that the CVT model places the shift window at a higher RPM than the recorded data shows.

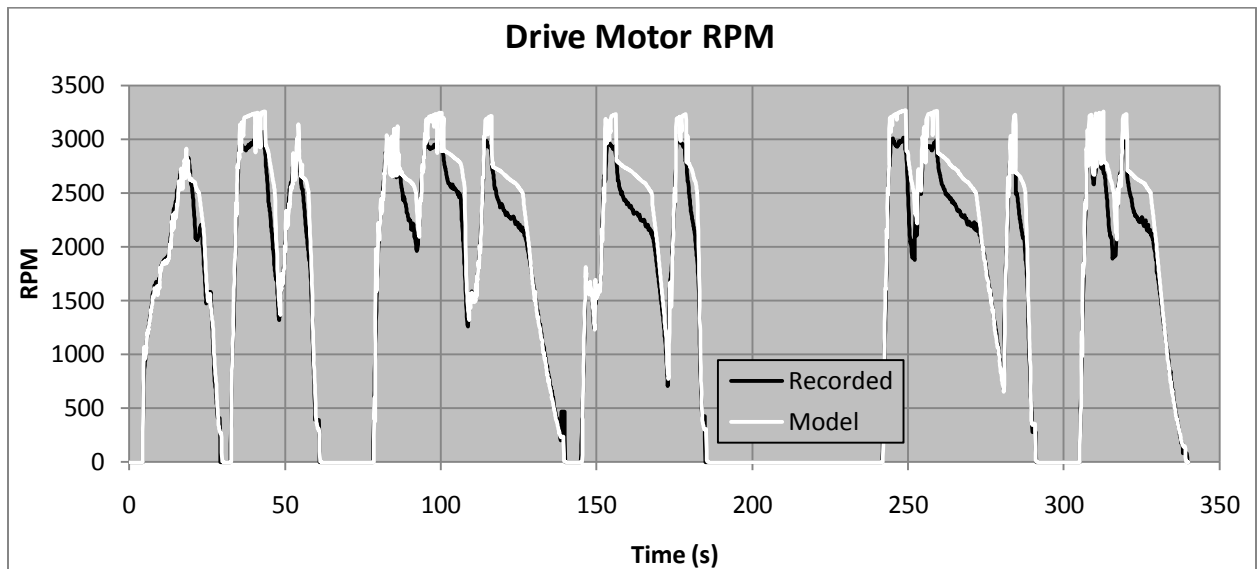


Figure 30: Drive motor RPM plot for complete model validation.

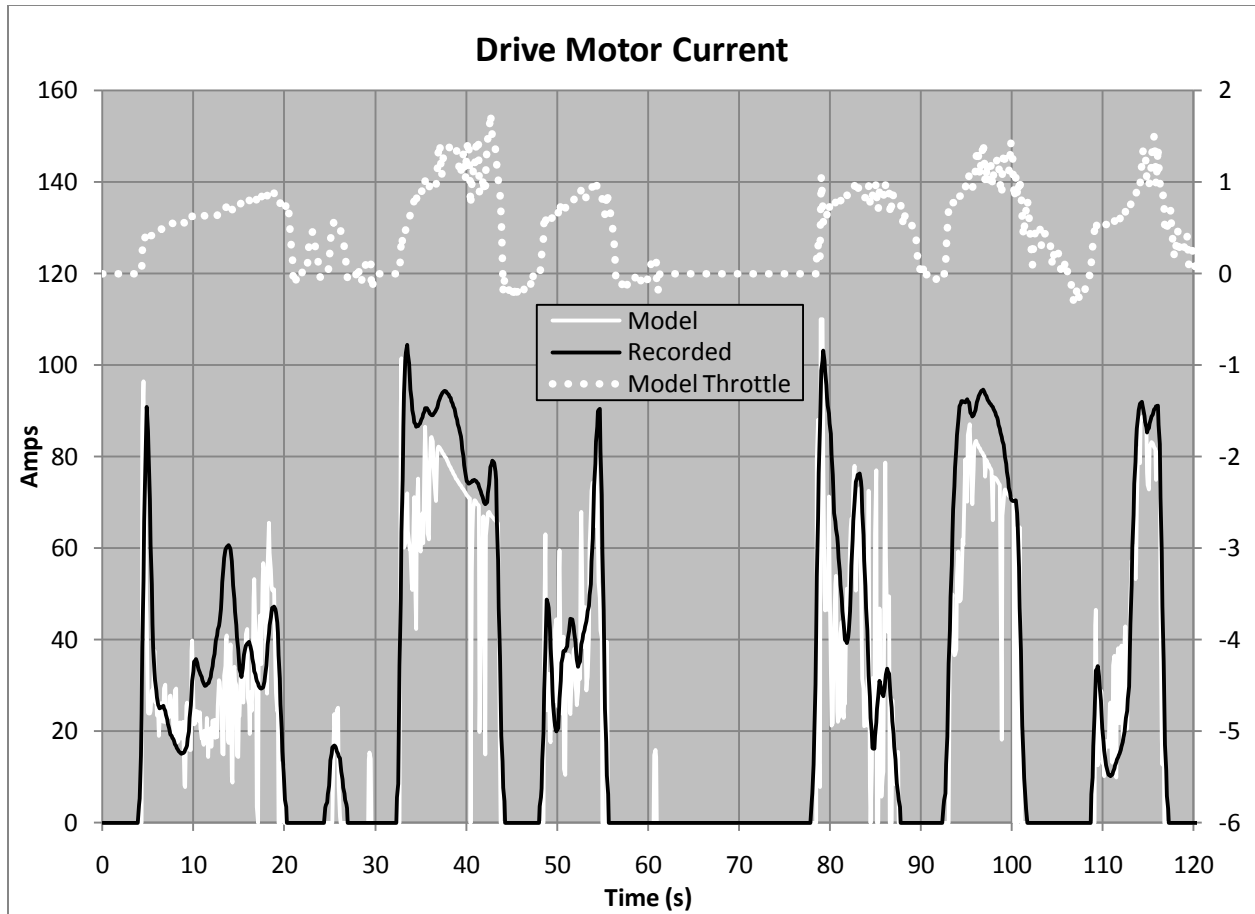


Figure 31: Drive motor current plot for complete model validation.

The drive motor current has proven to be more difficult to reproduce than other model signals. Note that for clarity purposes figure 31 shows a window of only the first 120 seconds of the data. The goal for reproducing the motor current is to capture the natural tendency of the system to limit the motor current below the limit imposed by the controller current limit. In figure 31, looking at the peaks beginning at 33 and 93 seconds, it is clear that the model indeed captures this effect. Noting that the throttle signal of the model is above 1 for the duration of these current peaks, the only explanation for the model motor current to be below the controller limit of 110 amps is the natural limiting effect of the system. Although there is some error present with the model's ability to capture the effect, the fact that it indeed does capture it, is the basic necessity for the powertrain investigation. The error present is tolerable since the goal is compare how different CVT and fixed ratio configurations affect the performance of the model as all other parameters are held constant.

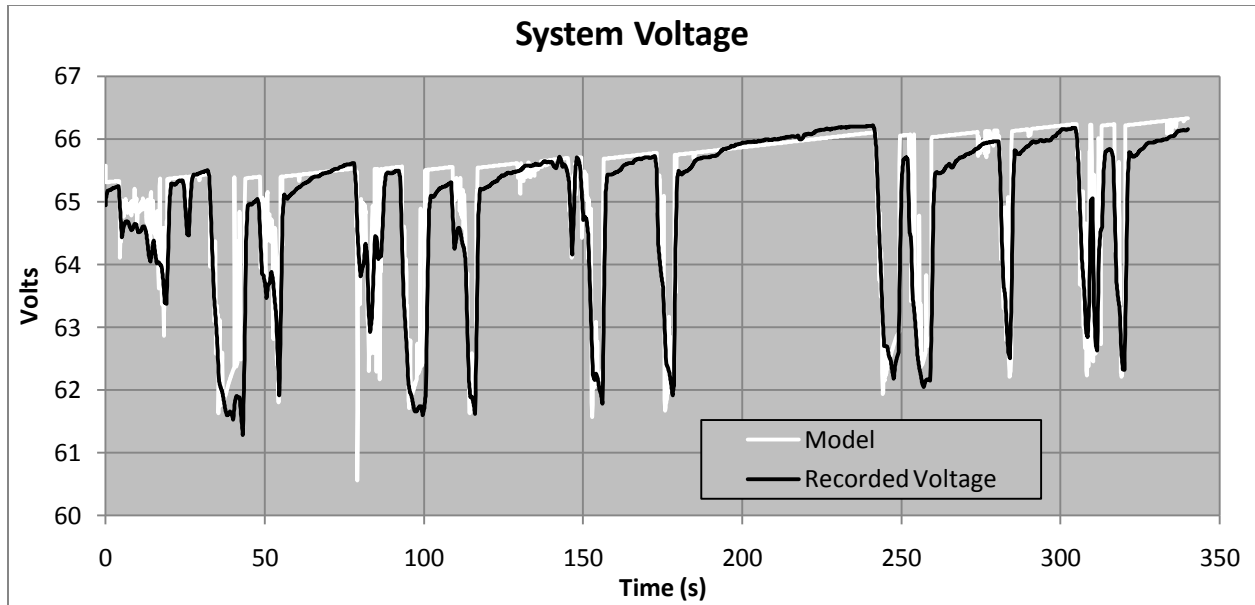


Figure 32: System voltage plot for complete model validation.

Although it may appear from figure 32 that there is significant error present in the system voltage plot, note that the vertical axis is not an absolute scale.

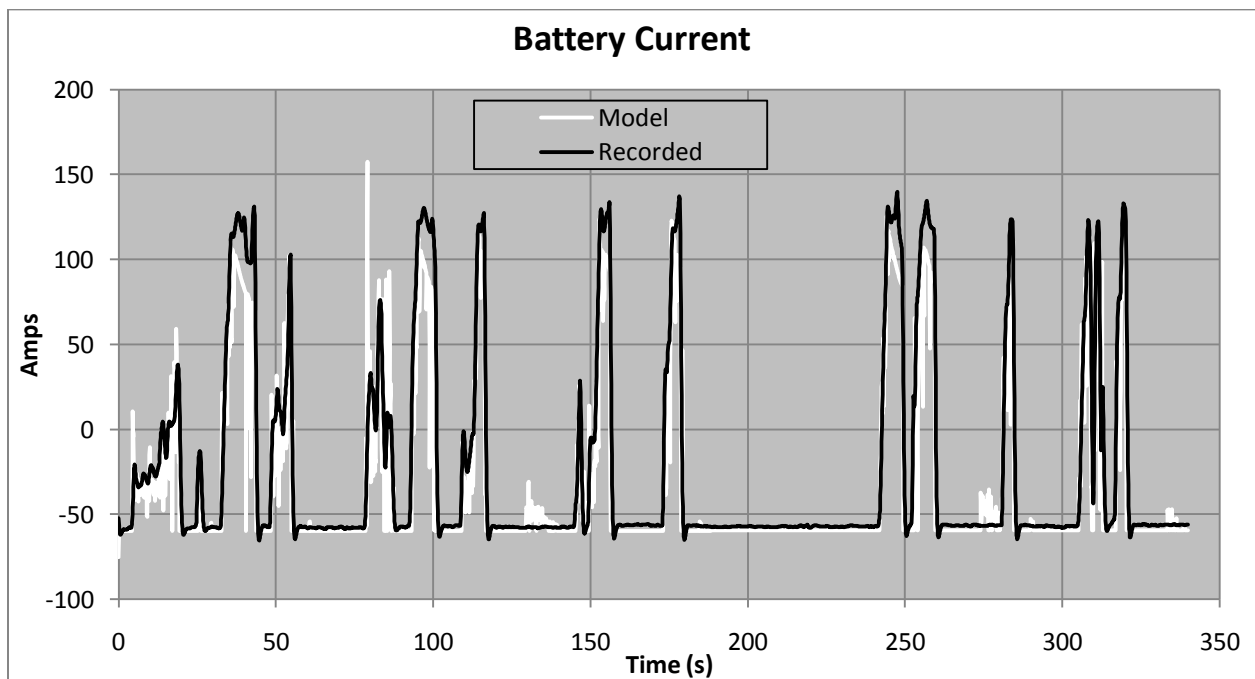


Figure 33: Battery current plot for complete model validation.

For investigations for which components of the vehicle model are the focus, the error in the battery current does not prevent the model from predicting the necessary signals with sufficient

accuracy. The energy system model is included only to provide a system voltage prediction. The system voltage prediction is crucial since as explained in section 3.3.2.1, the motor current and system voltage are interdependent.

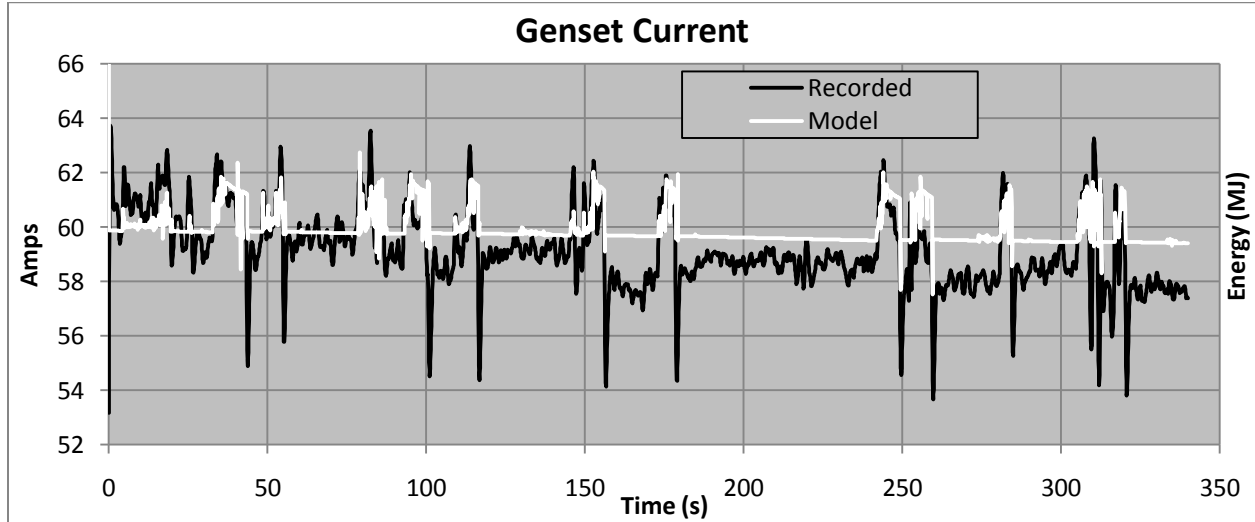


Figure 34: Genset current plot for complete model validation.

Note again that the vertical axis is not an absolute scale which means that the error visible in figure 34 is relatively small.

The vehicle model can also be validated without the energy system model. To validate the vehicle model without the energy system model, it is necessary to input the recorded system voltage as well as the vehicle speed. Validating the vehicle model without the energy system removes error in the output caused by the energy system model (i.e. poor prediction of system voltage). Removing this error allows us to see the influence on the output error in motor current originating from the interaction between the two systems, energy system and vehicle load. Figure 35 shows the average percent error for the selected signals shown in the series of plots above. Error data for the three energy system related signals does not apply for the case in which the vehicle model is validated without the energy system. From figure 35 we see that the error related to the drive motor is almost unaffected by removing the energy system. This confirms the conclusions of section 5.1.3 that the energy system model is capable of very closely reproducing the system voltage for a given load current.

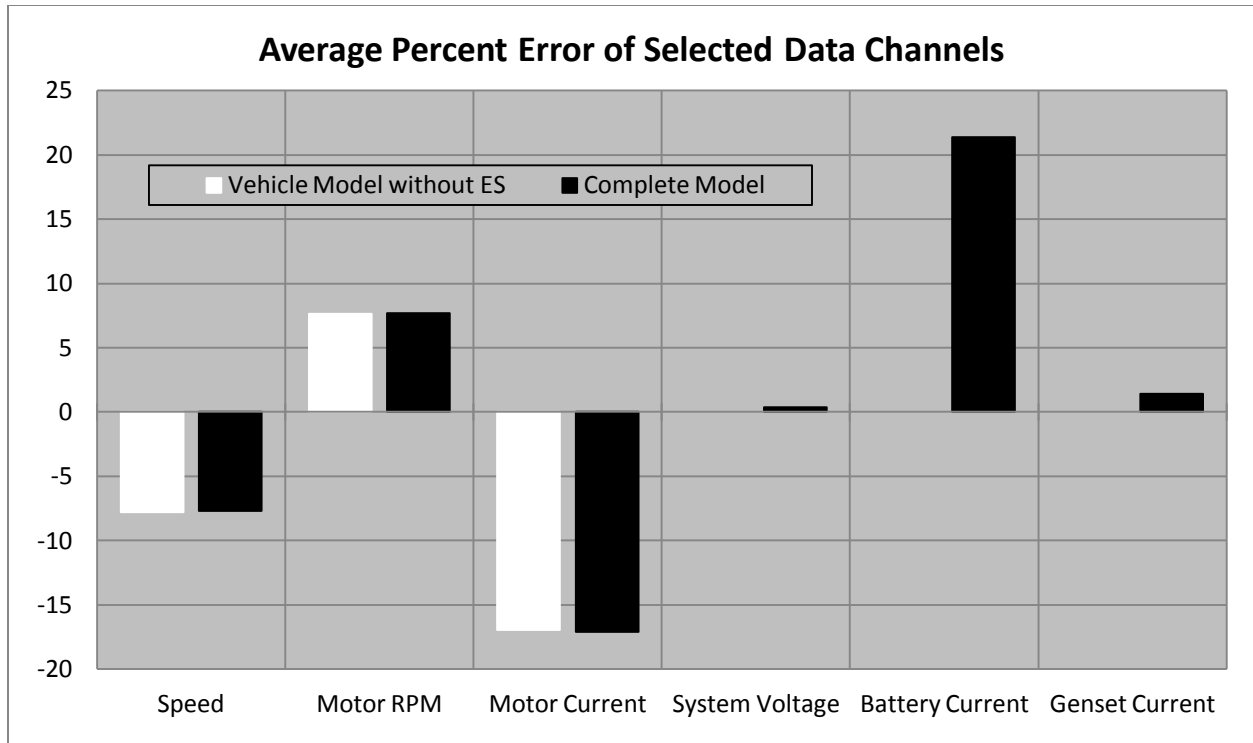


Figure 35: Average percent error of selected data channels for model validation.

Although all effort within the available time and resources was taken to improve the model, figure 35 shows that the prediction for motor current falls outside the criteria set for system level model accuracy. Since the error is negative indicating the model under-estimates the motor current, it will be important to take this into account when examining motor temperature predictions for the powertrain investigation. Also, given the error information here, we must be careful in drawing conclusions based on model predictions of motor current. If predictions for motor current fall within a window of 15%, then drawing conclusions may be risky.

This concludes the validation of the models developed in Simulink for both the genset and powertrain investigations. The model for the energy system presented above along with the load current data from the 2008 FH endurance event provide the necessary tools for genset investigation. The fidelity of the energy system model as shown multiple times in the two validation sections provides us with sufficient confidence that the recommendations of the genset investigation will be useful. Finally, although noticeable error is present in some critical signals for the system model, if we make the assumption that this error will be relatively constant throughout the powertrain investigation, we can be confident that the result will be useful. Since

the goal is to compare the different configurations holding all other parameters constant, the result will show us how the different configurations affect the otherwise unchanged model. It is important to note that since the motor current is heavily dependent on the performance of the CVT model, that the error in predicting motor current may increase or decrease when alternate CVT model maps are used.

5.2 *XMR Model*

The mathematical models of the XMR are not available due to copyrights; however, the vehicle configuration and output of the simulation are available which allows us to draw some conclusions on the validity of the model. The list of parameters which can be modified using the Vehicle Physics software indicate that XMR uses physics based equations to model a vehicle in a three-dimensional environment. For example, from Vehicle Physics, we know that that the forces and moments created at each tire are functions of the slip angle, slip ratio, camber, tire pressure, etc. as would be expected from the current understanding of the physical tire-road interaction. Since there are many parameters used to define the XMR model, the full list of these parameter settings as used for this study is made available in appendix 5.

5.2.1 XMR Vehicle

The main parameter of interest for this study is the torque curve applied to the XMR vehicle model. This curve represents the maximum torque available from the XMR vehicle power source for the entire RPM operating range of the source. For the hybrid powertrain these torque curves are produced from the Simulink model by the process described in section 4.1.2. Figure 36 shows the torque curves for configurations 1 and 21.

Validation of the XMR model is provided by a comparison of an acceleration and coast down cycle from Data Set 3. This validation is conducted by accelerating the XMR model to the same maximum speed as in the acceleration coast down cycle from Data set 3. Figure 36 shows the results of the validation exercise. The validation shows that the XMR model has greater acceleration initially but matches near the end of the acceleration section. This could be due to many factors including but not limited to differences in grip between the actual and simulated road surfaces, difference in grade of the two surfaces, and human error. What is important to note is that under similar conditions, the XMR model reacts in a similar manner to MHRT2.

Although an error analysis demonstrates that the model is within the criteria set for the Simulink models, as noted above, this error is not solely due to deficiencies of the model.

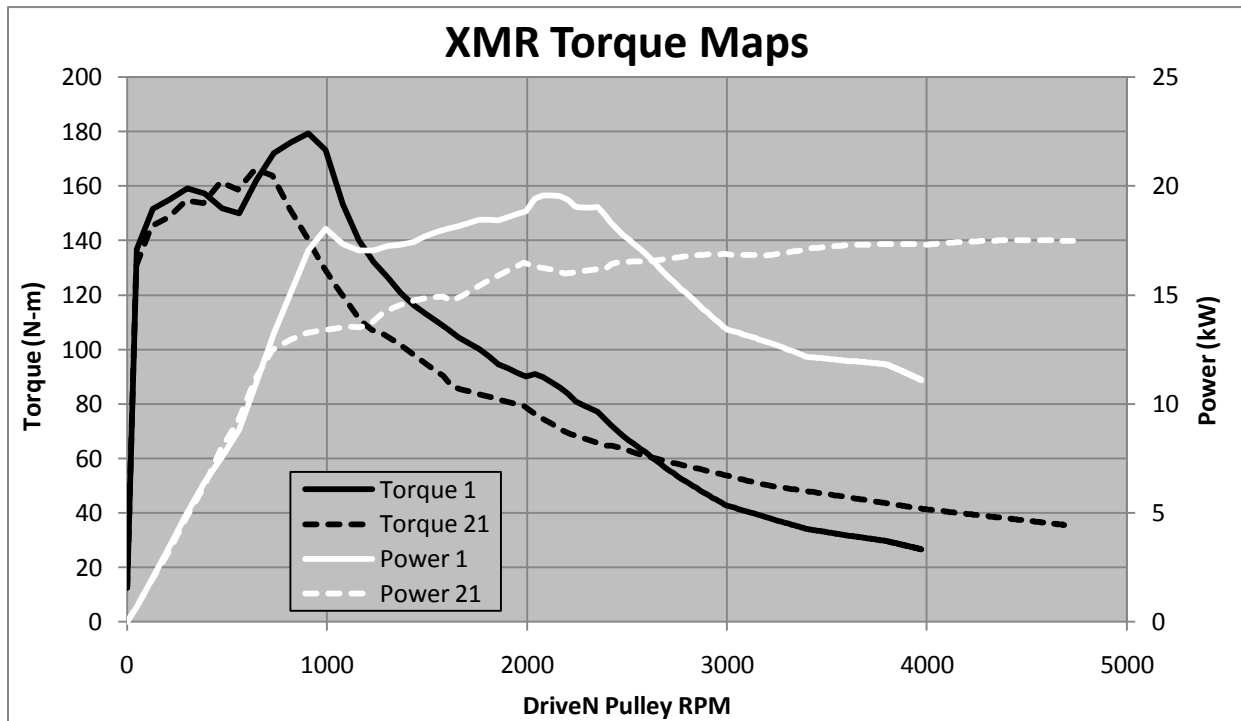


Figure 36: XMR torque maps.

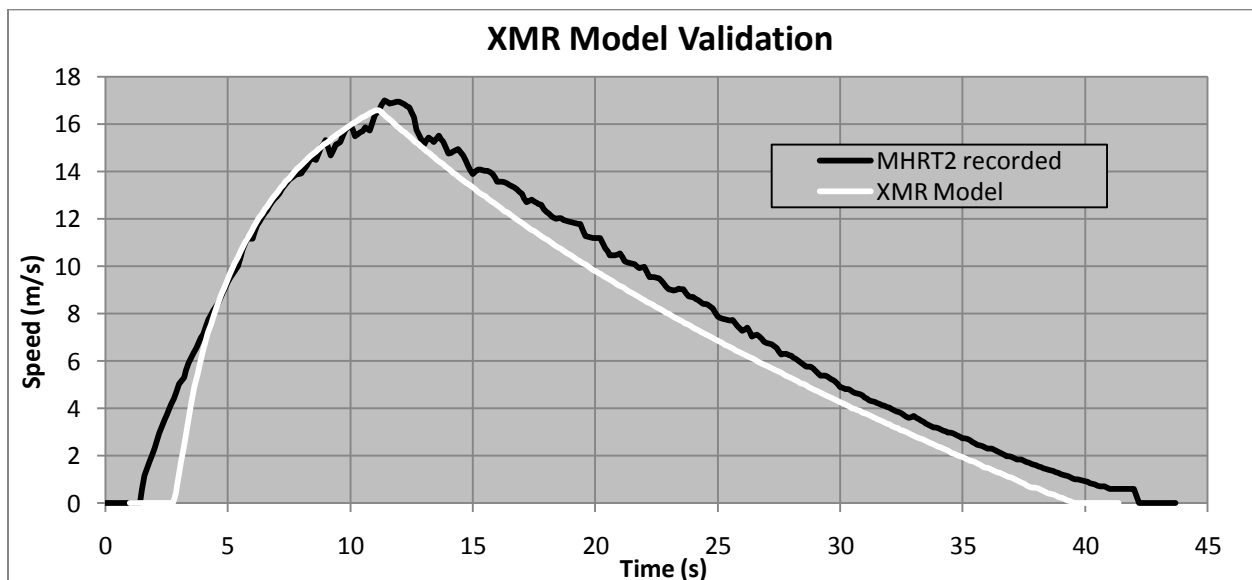


Figure 37: XMR model validation.

5.2.2 XMR Track

The track designed for the powertrain investigation is an attempted recreation of the 2008 FH endurance event race course. This is the most logical choice since a performance evaluation should be performed under conditions which mimic as closely as possible the conditions under which the vehicle will be required to operate. The track geometry was recreated using an aerial photograph of the FH competition grounds and the memory of the MHRT 2008 endurance event drivers. Figure 38 shows a schematic of the course. The total distance around the track is approximately 670 meters and the new lap line is indicated by the short black line crossing the white track path.

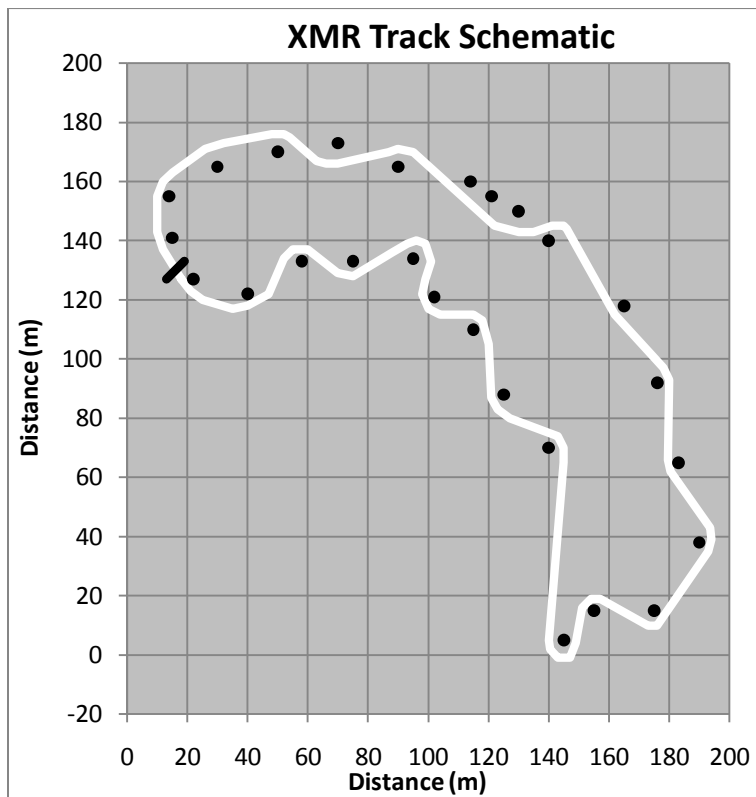


Figure 38: XMR track schematic.

5.3 Chapter Conclusion

A full vehicle model has been created. This model includes the following component models:

1. Engine
2. M/G
3. Battery
4. Drive Motor Controller
5. Drive Motor
6. CVT
7. Vehicle Drag and Inertia
8. Brakes
9. Driver Model

The model created has shown to possess the necessary capabilities to accomplish both specific objectives. Reproducing the natural limiting effect of the powertrain has been accomplished using the Simulink model while realistic behavior is achieved with the racing simulator. These tools coupled together are the resources required to carry out the two drive train investigations outlined in section 3.3.2.

It is also important to note that these models do not contain any special adjustment factors, added components etc. to improve the model. The component models are made to react just as the real components would and assembling them as system model, they interact in a similar fashion as the real system.

6 Drive Train Optimization and Results

6.1 Genset Investigation

The specific objective for the genset investigation is to determine how resources could best be allocated with respect to improving the genset performance. This investigation is performed using the energy system model presented in section 5.1.3, and the load current cycle from the 2008 FH endurance event presented in section 3.3.1.4. The proposed strategy for the investigation is to modify the genset model in ways representative of real possibilities which are of interest to the MHRT. These modified genset models will be coupled with the battery model to form a set of energy system models which will then be run using the load current data from the 2008 FH endurance event. Since the specific objective is to have the genset supply as much energy as possible, we will track the SOC of the battery and compare the results from each run to formulate the conclusions. A baseline run where the genset model is made to mimic the exact operation as in the 2008 endurance event is provided for reference.

The possibilities which are investigated are:

- Genset Possibility 1. The genset is able to run continuously. In this case, the heat issues and all other possible factors which prevent the genset from operating continuously are removed. The genset is operational for the entire duration of drivers A and B, but its operation time during the driver change break is not changed (i.e. charge 1 and 2 remain the same).
- Genset Possibility 2. The engine throttle controller is replaced with a proportional-integral controller acting on the error between engine RPM and the preset no-load RPM, determined by the maximum desired voltage.
- Genset Possibility 3. The engine throttle controller is made to act on the error between the system voltage and a set maximum desired voltage.
- Genset Possibility 4. The engine throttle controller is removed and the throttle is kept constant at its maximum.
- Genset Possibility 5. The mechanical ratio between the engine and the M/G is optimized.

The results of the genset investigation are shown in figure 38. Note that the variation in model prediction is significantly greater than the model error summary presented in section 5.1.3. As it turns out, the 1:1 ratio used for the original genset is near optimal as found from multiple runs with a range of ratios between 0.8 and 1.2 (speed ratio from engine to M/G, i.e. 1.2 means the M/G is rotating 1.2 times the speed of the engine), this data is available in appendix 6. Figure 39 shows that between all possibilities, it is clear that the greatest improvement comes with 1, which is mitigating the temperature issues. Possibility 3, applying the throttle control to the system voltage demonstrates slight improvement while both possibilities 2 and 4 demonstrate equal slightly greater improvement. 2 and 4 demonstrate equal improvement since error signal sent to the PI controller is large and positive due to the inability of the engine to maintain the set RPM value. This continuous positive error saturates the integral portion of the PI controller causing its output to be saturated at full throttle. Finally, combining possibilities 1 and 4, we see the greatest improvement.

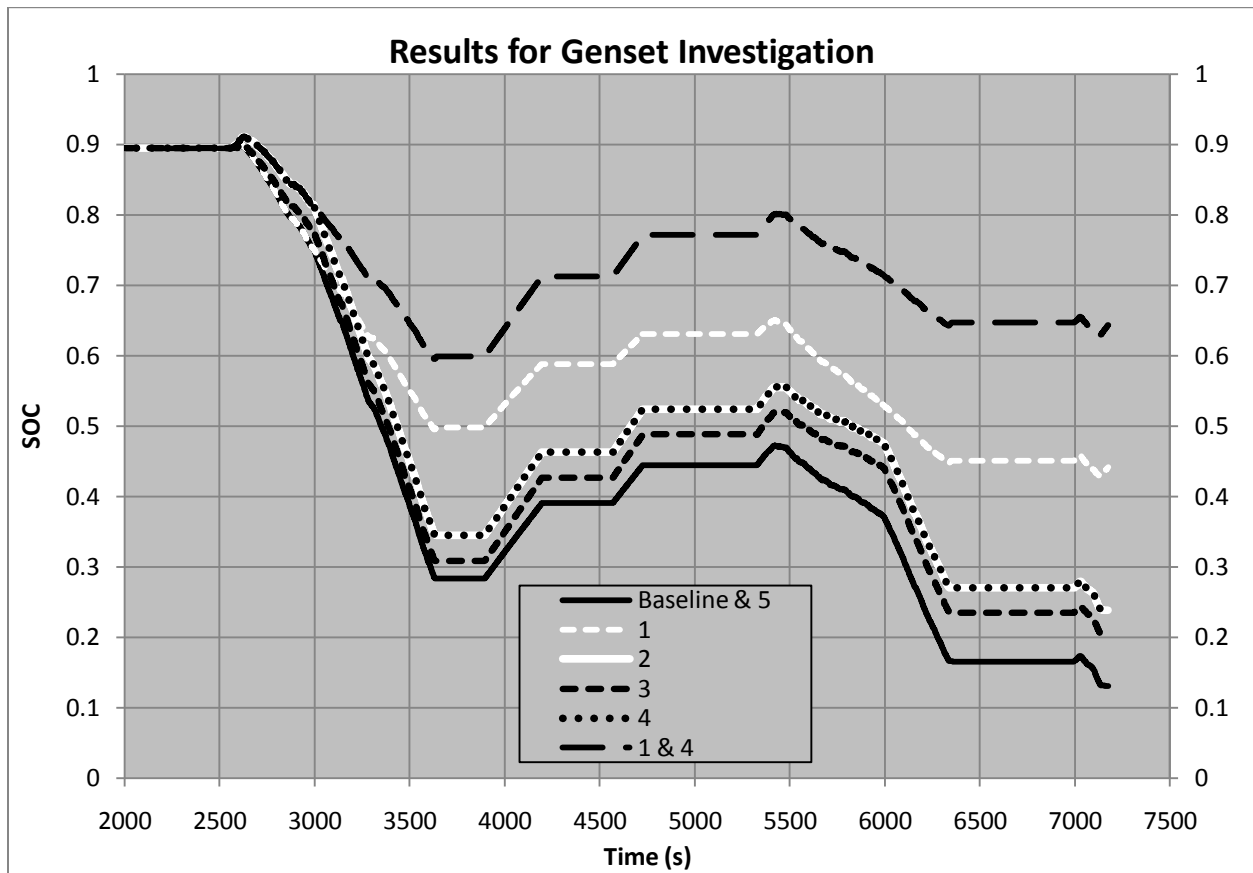


Figure 39: Results for genset investigation.

From these results it is easy to conclude that mitigating the heat issues should be the primary target of any resources devoted to genset improvement. Projects directed at modifying the engine throttle control do not appear to be worthwhile because the results show that the greatest improvements which can be achieved by such means are easily matched by simply constraining the throttle to maximum at all times.

It is important to mention that although it would not be difficult to modify the components of the energy system to investigate the benefits of using a more powerful engine or different cells to make up the battery pack; this is beyond the scope of this study but could be performed in another study using the models presented here.

The conclusions of the genset investigation suggest that efforts placed on improving the genset be focused on mitigating the heat issues such that the genset can operate continuously. Secondly, it suggested that the throttle for the genset be constrained to full throttle for all operation of the genset.

6.1.1 Outcome of MHRT Genset Improvement

Following the conclusion of the genset modeling, the MHRT made the decision to substitute the PMG M/G for the ME0709 M/G and fix the engine throttle at maximum. Following the implementation of these decisions a test was performed to evaluate the reliability of the solution. Figure 40 shows the results of this test. The motor casing temperature was taken from the outer casing surface of the ME0709, the mounting plate temperature was taken from the mounting plate surface near the ME 0709 sprocket; and the genset frame temperature was taken at a point on the frame approximately between the ME0709 and the engine. As we can see from the plot the ME casing and the frame temperatures approach steady state near the end of the test. The face plate temperature is still rising but appears to be leveling off. The total length of the test is approximately 25 minutes indicating that the solution should be sufficient for an FH endurance event during which driving sessions are 30 minutes maximum.

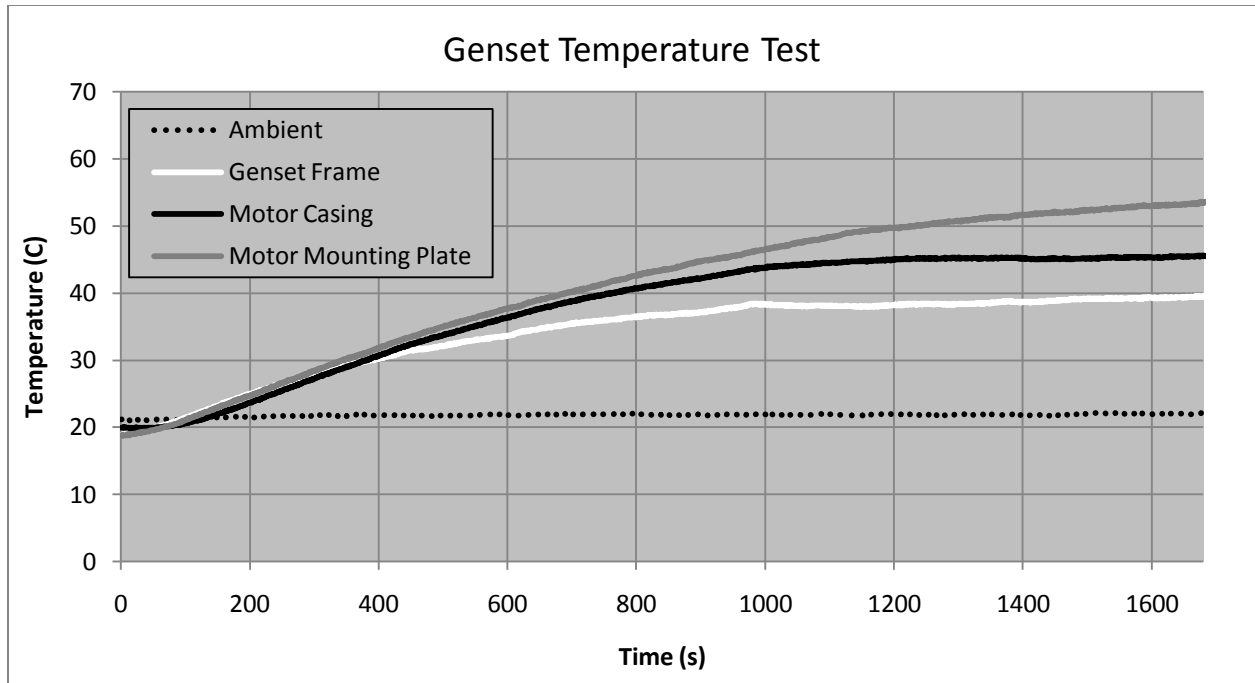


Figure 40: Genset Thermal Testing Results.

6.2 Powertrain Investigation

As described in chapter 2, the powertrain investigation involves ranking 24 different powertrain configurations using the XMR and Simulink models according to the procedure described in chapter 3. The criteria selected to compare the 24 configurations is based on the point scheme of the 2009 FH competition. Factors such as reliability, drivability, and acceleration play the major roles as the deciding factors. A weighted decision matrix is employed to provide insight into the relative performance of the different configurations.

6.2.1 XMR Trials

Two sets of trials were conducted with the XMR simulator to rank the 24 configurations in terms of fastest lap time. All efforts were made to provide equal opportunity to all configurations. The first set involved completing between 10 and 20 laps with each configuration such that the driver felt confident that lap times could not be significantly improved. This first set of trails was then compared by plotting the 3 best lap times as well as their average for all configurations. The first set of trials was conducted with the vehicle in slight under steer configuration; the suspension was modified to have slight over steer for the following set of trails. The suspension adjustments

were made to see how this might affect the ranking of the different configurations from the first set of trials. The second set of trials was conducted in order of the fastest configuration first, moving to the next fastest and so on. This way, the configurations which produced slower lap times in the first trial set were given an advantage as the driver became more accustomed to the new vehicle settings. Table 14 presents the identification used for the different configurations and figure 41 shows the result from both sets of trials.

Table 14: Powertrain configuration identification table.

	Fixed Ratio					
	3.21	3.46	3.75	4.29	4.62	5
CVT1	1	2	3	4	5	6
CVT2	7	8	9	10	11	12
CVT3	13	14	15	16	17	18
CVT4	19	20	21	22	23	24

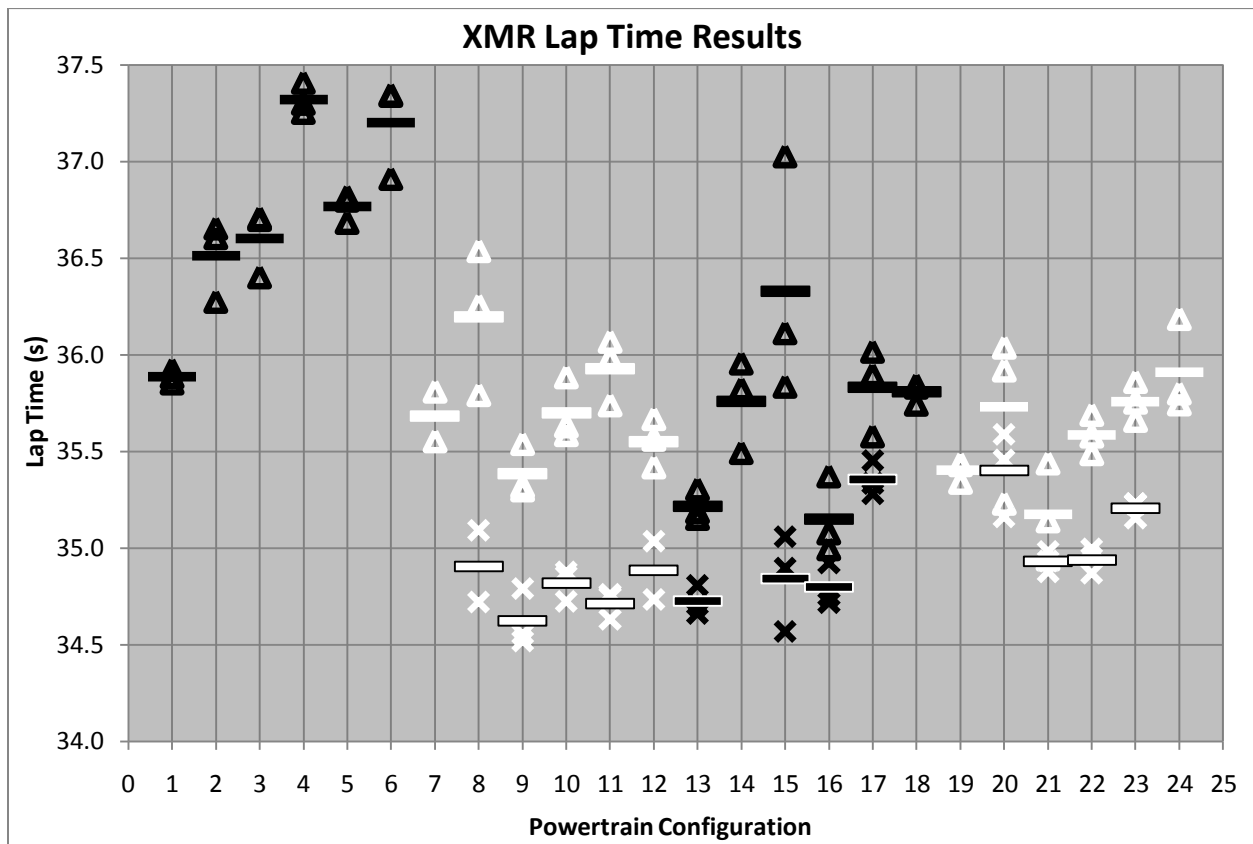


Figure 41: XMR lap time results. See text for plot marker description.

In figure 41 the lap times for the first trial set are shown as Δ , and those for the second set shown as X. The alternating color pattern helps identify the configurations by CVT number. Averages for each lap time group are indicated by bars. Average bars for the second trial set are shown with outlines in the opposite color to avoid confusion with average bars from the first trial set. The cumulative distance driven for both trial sets was approximately 850 km which for a lap distance of 670 m equates to well over 1000 laps.

For the second trial set there are eleven configurations which are not included, within these eleven are all six for CVT1. CVT1 was not included in second trial set because of its poor performance in the first set. In addition, the decision was made that CVT1 would not be included in further analysis unless all other configurations demonstrated severe negative impacts on the vehicle performance or reliability.

Note that besides the data for CVT1, there is almost no correlation between lap time and the fixed ratio. A slight pattern is noticeable for ratios 3.75 and 4.29 as they perform well for CVTs 2, 3, and 4; however, this is not sufficient to draw solid conclusions. Finally, noting that the average lap times for the 10 fastest configurations fall within the 34.5 to 35 second range, is it clear that other factors affecting the vehicle will necessarily need to play a role in selecting the final configuration. The apparent minimum lap time of approximately 34.5 seconds could be due to the performance limits of the simulated vehicle on the given course, or similarly the skill of the drivers with the given simulated vehicle and course. The fact that ten out of twenty configurations produce best average lap time all within 2.3 % of each other seems unlikely to be a result arising from similar effect on total vehicle ability and performance. Noting that a suspension setup modification between rounds one and two of the XMR trials produced improved laps times for most configurations, this suggests that maybe a third round would shed even more light on the difference in performance between the fastest ten configurations. Other possibilities include changing the course to see which configurations improve lap time for a more open course, and which improve lap time for a slower course. Examining either of these possibilities is left for future work. Further analysis will only include the ten fastest configurations from trial set 2. The lap time data from trial set 2 is used as the drivability criteria for the decision matrix.

6.2.2 Simulink Output

The figures 42 and 43 show the motor temperature and SOC estimates for the 10 configurations producing the fastest lap times in trial set 2. The majority of the plots are shown in black since the amount of overlap does not allow for much detail. With the majority of the plots black, configuration 9 shown in white, is highlighted demonstrating the general trend followed by all plots. Also, the plots making the lower and upper bound for each figure have been identified by dotted or dashed lines. Tabulated data is provided in table 16 for the final values for SOC and average values for motor temperature taken near the end of the second session.

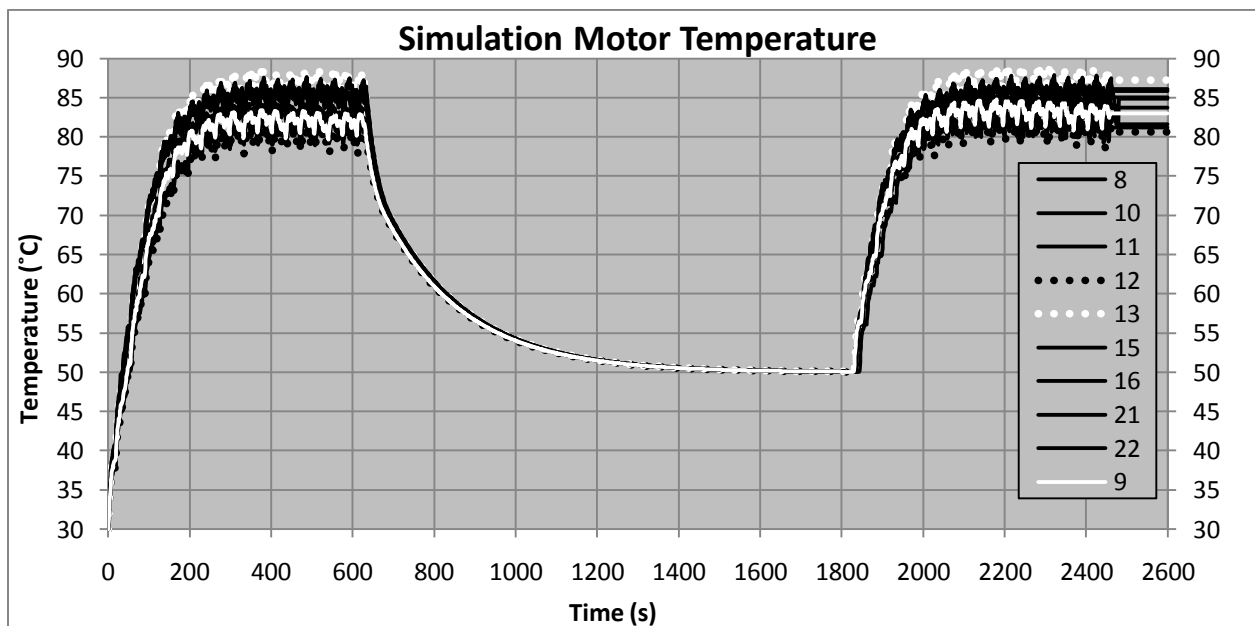


Figure 42: Powertrain investigation motor temperature output.

Note that the motor temperature approaches an asymptote near 50 degrees Celsius as the motors cool down during the driver change period. This matter is discussed in section 5.1.4.2. The maximum temperature suggested by the motor manufacturer is 120 degrees Celsius. The fact that none of the plots approach the maximum temperature does not necessarily mean that motor temperature can be disregarded. As we saw in section 5.1.6, motor current is underestimated by the model by approximately 15%; therefore, since motor current is the sole input into the temperature tracking model, it is safe to assume that the actual motor may become 5 - 20% hotter than shown in figure 42. Such an increase from the model prediction would bring the hotter predictions close to the limit.

The SOC plots also demonstrate a relatively small span between the upper and lower bounds. The data between 1800 and 2400 seconds suggests that in general approximately 30 % of the battery capacity is required for one driving session. This places some importance on SOC as a deciding factor because in the event that the genset cannot operate for the same period of time as assumed for the simulation, SOC will drop further, thus decreasing the margin of safety before the BMS shuts the pack off.

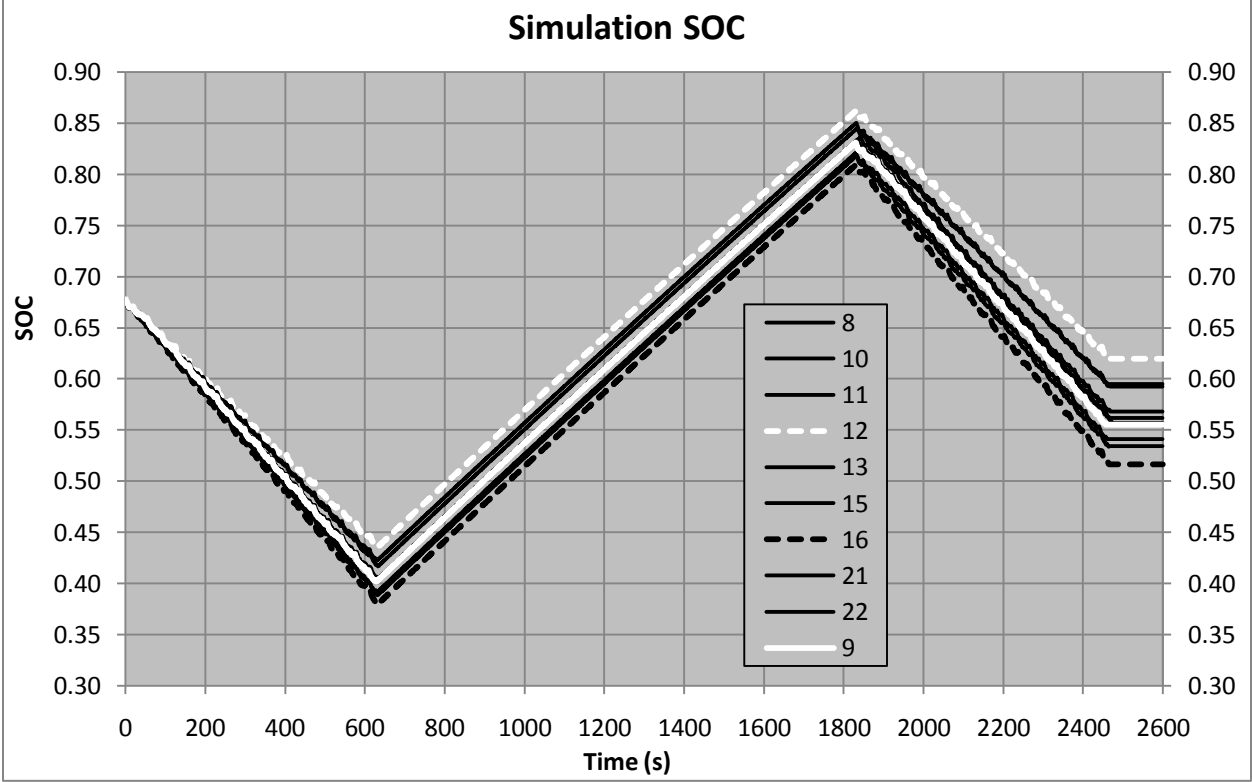


Figure 43: Powertrain investigation SOC output.

Figures 44 and 45 graphically demonstrate the variation in the final values of motor temperature and SOC produced by the Simulink simulations. This data is also provided in table 16.

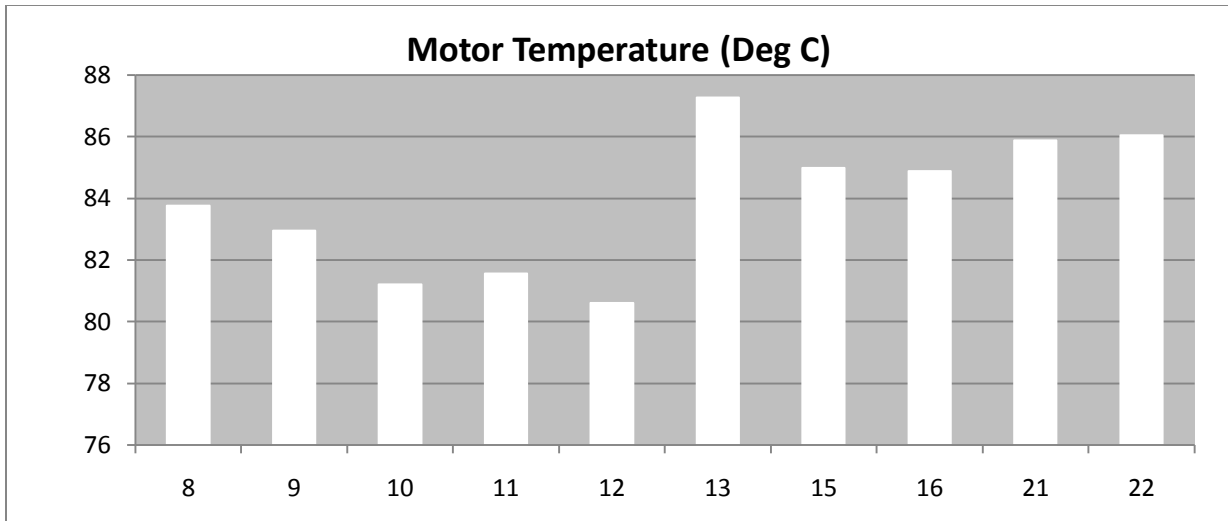


Figure 44: Bar graph of motor temperatures from powertrain investigation.

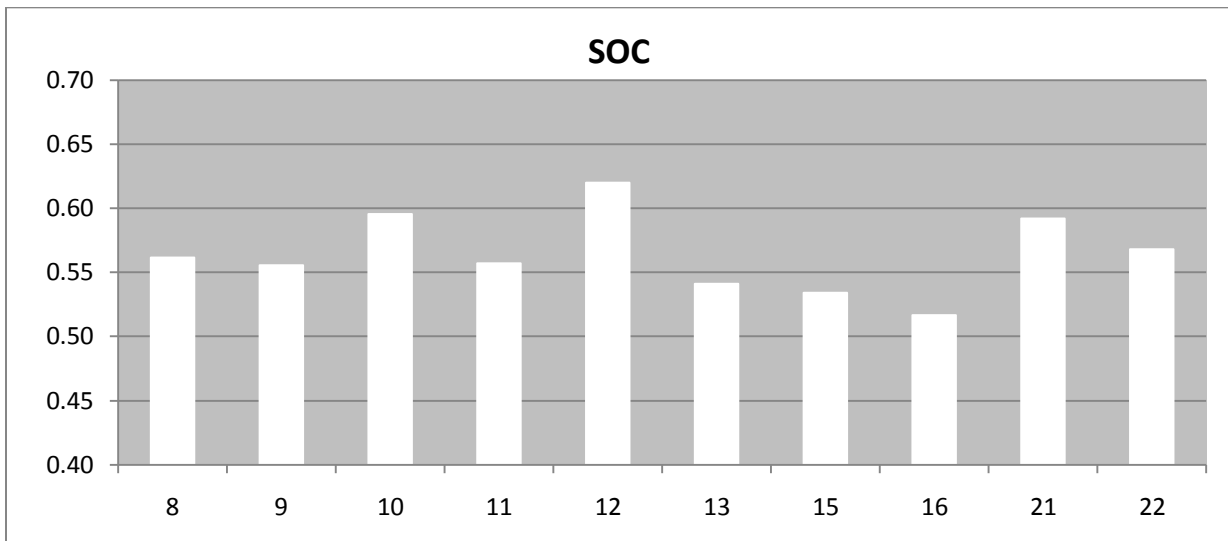


Figure 45: Bar graph of final SOC values from powertrain investigation.

The ranking of the different configurations according their final values for SOC and motor temp will each serve as a criterion for the decision matrix.

Using the Simulink model by itself, we can also perform simulations of the FH acceleration event for the 10 configurations of interest, figure 46 summarizes the results. Note the inverse correlation between the acceleration results and the motor temperature values. This observation fits with our expectations that short acceleration times require large motor torque, and hence large motor current. This greater availability of torque and current causes the motor to be hotter

in comparison. The acceleration data serves as the fourth and final criterion for the decision matrix.

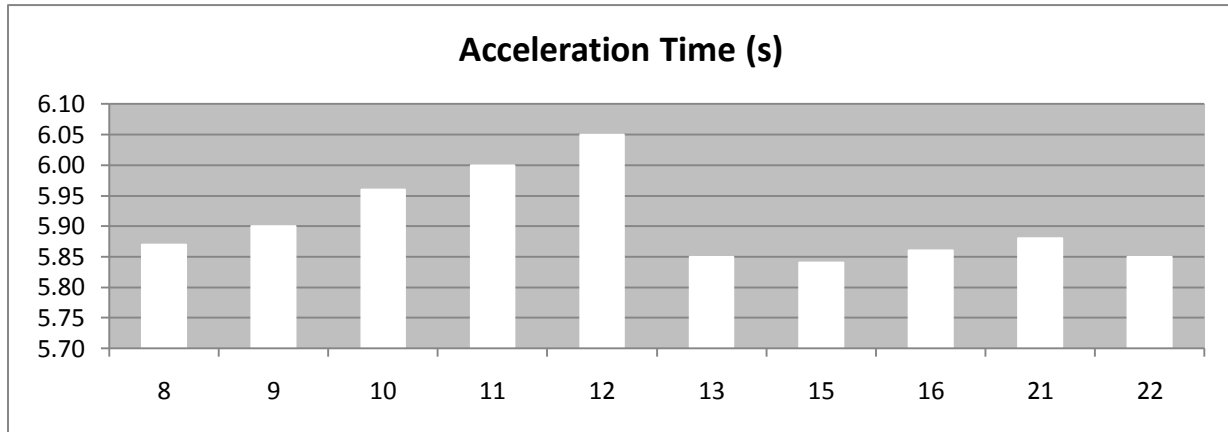


Figure 46: Acceleration results for the powertrain investigation.

The predicted amount of fuel consumed by the genset during the endurance event is reviewed here; however, this factor is not considered as one of the criteria for this investigation since in section 3.3.2, efficiency was not found to be a weakness of the previous MHRT vehicles. The simulations predict that the difference for the volume of fuel consumed for each configuration is very small. The fuel consumption rate during the endurance event is constant because the genset operates at almost constant power output for duration of the simulation. The difference in fuel consumed therefore comes from the different lengths of time required for each configuration to complete 22 km. A summary of the fuel consumption estimates is provided in table 15.

Table 15: Fuel consumption data for the powertrain investigation.

Fuel Consumption (liters)			
Max	Min	Average	Standard Deviation
1.420	1.408	1.412	0.00352

6.2.3 Powertrain Investigation Conclusion

To compile the information provided by the XMR and Simulink simulations, a weighted decision matrix is used to rank the 10 powertrain configurations against the 4 criteria simultaneously. The criteria are: acceleration time, lap time, final SOC value, and the average motor temperature as seen during sustained driving. The weights assigned to the criteria are effectively a judgment

decision made by the designer(s) of the MHRT vehicles. The individual assignment of weights to the criteria determines the importance that the designer feels the criteria has on the success of the vehicle in the FH dynamic events. Since assigning the weightings is based on judgment, 4 top members of the MHRT including the author have each provided a weighting scheme with a maximum point weight of ten points. The decision matrix will be evaluated for each scheme to see how sensitive the outcome is to different weighting schemes. The weighting schemes are presented in figure 47.

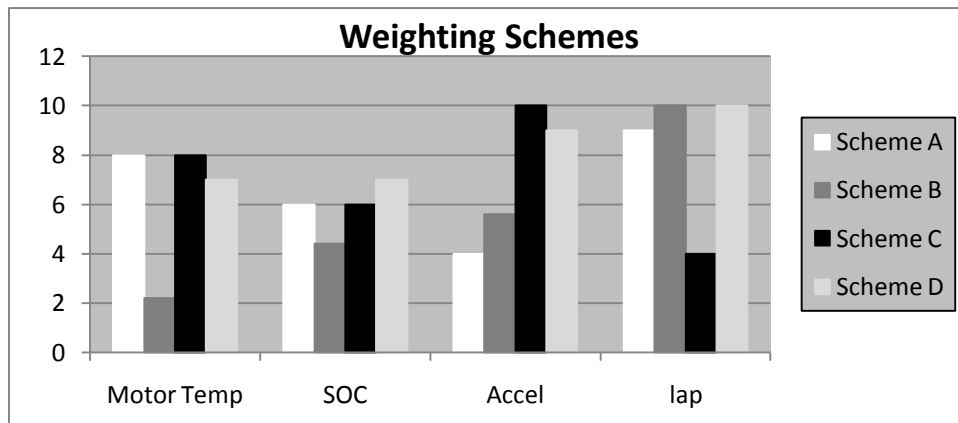


Figure 47: Bar graph of decision matrix weighting schemes.

Note that the different weighting schemes do not resemble each other. Although the dissimilarity of the weighting schemes is unintentional, it is convenient in that it allows us to see how the decision matrix is affected by the different inputs. Table 16 shows the tabulated results of the four criteria as well as the scores and outcomes from applying the 4 weighting schemes. As we can see from table 16, configuration 9 shows consistent dominance over the other configurations regardless of the weighting. This demonstrates the insensitivity of the outcome to the weighting scheme applied to the four criteria. Such an outcome allows us to make the final decision quite easily with the confidence that configuration 9 is the best choice. This confidence is of course limited by the accuracy of the models, but in this case, we have greater confidence than the case where the decision matrix outcome does not converge as nicely.

Table 16: Decision matrix for the powertrain investigation.

Criteria		Powertrain Configurations									
		8	9	10	11	12	13	15	16	21	22
Motor Temp. (Deg C)		83.8	83.0	81.2	81.6	80.6	87.3	85.0	84.9	85.9	86.1
SOC		0.562	0.556	0.595	0.557	0.620	0.541	0.534	0.517	0.592	0.568
Acceleration (s)		5.87	5.90	5.96	6.00	6.05	5.85	5.84	5.86	5.88	5.85
Lap Times (s)		34.9	34.6	34.8	34.7	34.9	34.7	34.8	34.8	34.9	34.9
Scheme A	Score	12.0	20.8	13.8	17.9	9.6	14.4	14.5	16.5	6.7	8.3
	Rank	7	1	6	2	8	5	4	3	10	9
Scheme B	Score	9.5	18.2	9.2	13.0	3.9	15.4	13.1	14.7	6.4	7.9
	Rank	6	1	7	5	10	2	4	3	9	8
Scheme C	Score	16.6	20.1	14.5	15.8	8.7	16.8	18.9	19.7	11.5	14.0
	Rank	5	1	7	6	10	4	3	2	9	8
Scheme D	Score	16.4	25.3	15.7	19.5	8.7	20.6	20.3	22.1	10.9	13.3
	Rank	6	1	7	5	10	3	4	2	9	8
All Schemes Combined	Score	54.4	84.3	53.3	66.2	30.9	67.2	66.8	72.9	35.4	43.5
	Rank	6	1	7	5	10	3	4	2	9	8

6.3 MHRT3 Results

As mentioned before, MHRT3 did not perform as expected during the 2009 FH competition. Due to this, it was impossible to make use of the majority of the data gathered during the competition since not much stands to be learned with regards to this study by forcing the models to recreate the poor performance of MHRT3 at the competition. Data set 4 however provides us with much of the needed information upon which we can compare the outcome of the optimization process presented above. In addition to the description provided in section 4.2.1 for data set 4, two additional details which cannot be found in the recorded data are necessary in order for the reader to grasp the full meaning of the data. The first detail has to do with the lack of autocross data for CVT4. The intention was to gather autocross data for an equal number of laps for each CVT, however, approximately half way through the targeted number of laps for CVT4, the BMS shut off the battery due to a cell over temperature error. To avoid this situation a second time, the autocross data taken for CVT4 was limited to four laps. The second detail has to do with the maximum torque that the powertrain is capable of applying at wheels. The observation was made that with CVT4 the vehicle demonstrated the ability to break the tires loose causing them to squeal, indicating large slip ratio. Although this is not solid evidence of greater power

availability, correlating these observations with the data gathered produces interesting conclusions. With the added details we are ready to review the data and compare it to the model output.

6.3.1 MHRT3 Acceleration Performance

Figure 48 shows the vehicle speed and motor current data for the three acceleration runs performed for data set 4. Here the inputs to the model are the initial voltage of the battery before the acceleration run, and the duration of time for which the throttle was maintained at 100%.

Figure 48 clearly illustrates the ability of the model to capture the natural limiting effect on motor current. For all models runs and data shown, the controller motor current limit was set at 200 amps. As we can see, in all cases the motor current initially spikes to 200 amps and then proceeds to the natural limit. For CVT4, the motor current remains at 200 amps indicating that the natural limit may be higher. The interesting conclusion which we can draw from the correlation between the motor current data of figure 48, and the observation of wheel slippage for CVT4 is that of maximum transmissible torque of the CVT at very low vehicle speeds. Since all cases demonstrate the same initial motor current spike, this means that they experienced the same initial motor torque spike. Knowing this, we can conclude that CVT4 must pass greater torque at lower speeds since this is the only configuration which consistently caused the tires to break loose. This notion is consistent with the expectation that heavier weights and a softer spring will tend to produce a greater clamping force on the CVT belt at the DriveR pulley.

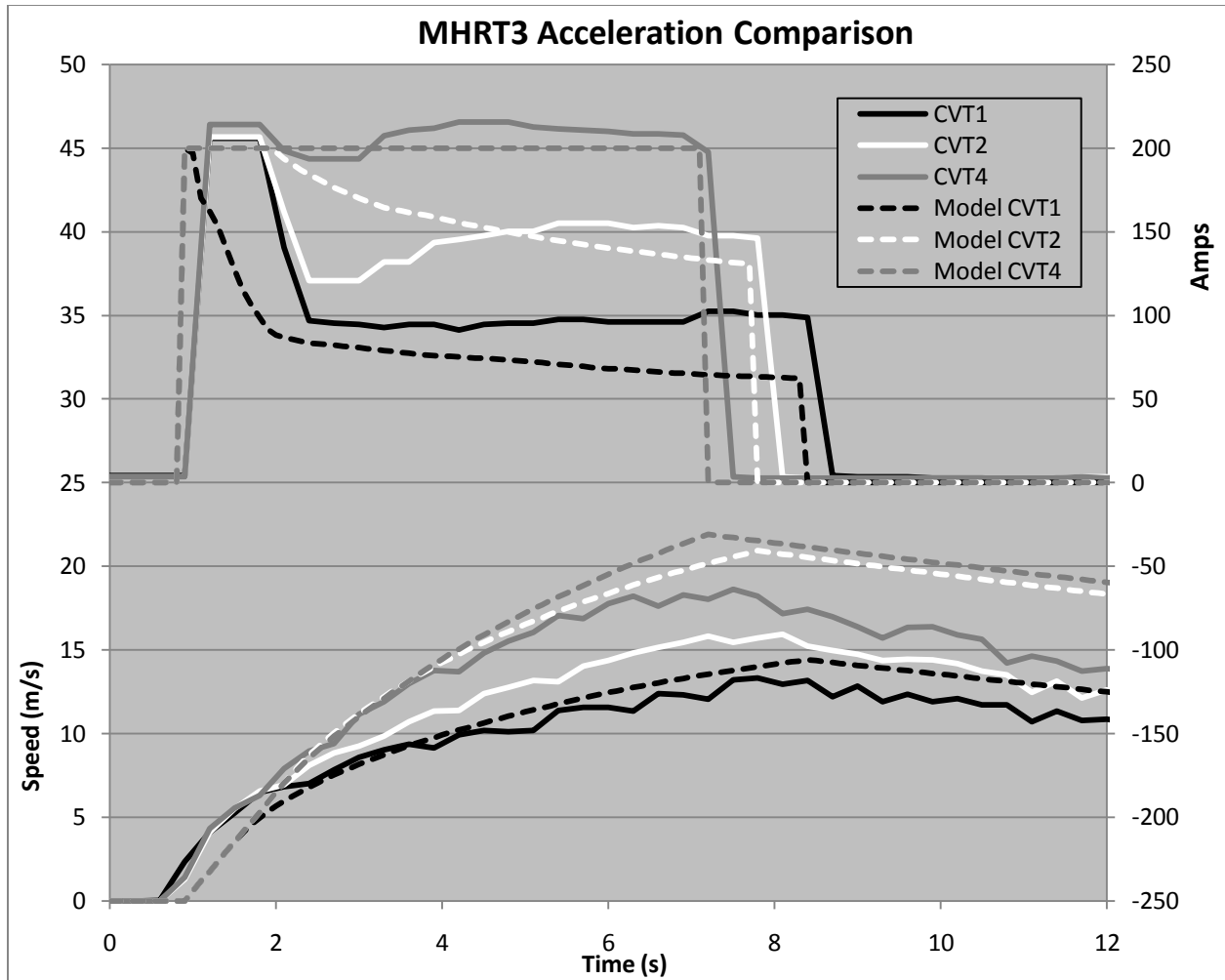


Figure 48: MHRT3 and model acceleration data.

Also from figure 48 we see that there is noticeable difference in speed between the model and the recorded data for CVT2. This difference originates from the motor RPM and output torque maps of the CVT model. This conclusion is fair since we see that for CVT1, motor current is under estimated but the speed curve matches fairly well. For CVT4, the motor current is only slightly under estimated, while the model speed is slightly over estimated. The model run for CVT2 significantly over estimates the motor current, it therefore makes sense that it would over estimated the vehicle speed as well. Note that for all configurations the model demonstrated greater energy conversion efficiency between the motor and the road than did the MHRT3 prototype. To investigate this further, we can compare the drag relationship developed for MHRT2 with a drag relationship developed using the MHRT3 data. Figure 49 shows a comparison of the drag relationships.

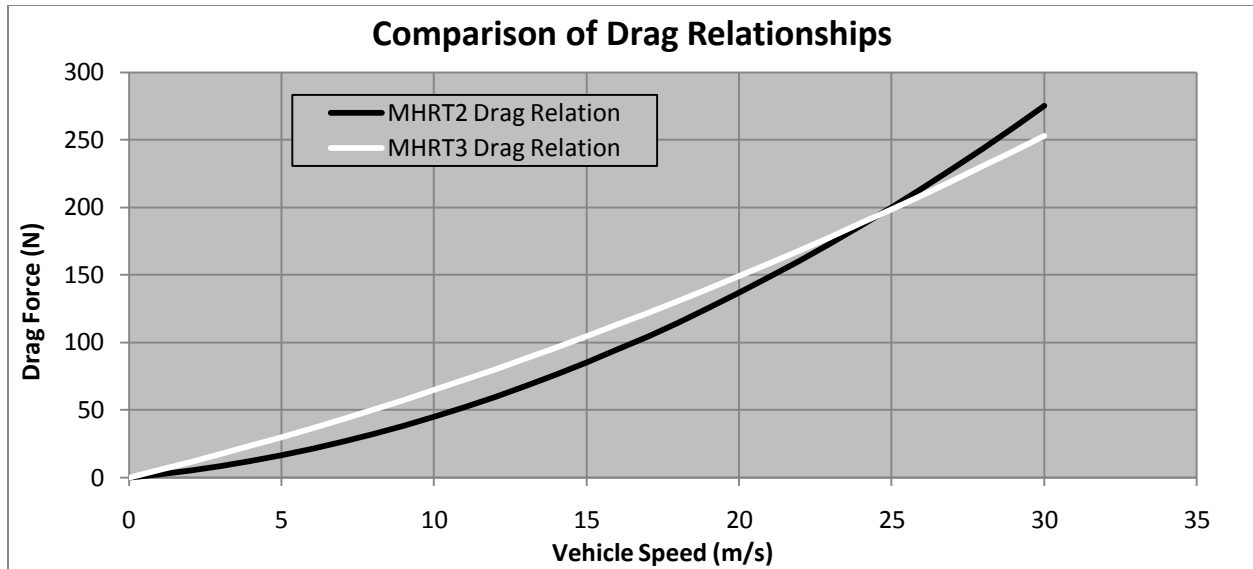


Figure 49: Comparison of drag relationships for MHRT2 and MHRT3.

The MHRT3 relationship does demonstrate greater drag below 25 m/s which provides some of the explanation for the difference between the models and the data for MHRT3. Rerunning the model with the MHRT3 drag relationship however does not noticeably affect the output; therefore there must be other factors creating the difference. The difference between the two is that of torque loss, a greater amount of torque is lost somewhere in powertrain for the recorded data. For the recorded data, we can calculate the torque at several locations along the powertrain using component relationships presented in section 5.1.4; however, we will not see anything new in doing so since we will not be creating any new data, just modifying the available data. What we will see is that areas which currently demonstrate agreement will continue to agree, while areas where we see disagreement will remain in disagreement. Effectively, what we need in order to determine where this discrepancy arises is recorded torque data at several points along the powertrain, for example at each end of the half shafts, each end of the fixed ratio, etc. Without further recorded information of the torque flows we cannot draw further conclusions about the difference in the motor to road efficiency between the model and the prototype.

6.3.2 MHRT3 Lap Performance

Data set 4 contains the data for 22 laps with CVT2, 4 laps with CVT4, and 4 laps with CVT1. The laps for CVT2 were conducted first, followed by those with CVT4, and finally CVT1. All were conducted with a fixed ratio of 3.75. Table 17 provides a statistical analysis of vehicle

speeds for three separate scenarios to show how the speeds of data set 4 compare to that of the simulations and the 2009 FH endurance event.

Table 17: Vehicle speed statistics for different tracks.

	2009 Endurance Event	Data Set 4 CVT2	Configuration 9 XMR Simulation	
Maximum Speed	16.5	14.9	22.3	m/s
Minimum Speed	8.3	5.5	4.8	m/s
Average Speed	12.1	9.4	17.6	m/s
Standard Deviation	1.6	1.9	4.3	m/s

As we can see the range of vehicle speeds for the simulation spans those of data set 4 and the 2009 endurance event. Most importantly, the close match between the 2009 endurance speeds and the data set 4 speeds indicates that the track used to gather the data of data set 4 was fairly representative of an FH endurance event race course. The data acquisition system of MHRT3 does not allow us to record lap time directly; however, we can estimate it by calculating the time between the peaks in speed of each lap. A summary of the lap times for data set 4 is provided in table 18.

Table 18: Lap time statistics for data set 4.

	CVT1	CVT2	CVT4	
Best Lap	22.8	20.4	22.2	s
Worst Lap	23.7	23.4	23.4	s
Average Lap	23.2	22.1	22.7	s
Standard Deviation	0.11	0.75	0.2	s

Configuration 9 again produces the fastest lap time, followed by configuration 21, and then configuration 3. The fact that these lap times match the order presented in figure 41 is not necessarily entirely due to the powertrain performance. The fact that Configuration 9 recorded the best time here could be due to the greater number of laps driven, hence giving configuration 9 a statistical advantage and greater driver experience. Otherwise, noting that configuration 21 has greater acceleration; one might suspect that the lap times may be slower simply because the driver had greater difficulty keeping control. If this is the case then we would expect that

eventually this powertrain would produce the fastest lap times as the driver became accustomed to the available power.

However, only taking into account the power availability leaves out the important detail noted at the beginning of this section. The fact that configuration 21 with CVT4 cause a cell over temperature in the battery pack while configuration 9 with CVT2 did not for approximately twice the amount of laps, indicates that the driver would have to learn far more about the vehicle before producing consistent faster lap times with the reliability demonstrated by configuration 9. Many different scenarios for power control and component cooling can be imagined to mitigate the issues demonstrated by configuration 21 in order to make use of the greater power availability of configuration 21. The decision as to which scenario best fits the MHRT is left to future MHRT designers with suggestion that increased ventilation of cells within the battery pack be investigated.

In conclusion, given that overheating the battery was not considered as a possibility for this study, the fact that the final decision for the powertrain included criteria based on motor temperature and SOC as proxies for the system duty cycle was in retrospect a safe and well made decision.

6.3.2.1 Drive Motor Temperature

Using the CVT2 lap data from data set 4 we can compare motor temperature data with the model output. Figure 50 shows motor temperature data and model output with the corresponding vehicle speed for each. As we can see, given the same initial temperature, both the model and the data agree quite favorably near the end of the 22 laps; however two aspects of the motor temperature model need to be addressed. First, it does appear that if the data were to continue, the model would reach equilibrium at a lower temperature than the real motors. This could be due to the under estimation of motor current by the model however, section 6.3.1 shows that the model over estimates motor current for CVT2 therefore more information is required in order to draw any conclusions. The temperature map should be expanded to include motor temperatures (relative to ambient) beyond the required limits to ensure that the model is not restricting the range of the signal produced. This could prove extremely expensive if destructive testing is found to be the only means to do so, if this is the case, then perhaps an analytical model should be explored.

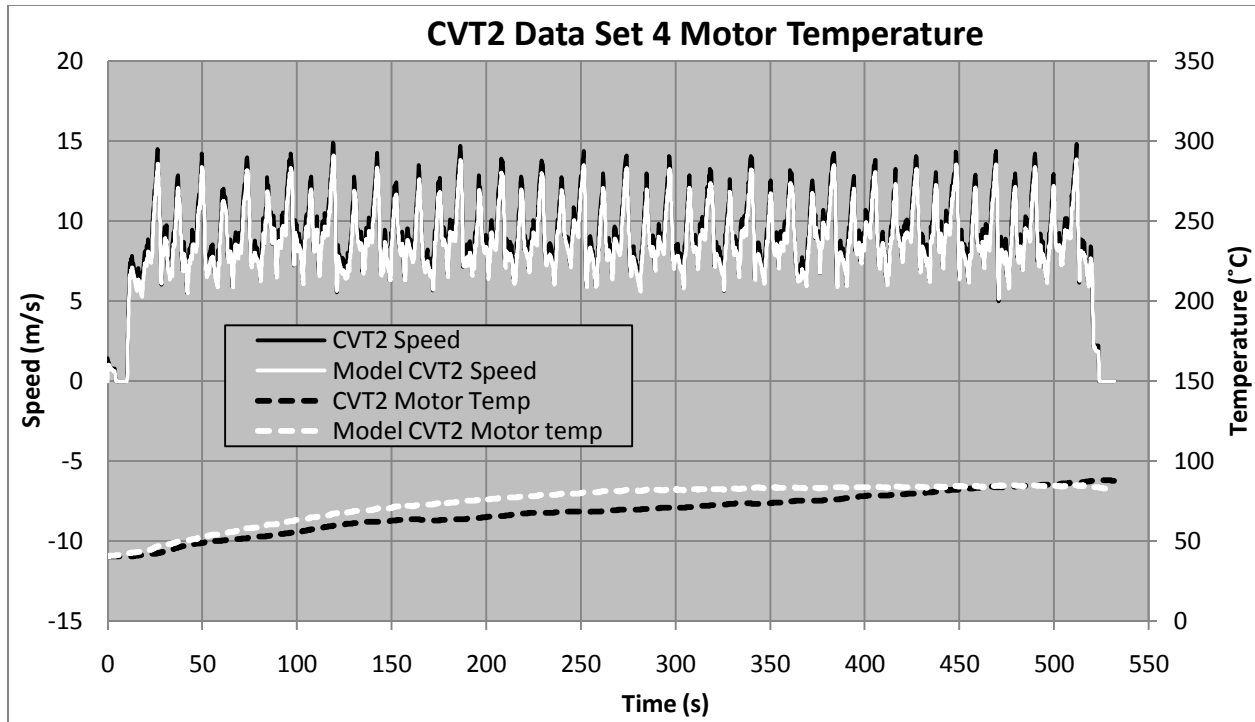


Figure 50: Motor temperature data and model validation for data set 4.

6.4 Chapter Conclusion

Comparison of the optimization predictions with prototype data demonstrates that the models and methodology have proven to be powerful means to improve the performance of the MHRT vehicle. Deriving quantitative results for the improvement is difficult since MHRT 3 cannot be directly compared to MHRT2¹⁵; however, from data set 4 and the added information regarding battery over heating it appears that for configuration 9 the reliability for the drive train has not been affected while performance has been improved. Therefore it is fair to state that implementing the methodology developed for this study has realized significant improvement of the powertrain without compromising reliability.

¹⁵ MHRT2 and MHRT3 share several major components, for example, battery, genset, drive motors, CVTs etc.

7 Conclusion

The objectives of this study are:

1. Identify areas of the drive train where significant improvements are possible.
2. Determine what actions should be taken in order to improve the performance of the MHRT vehicle for the FH dynamic events.
3. Predict the performance improvement of the system.
4. Compare these predictions with measured performance of a second generation prototype.
5. Discuss any discrepancies between predictions and measurements.

Analyzing data from past competitions and from subsequent tests provided the necessary information to accomplish objective number one. The conclusion was that the genset and powertrain were the two major weaknesses of the MHRT vehicle. Completion of objective number two is summarized by the specific objectives derived to eliminate these weaknesses, these specific objectives are:

- A. Mitigate the natural power limitation of the powertrain without compromising the vehicle reliability during an FH endurance event.
- B. Determine how best to allocate resources devoted to genset improvement.

Chapter 6 presents the work performed to accomplish objective 3, 4 and 5. For the genset investigation the prediction was made that mitigating the heat issues should be given all resources dedicated to genset improvement. The simulation and test results both indicate that the genset could produce between two and three times more energy during an endurance event as compared to previously possible. The powertrain investigation provided the necessary performance predictions required for the implementation of the decision matrix to select an optimum configuration. The optimum configuration is defined by the specific objective set for the powertrain investigation, point A above. The predictions of the investigation agreed favorably with subsequent testing of the MHRT3 vehicle. As shown in section 6.3, performance improvement was indeed realized without affecting the vehicle reliability.

The goal of this study has been successfully completed by the work outlined above. Clearly defining the specific objectives of the powertrain and genset investigation provided the necessary

information required to develop an appropriate methodology to achieve the goal. The methodology employing modeling and simulation has been successfully implemented to realize significant improvement in the powertrain as well as to appropriately allocate resources dedicated to genset improvement.

The results of the powertrain investigation in conjunction with the results from MHRT3 show that the configuration of the CVT and fixed ratio can have a significant impact on both the performance and reliability/durability of the vehicle. Given the state of the modeling abilities presented above, it is possible to generate a significant amount of knowledge about how the vehicle will perform in a given event. For certain events, such as acceleration, the available options are fairly obvious, but for events only modestly different than the standard endurance event as described above, simulations could help make the decision between two configurations which have very similar performance. If the simulation capabilities were improved to include added outputs for variables which become known to be important in terms of reliability, such as battery temperature, or performance, such as tire modeling, then the predictive abilities become of even greater value.

In addition to completing the optimization and improvement goals of this study, the simulation capabilities and methodology developed provides future MHRT designers with the tools to optimize the specific powertrain studied here. If MHRT designers desire to investigate alternate powertrain architectures or components, the overall procedure and methodology remain the same and only models need to be modified and validated. The possibilities for improving the capabilities for future work are numerous therefore only the most important ones are mentioned here.

Investigating the possibility of direct patch between the driving simulator and the powertrain simulator is where the greatest benefits are foreseeable. This “all-in-one” software would give real-time information about the drive train under investigation and could significantly reduce the time required to draw conclusions from simulation based investigations. Acquiring a license for rFactor Pro maybe the most logical solution since the Simulink models developed here are already compatible with rFactor Pro.

Investigating replacement options for MATLAB models could also provide several gains. Substituting commercially available powertrain simulation software packages such as PSAT or AVL CRUISE could significantly increase the fidelity of the powertrain simulations. Increased fidelity would place greater confidence in the final conclusions drawn from the simulation based investigations allowing for more precise simulation based design. Whether increased fidelity comes from the substitution of Simulink for alternate software or by increasing the fidelity of the existing Simulink models; this approach will most certainly be necessary for further refinement of the current powertrain. If the powertrain architecture becomes the topic of investigation clearly the Simulink models will require modification. At this point, employing alternate software may not be a significant increase in effort.

8 Bibliography

1. **F1.** Rules & Regulations: Formula One. *Formula One*. [Online] 2009. [Cited: 07 15, 2009.] http://www.formula1.com/inside_f1/rules_and_regulations/sporting_regulations/8692/fia.html.
2. **ATA.** Formula EHI. [Online] 2008. [Cited: 07 15, 2009.] <http://www.ata.it/it/formulaata/25/formula-ehi/>.
3. **Washburn, Wynne C.** About: Formula Hybrid. *Formula Hybrid*. [Online] 2009. [Cited: 07 15, 2009.] <http://www.formula-hybrid.org/about.php>.
4. *Effeiciency Analysis of an Electric Delivery Truck using Computer Modeling and Simulation.* **Mathews, Albert.** France : IFP, 2008. International Conference on Advances in Hybrid Powertrains.
5. *Model-Based Design Approaches for Plug-In Hybrid Vehicle Design.* **Mendes, C.** Winnipeg : PHEV 2007, 2007.
6. *PHEV Hymotion Prius Model Validation and Control Improvements.* **Cao, Qiandong.** Costa-Mesa : s.n., 2001. Future Transportation Technology Conference.
7. *Automated Model Generation for Hybrid Vehicles Within a Hardware-in-the-Loop Environment.* **Verdonck, Nicolas.** France : IFP, 2008. International Conference on Advances in Hybrid Powertrains.
8. *HARDWARE IN THE LOOP PLATFORM DEVELOPMENT FOR HYBRID VEHICLES.* **Wilhelm, Erik.** Winnipeg : s.n., 2007. PHEV 2007.
9. **rFactor-Pro.** Brochure: rFactor-Pro. *rFactor-Pro*. [Online] 2008. [Cited: 07 15, 2009.] <http://www.rfactor-pro.com/rFactorPro/Summary.aspx>.
10. *Tire Thermal Model for Enhanced Vehicle Dynamics Simulation.* **Somiotti, Aldo.** s.l. : SAE, 2009. 0148-7191.
11. *Selecting an Optimal Hybrid Car Configuration by means of a Simulation Automation System.* **Bröcker, Eduard.** France : IFP, 2008. International Conference on Adavances in Hybrid Powertrains.

12. *Hydraulic Hybrid Propulsion for Heavy Vehicle: Combining the Simulation and Engine-in-the-Loop Techniques to Maximize the Fuel Economy and Emissions Benefits.* **Filipi, Zoran.** France : IFP, 2008. International Conference on Advances in Hybrid Powertrains.
13. **Frey, H. Christopher.** *Comparing real-world fuel consumption for diesel- and hydrogen-fueled transit buses and implication for emissions.* s.l. : Elsevier, 2007.
14. *Race driver model.* **Braghlin, F.** 13-14, Milan : Elsevier; Computers and Structures, 2007, Vol. 86.
15. **Mueller, R. L.** Full Vehicle Dynamics Model of a Formula SAE Racecar using ADAMS/Car. *Mech. Eng. Thesis.* s.l. : Texas A&M University, 2005.
16. **B. A. Guvenc, E. Kural.** Adaptive Cruise Control Simulator. *IEEE Control Systems Magazine.* 2006.
17. **Keith, K.** *Roadway human factors and behavioral safety in Europe.* s.l. : Federal Highway Administration, 2005.
18. **Pauzie, A.** *International Harmonised Research Activity - Intelligent Transport Systems.* s.l. : INRETS, 2007.
19. *A driveng simulator platform applied to develop driver assistance systems.* **Jianquang, W.** Beijing : IEEE; State Key Lab. of Automotive Safety and Energy, 2009.
20. **F1, Williams.** Williams F1. [Online] [Cited: 01 30, 2010.] <http://www.williamsf1.com/>.
21. *Effects of control structure on performance for a automotive powertrain with a continuously variable transmission.* **Liu, S.** 5, s.l. : IEEE; Transactions on Control Systems Technology, 2002, Vol. 10.
22. **SAE.** Collegiate Design Series: SAE. *SAE Student.* [Online] 2009. [Cited: 07 15, 2009.] <http://students.sae.org/competitions/>.
23. **MRT.** MRT. *MRT.* [Online] 2006. [Cited: 07 15, 2009.] <http://fsae.mcgill.ca/en/indexen.htm>.

24. **MHRT.** MHRT. [Online] 2009. [Cited: 07 15, 2009.] <http://formulahybrid.mcgill.ca/Home.html>.
25. **FH.** Past Events: Formula Hybrid. *Formula Hybrid*. [Online] 2007. [Cited: 07 15, 2009.] <http://www.formula-hybrid.org/history/2007-competition.php>.
26. —. Past Events: Formula Hybrid. *Formula Hybrid*. [Online] 2008. [Cited: 07 15, 2009.] <http://www.formula-hybrid.org/history/2008-competition.php>.
27. **Thayer School of Engineering.** 2009 Competition: Formula Hybrid. *Formula Hybrid*. [Online] 2009. [Cited: 07 27, 2009.] http://www.formula-hybrid.org/pdf/2009_Program.pdf.
28. *Development of a a Series PHEV "Formula Style" Race Car.* **Ouellette, Simon.** Winnipeg : Center for Sustainable Transportation, 2007. PHEV 2007.
29. **Alltrax Inc.** Document Depot: Alltrax Inc. *Alltrax Inc.* [Online] 03 20, 2007. [Cited: 07 15, 2990.] http://www.alltraxinc.com/files/Doc100-055-B_SPEC-AXE-Product-Family.pdf.
30. **PERM GMBH.** DC Motors: Products: PERM GMBH. *PERM GMBH*. [Online] 2009. [Cited: 07 15, 2009.] http://www.perm-motor.de/site/pdf/Gleichstrommotoren_PMG/Technische_Daten/PMG_132_TD_Technische_Daten_und_Beschreibung_English_02-08.pdf.
31. **CVTech.** Our Products: CVTech R&D. *CVTech R&D*. [Online] 2009. [Cited: 07 15, 2009.] <http://www.cvttech-rd.com/client/pagesoussection.asp?clef2=2>.
32. **Robin America.** EX21: Overhead Cam Engines: Industrial Engines. *Robin America*. [Online] 2009. [Cited: 07 15, 2009.] <http://www.robinamerica.com/pfeatures.aspx?pid=9>.
33. **Mars Electric LLC.** ME0709: Brushed DC Motors. *Mars Electric LLC*. [Online] 2009. [Cited: 07 15, 2009.] <http://marselectricllc.com/me07091.html>.
34. **LTC, Gaya.** Products. *LTC, Gaya*. [Online] 2009. [Cited: 07 15, 2009.] http://www.gaia-akku-online.de/DOWNLOAD/45AhHP_NCA.pdf.
35. **I+ME Actia.** Downloads. *I+me Actia*. [Online] 2009. [Cited: 07 15, 2009.] http://www.ime-actia.de/download/IR11652_BMS_GB.pdf.

36. **Formula Hybrid Committee.** *2008 Formula Hybrid Rules.* Dartmouth : Thayer School of Engineering, 2008.
37. **Bruce D. Anderson, John R. Maten.** *Continuously Variable Transmission.* s.l. : SAE, 2006.
38. **Albert Mathews, Simon Ouellette, Peter radziszewski.** *AVPRnet Simulation Onfrastructure.* Montreal : McGill University, 2008.
39. *Validation process of a HEV system analysis model: PSAT.* **Rousseau, Aymeric.** Detroit : SAE paper 2001-01-0953, 2001. SAE 2001 World Congress.
40. **Image Space Inc.** Features: rFactor. *rFactor.* [Online] 2009. [Cited: 07 15, 2009.] [http://www.rfactor.net/index.php?page=features.](http://www.rfactor.net/index.php?page=features)
41. **The MathWorks Inc.** Simulink: Products. *The MathWorks.* [Online] 2009. [Cited: 07 15, 2009.] [http://www.mathworks.com/products/simulink/.](http://www.mathworks.com/products/simulink/)
42. **Exotypos.** X Motor Racing. [Online] 2009. [Cited: 07 15, 2009.] [http://www.xmotorracing.com/.](http://www.xmotorracing.com/)
43. **University of Chicago Argonne LLC.** PSAT: Modeling and Simulation. *Argonne National Laboratories.* [Online] 06 5, 2007. [Cited: 07 15, 2009.] [http://www.transportation.anl.gov/modeling_simulation/PSAT/index.html.](http://www.transportation.anl.gov/modeling_simulation/PSAT/index.html)
44. **Clive L. Dym, Patric Little.** *Engineering Design.* s.l. : John Wiley & Sons, Inc., 2004. 0-471-25687-0.
45. **Norton, Robert L.** *Design of Machinery.* s.l. : McGraw-Hill, 2001. 0-07-237960-X.
46. **Kevin Otto, Kristin Wood.** *Product Design.* s.l. : Prentice Hall, 2001. 0-13-021271-7.
47. **Isaac Instruments.** Recorders. *Isaac Instruments.* [Online] 02 2008. [Cited: 07 15, 2009.] [http://www.isaac.ca/Downloads/datasheets/BOXV73_PRO%20V73%20Professional%20System .pdf.](http://www.isaac.ca/Downloads/datasheets/BOXV73_PRO%20V73%20Professional%20System.pdf)
48. FSAE Tire Test Consortium Data. s.l. : FSAE Tire Test Consortium and Calspan Tire Research Facility.

49. *Validating Simulation Tools for Vehicle System Studies Using Advanced Control and Testing Procedure.* **Pasquier, Maxime.** Berlin : s.n., 2001. 18th International Electric Vehicle Symposium.
50. *Honda Insight Validation Using PSAT.* **Rousseau, Aymeric.** Cost-Mesa : s.n., 2001. Future Transportation Technology Conference.
51. *Li-ion Battery Models for HEV Simulator.* **Debert, Maxime.** France : IFP, 2008. International Conference on Advances in Hybrid Powertrains.
52. *A model of the tension and transmission efficiency of a bush roller chain.* **Lodge, C. J.** Part C, Bristol : Journal of Mechanical Engineering Science, 2001, Vol. 216.
53. **Stevens, Matthew.** *Unicell Quick Sider Vehicle Powertrain Simulation.* Montreal : McGill University, 2008.
54. *A semi-empirical dynamic tire model for combined-slip forces.* **Svendenius, Jacob.** Lund : Vehicel system Dynamics, 2006. 0042-3114.
55. *Dynamic Tire Friction Models for Vehicle Traction Control.* **Wit, Carlos Canudas De.** Phoenix : 38th Conference on Decision and Control, 1999.
56. **The Math Works.** Documentation/SimDriveline. [Online] The Math Works. [Cited: 07 29, 2009.]
<http://www.mathworks.com/access/helpdesk/help/toolbox/phymod/drive/index.html?/access/helpdesk/help/toolbox/phymod/drive/tire.html&http://www.google.ca/search?q=tire+slip+model+in+vehicle+simulation&ie=utf-8&oe=utf-8&aq=t&rls=org.mozilla:en-US:official&>
57. **Argonne National Laboratory.** Powertran Systems Analysis Toolkit Components. *PSAT Documentation.*
58. **Pacejka, H. B.** *Tire and Vehicel Dynamics.* s.l. : Oxford, 2002.
59. *Accident Analysis and Prevention; Driving simulator for spee research on two-lane rural roads.* **Bella, F. 3,** Rome : Elsevier, 2008, Vol. 40. 0001-4575.

APPENDIX 1

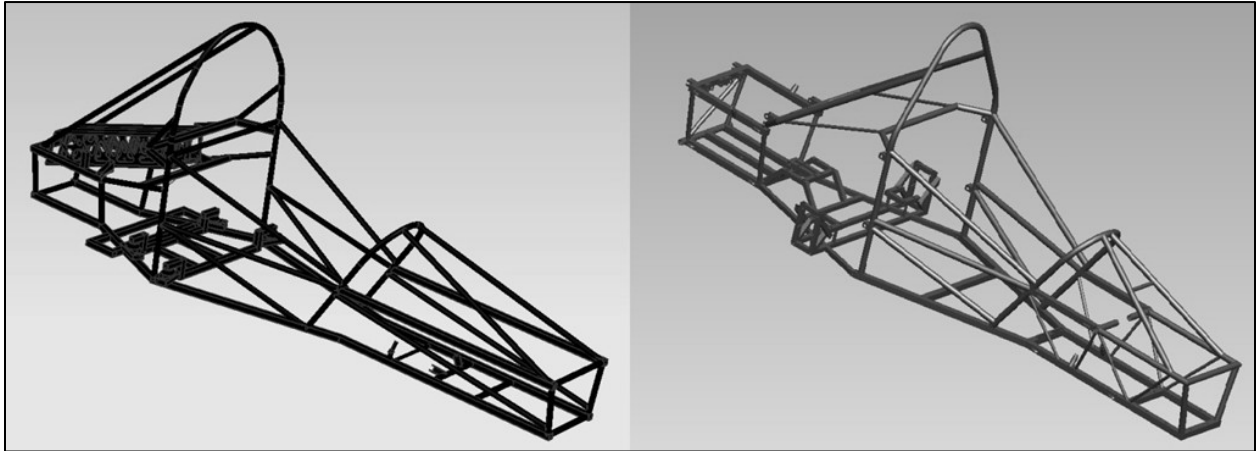


Figure 51: Chassis CAD views for MHRT3 (left) and MHRT2 (right).

The two chassis have the same basic design. For MHRT3, the driver compartment was elongated while the powertrain compartment was shortened.

APPEENDIX 2

Figure 52 shows the relation used for equation 2 of the battery model.

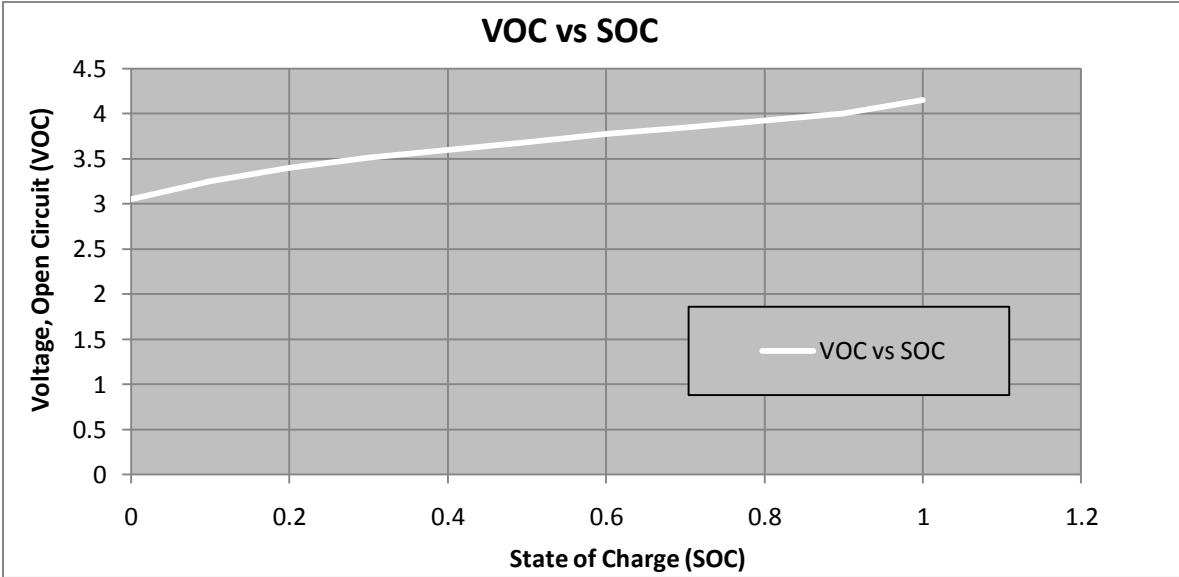


Figure 52: Battery model relation for open circuit voltage to state of charge.

Previous work performed on modeling of the LTC cells proved that linear fits to the given Voc vs SOC table could not produce adequate accuracy in reproducing battery performance. For this reason the table has been develop through careful data analysis and subsequence adaptation to produce the desired accuracy.

APPENDIX 3

Relationships used for the PMG and ME0709 models are show in figures 53 and 54.

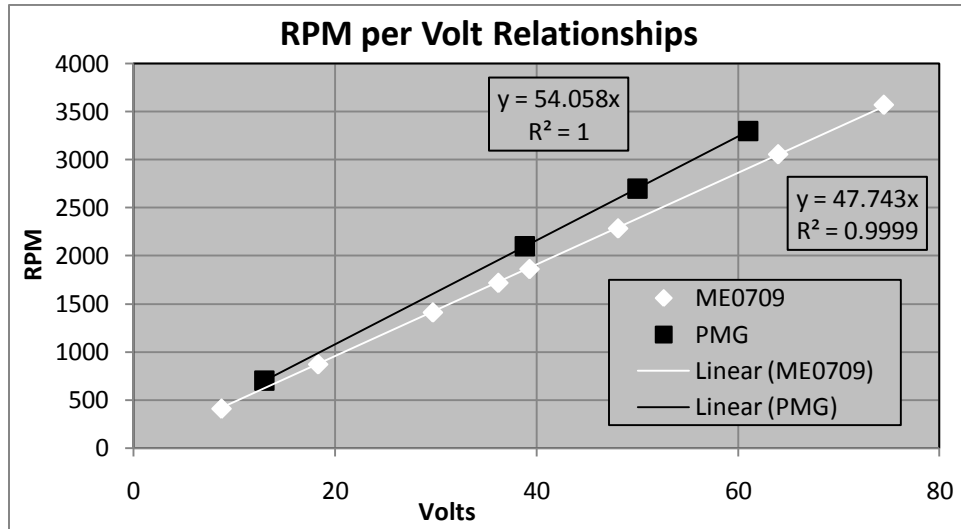


Figure 53: RPM per Volt relationships.

Figure 53 shows that for the same voltage, the ME0709 will produce a lower speed.

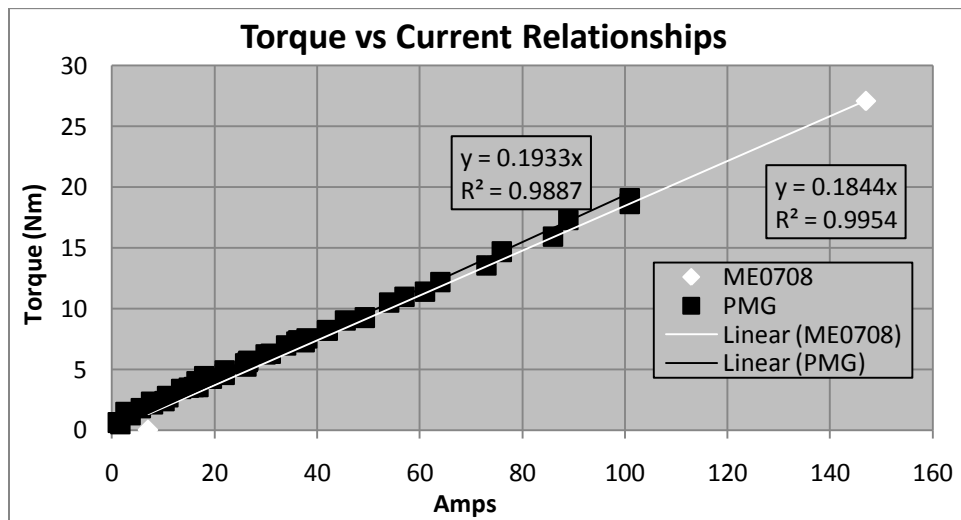


Figure 54: Torque versus current relationships.

Note that both the PMG and the ME0709 have similar relationships between current and torque. The coil resistance used for each is 0.016 Ohms.

APPENDIX 4

Table 19 shows the dynamometer data obtained for the output torque of CVT3, note that due to limited power available from the electric drive system used to power the CVT, some high torque data points are missing. These points are filled in by extrapolating the existing data using a curve fit for a plot of the output torque versus the input torque. This is carried out for each RPM value as indicated by the arrow at 600 RPM.

Table 19: Dynamometer data for CVT3.

DriveN Torque (Nm)	DriveR Torque (Nm)								
	0	3.9	7.9	12	16	20	24	28	
DriveN RPM	200	-6.8	9	25	40	54	68	81	
	400	-7	8.5	24	37	52	67		
	600	-6.6	8	22	36	—	—	—	→
	800	-6.2	6	18	29	40	51		
	1000	-5.8	4.1	14	24	33	43	51	
	1200	-4.9	3.7	13	20	28	35	43	
	1400	-4.3	3.3	10	17	25	31	39	
	1600	-4.2	2.6	9.3	16	22	29	33	
	1800	-4.6	2.3	8.2	15	20	26	32	
	2000	-4.5	1.5	7.2	13	19	24	28	
	2200	-4.2	1.6	6.4	12	17	22	27	
	2400	-3.7	1.2	5.9	11	15	21	24	
	2600	-3.6	1	5.5	10	15	19	23	
	3000	-3.6	0.6	4.5	8.8	12	17	20	
	3400	-3.6	0.1	3.6	7.5	11	15		
	3800	-3.6	-0.1	3.3	6.4	9.7	13		
4400	-3.5	-0.6	2.3	5.4	8.4				

Figure 55 shows plots and curve fits for some RPM values, the equations of the curve fits are used for the extrapolation. This procedure is performed for both the DriveN torque and the DriveR RPM data tables for all four CVT configurations.

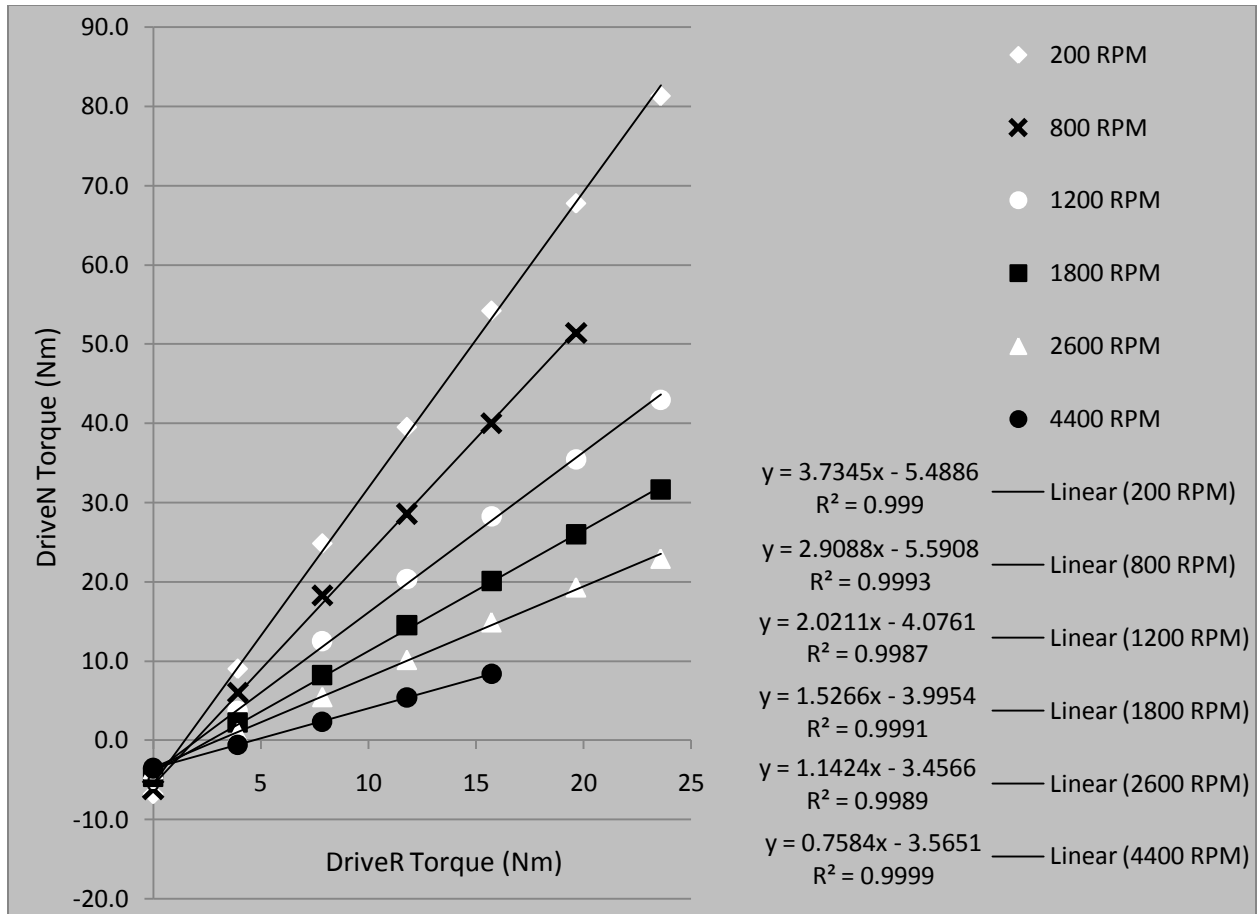


Figure 55: Curve fits used to extrapolate CVT3 torque data.

APPENDIX 5

The XMR Vehicle Physics program is used to modify the parameters used in the physical modeling of the vehicle in the three dimensional environment. For each vehicle modeled in XMR, vehicle physics can be used to create as many different profiles as one desires. The program has tabs to categorize the many parameters which can be adjusted. Within each tab, the window is separated into several boxes. The list below is setup with tabs identified by numbers, boxes by letters, and parameters by roman numerals. The settings provided here are those for trails set two.

XMR Vehicle physics Parameters, some are dimensionless parameters:

1. Common
 - a. Mass
 - i. Mass/Sprung = 300 kg
 - ii. Wheel/Unsprung Mass = 10 kg per wheel
 - b. Center of Mass / CG
 - i. Height offset = 0.14m
 - ii. Weight dist (front/rear) = 0.44
 - c. Body Geometry
 - i. Width = 0.66m
 - ii. Height = 0.66m
 - iii. Length = 2.5m
 - iv. Offset X longitude= 0m
 - v. Offset Y vertical= 0.07m
 - vi. Offset Z lateral= 0m
 - vii. Front Wheel Radius = 0.25m
 - viii. Rear Wheel Radius = 0.25m
 - ix. Front Tire Width = 0.203m
 - x. Rear Tire Width = 0.203m
 - xi. Front Tire Height = 0.07m
 - xii. Rear Tire Height = 0.07m
 - d. Mass Distribution
 - i. Width = 0.9m
 - ii. Height = 0.4m
 - iii. Length = 2.44m
 - iv. Wheel Radius = 0.2m
 - e. Driving Wheel = Rear Wheel Drive
2. Aerodynamics – “Forces Only”
 - a. Drag Coefficient = 0.426
 - b. No lift coefficients are used.
 - c. Side force Coefficient = 0.43
 - d. Pitching Moment = 0.04

- e. Yawing Moment = 0.01
 - f. Rolling Moment = 0.01
 - g. Frontal Area = 0.903 m²
 - h. No hydro dynamics
3. Steering
- a. Maximum steering angle = 30 deg
 - b. Parallel steer = 1
 - c. Max steering at velocity = 30 deg
 - d. Caster angle = 3.5 deg
 - e. King pin inclination = 0.75 deg
4. Brakes
- a. Brakes
 - i. Max Front Brake Torque = 350 N-m
 - ii. Max Rear Brake Torque = 350 N-m
 - iii. Max Hand Brake Torque = 10 N-m (min allowable)
 - b. Traction Control – All parameters at minimum
 - c. ABS – All parameters at minimum
 - d. Stability Control – All parameters at minimum
5. Engine
- a. Min RPM = 0
 - b. Max RPM = Defined by Powertrain Configuration
 - c. Redline RPM = Defined by Powertrain Configuration
 - d. FF to engine = 1
 - e. Shutdown RPM = 0
 - f. Inertia = 0.15 kg-m²
 - g. Dissipation = 0.0047053
 - h. Vapor Dissipation = 0.018
6. Suspension
- a. Front Suspension
 - i. Double wishbone
 - ii. Travel = 0.05m
 - iii. Stiffness k = 45250 N/m
 - iv. Anti roll bar stiffness = 15000 N-m
 - v. Bump Damping = 3218 Ns/m
 - vi. Rebound Damping = 3218 Ns/m
 - vii. Hardness Part = 0.97, default
 - viii. Hardness Part Fun = 4.5, default
 - ix. Roll Center Height = 0 m
 - b. Rear Suspension
 - i. Double Wishbone
 - ii. Travel = 0.05m
 - iii. Stiffness k = 55313 N/m
 - iv. Anti roll bar stiffness = 5000 N-m
 - v. Bump Damping = 4422 Ns/m
 - vi. Rebound Damping = 4422 Ns/m
 - vii. Hardness Part = 0.97, default

- viii. Hardness Part Fun = 4.5, default
 - ix. Roll Center Height = 0 m
 - c. Ride Height Reduction
 - i. Front = 0m
 - ii. Rear = 0 m
 - d. Anti
 - i. Anti Squat = 0
 - ii. Anti Dive = 0
- 7. Transmission
 - a. Differential
 - i. Type = Active
 - 1. Active f = 3.4
 - b. Central = Open
 - c. Auto Clutch
 - i. Auto clutch delay start = 500 ms
 - ii. Auto clutch delay shifting = 100 ms
 - d. Key clutch delay – This parameter is not used
 - e. Transmission
 - i. Transmission inertia = 0.02 kg-m²
 - ii. Transmission dissipation = 0.1
 - f. Gears
 - i. Gear num = 1
 - ii. Main Gear ratio = 1
 - iii. Gear Ratios
 - 1. -1 (reverse) = -5
 - 2. Defined by Powertrain Configuration
 - g. Axel Shaft
 - i. Axel Shaft Inertia = 0.028 kg-m²
 - ii. Axel Shaft dissipation = 0.025
- 8. Tires
 - a. Front Wheels
 - i. Surface = Asphalt
 - ii. Long. Friction Coeff. = 2.5
 - iii. Lat. Friction Coeff. = 2.3
 - iv. Rolling Resistance = 0.007
 - v. Pressure = 110 kPa
 - vi. Camber Angle = -2 deg
 - vii. Toe Angle = 0 deg
 - b. Rear Wheels
 - i. Surface = Asphalt
 - ii. Long. Friction Coeff. = 2.5
 - iii. Lat. Friction Coeff. = 2.3
 - iv. Rolling Resistance = 0.007
 - v. Pressure = 110 kPa
 - vi. Camber Angle = -2 deg
 - vii. Toe Angle = 0 deg

9. Tire Model
 - a. Spline = 0.5
 - b. Tire Model Maps Created from (48)

APPENDIX 6

Figure 56 shows the results from optimization of the genset ratio with all other variables held constant. Comparing the output of ratios 1.0 and 1.05, we see that 1.05 performs better at high SOC while 1.0 performs better at low SOC. Noting that a ratio of 1.1 performs better than 1.05 at very high SOC, it is possible that greater benefit could be achieved with ratios greater than 1.0 but only if the heat issues are non-existent. However, care must be taken since as the SOC becomes dangerously low, the performance of higher ratios decreases relative to that of 1.0. Since 1.0 performs adequately over the entire SOC range, it appears to be the safest choice.

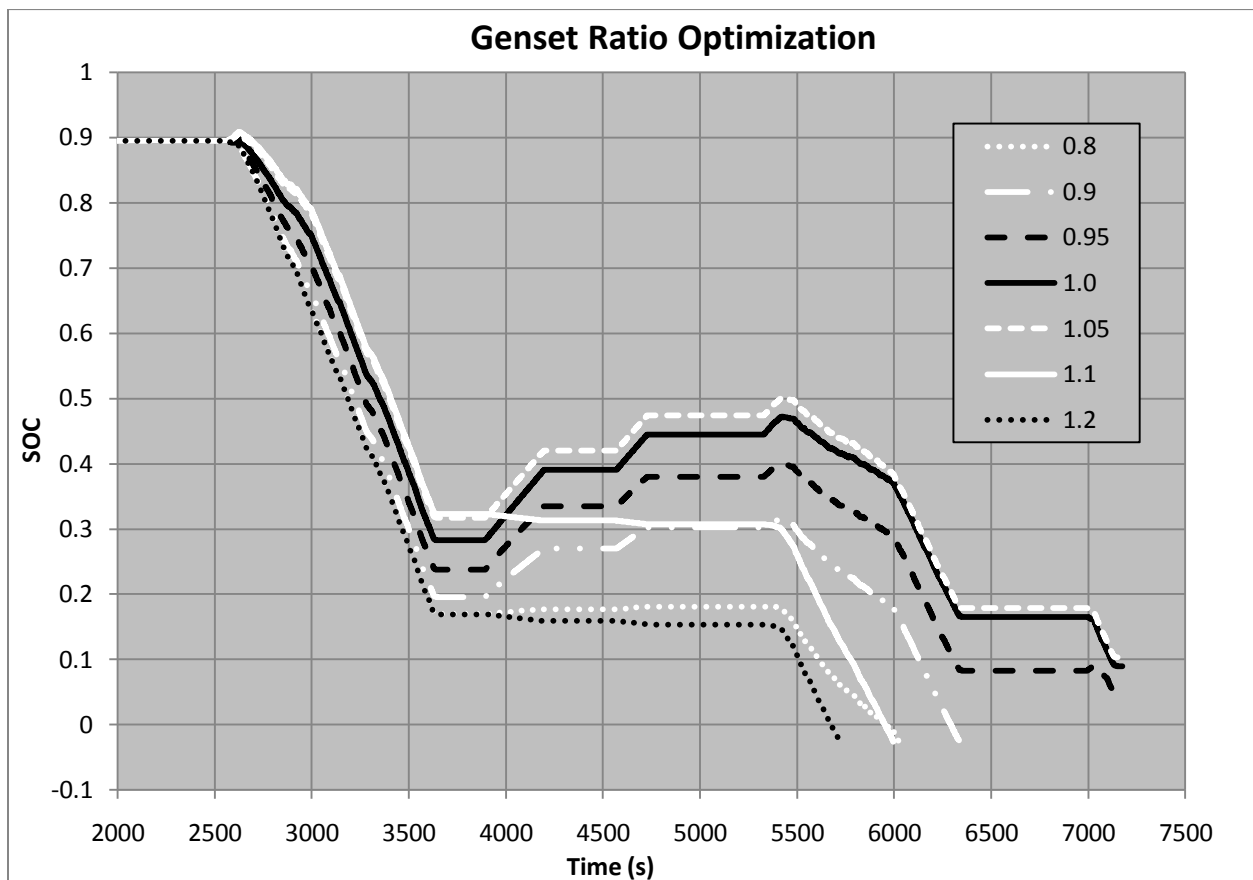


Figure 56: Genset ratio optimization.